Establishment and maintenance of 35S rRNA gene chromatin states in *Saccharomyces cerevisiae*

DISSERTATION ZUR ERLANGUNG DES DOKTORGRADES DER
NATURWISSENSCHAFTEN (DR. RER. NAT.)
DER FAKULTÄT FÜR BIOLOGIE UND VORKLINISCHE MEDIZIN
DER UNIVERSITÄT REGENSBURG

vorgelegt von

Manuel Wittner aus Ingolstadt

im Februar 2012

Das Promotionsgesuch wurde eingereicht am: 07. Februar 2012

Die Arbeit wurde angeleitet von: PD Dr. Joachim Griesenbeck

Prüfungsausschuss:

Vorsitzender:	Prof. Dr. Herbert Tschochner
1. Prüfer:	PD Dr. Joachim Griesenbeck
2. Prüfer:	Prof. Dr. Michael Rehli
3. Prüfer:	Prof. Dr. Wolfgang Seufert

Die vorliegende Arbeit wurde in der Zeit von Dezember 2008 bis Februar 2012 am Lehrstuhl Biochemie III des Institutes für Biochemie, Genetik und Mikrobiologie der Naturwissenschaftlichen Fakultät III der Universität Regensburg unter Anleitung von PD Dr. Joachim Griesenbeck im Labor von Prof. Dr. Herbert Tschochner angefertigt.

Ich erkläre hiermit, dass ich diese Arbeit selbst verfasst und keine anderen als die angegebenen Quellen und Hilfsmittel verwendet habe.
Diese Arbeit war bisher noch nicht Bestandteil eines Prüfungsverfahrens.
Andere Promotionsversuche wurden nicht unternommen.

Manuel Wittner

Regensburg, 07. Februar 2012

Table of Contents

1 Summary

The ribosomal DNA (rDNA) locus of *Saccharomyces cerevisiae* (hereafter called yeast) represents an ideal model system to study the interplay between chromatin and all DNA-dependent processes such as transcription, replication and DNA repair. This multicopy gene locus harbours the 35S ribosomal RNA (rRNA) genes which are transcribed by the specialised RNA polymerase I (Pol I). Importantly, each 35S rRNA gene exists in either a Pol I transcribed and nucleosome depleted, open chromatin state or a nucleosomal, closed chromatin state. Open rRNA genes guarantee the cell's supply with structural and catalytic components of the ribosome, whereas closed rRNA genes ensure genomic integrity. In this study, the molecular processes leading to chromatin transitions from the open to the closed chromatin state or *vice versa* were analysed. To this end, alterations in the 35S rRNA gene chromatin states were investigated in course of the cell cycle and after UV-induced DNA damage and subsequent nucleotide excision repair (NER).

The analyses of 35S rRNA chromatin during the cell cycle revealed that the observed balance between open and closed rRNA gene chromatin states in proliferating yeast cells is due to a dynamic equilibrium of transcription-dependent removal and replication-dependent assembly of nucleosomes. Besides, a molecular role for Hmo1, an HMG box protein which is a component of the open 35S rRNA gene chromatin state, could be identified. Hmo1 counteracts replication-independent nucleosome deposition and thereby maintains the open rRNA gene chromatin state outside of S phase. These findings indicate that the opposing effects of replication and transcription lead to a *de novo* establishment of rRNA gene chromatin states during each cell cycle.

The analyses of 35S rRNA gene chromatin states after irradiation of yeast cells with UV light demonstrated that UV induced DNA damage triggers nucleosome assembly at open rRNA genes. In contrast to the situation in non-damaged cells, where Pol I and Hmo1 are exclusively associated with the nucleosome depleted, open rRNA genes, DNA damage induced nucleosome deposition converts the former open rRNA genes to a mixed chromatin state, harbouring Pol I, Hmo1 and nucleosomes. NER is then required for re-opening rRNA gene chromatin in a 5'-3' gradient. Interestingly, the opening of rRNA genes during NER leads to a higher fraction of open rRNA genes than the one observed in exponentially growing cells before DNA damage. In accordance with the results obtained in the analysis of 35S rRNA gene chromatin during the cell cycle, the latter might be a consequence of DNA damage induced cell cycle arrest.

2 Introduction

2.1 Eukaryotic chromatin structure

In eukaryotes, genomic DNA is arranged in a set of linear chromosomes and located to a specialised compartment, called the nucleus. In the chromosomal context, the DNA is associated with numerous proteins and forms a structure, called chromatin. On the one hand, these protein-DNA interactions lead to strong compaction and thus enable the DNA to fit inside the confined volume of the nucleus. On the other hand, chromatin serves as a central regulator of all DNA-dependent metabolic processes occurring in eukaryotic cells. Accordingly, the structure of chromatin has to be highly dynamic to enable processes such as transcription, DNA repair or DNA replication (Kornberg and Lorch, 1995; Li et al., 2007; Clapier and Cairns, 2009).

2.1.1 Histone molecules represent the main components of chromatin

The basic repeating structure in chromatin is termed the nucleosome core particle (Fig. 2-1). The nucleosome is formed by 147 base pairs (bp) of DNA wrapped around an octamer of two subunits of each of the core histones H2A, H2B, H3, and H4 (Luger, 2003). Each core histone comprises two separate functional domains. The “histone-fold” motif sufficient for both histone-histone and histone-DNA contacts within the nucleosome, and the N- and C-terminal “tail” domains that contain sites for posttranslational modifications (e.g. acetylation, methylation, phosphorylation, and ubiquitination) (Jenuwein and Allis, 2001; Horn and Peterson, 2002; Peterson and Laniel, 2004). Histone proteins are highly conserved among all eukaryotic organisms, with *Saccharomyces cerevisiae* (hereafter called yeast) histones being one of the most divergent from mammalian histones (Baxevanis and Landsman, 1998). The distinct sequence divergence between the histone proteins of yeast and metazoans might be reasoned by the different requirements for DNA compaction between uni- and multicellular organisms. Indeed, it was reported that yeast mononucleosomes are less stable towards salt-dependent and thermal unfolding, suggesting a more flexible structure (Lee et al., 1982; Piñeiro et al., 1991). Besides, there is also a difference in the spacing of nucleosomes in yeast and higher eukaryotes. Whereas in metazoan the average nucleosomal repeat length is approximately 190bp, in yeast, nucleosomes are

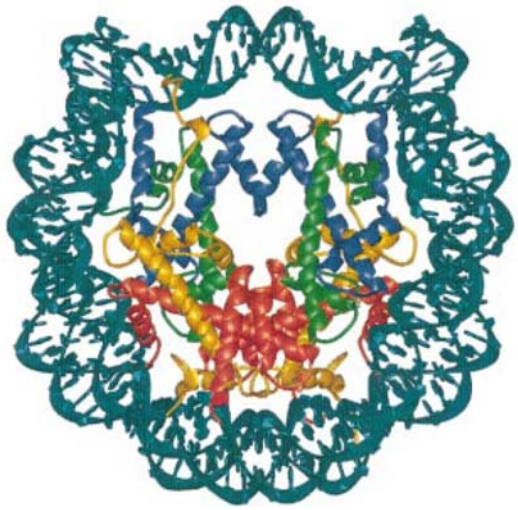

Figure 2-1. Structure of the *S. cerevisiae* nucleosome core particle
Front view of the yeast nucleosome core particle, viewed down the superhelical axis. Histone chains are coloured yellow for H2A, red for H2B, blue for H3 and green for H4. The DNA is shown in turquoise. α-helices and the location of the N- and C-terminal tails are shown. (from White et al., 2001)

very closely spaced, with an average repeat length of 162±6bp (Hörz and Zachau, 1980), resulting in a linker length of only 15-20bp (White et al., 2001).

In addition to the four core histones, a fifth histone, H1 or linker histone, associates with DNA at the nucleosomal entry/exit site, leading to increased protection of the nucleosomal DNA. Although the precise location of H1 in chromatin is still unknown, it was shown that H1 is implicated in salt dependent compaction of a nucleosomal array into a regular 30nm chromatin fibre *in vitro* (reviewed in Woodcock and Ghosh, 2010). By establishing higher order chromatin structures, H1 also modulates the accessibility of regulatory proteins, chromatin remodelling and histone modifying enzymes to their target sites (Happel and Doenecke, 2009). In mammalian cells, at least six different isoforms of H1 are expressed, often in a tissue specific way (Sancho et al., 2008). Depletion of H1 prevents the establishment of the most condensed chromatin structure (Maresca and Heald, 2006), the metaphase chromosome, and is lethal during mice and *Drosophila* development (Fan et al., 2003; Lu et al., 2009). In yeast, the putative histone H1 homolog is encoded by *HHO1* (Landsman, 1996; Ushinsky et al., 1997). Surprisingly, yeast cells harbouring a deletion of this gene do neither reveal defects in growth nor in mating (Patterton et al., 1998). In contrast to other organisms, yeast histone H1 is present in substoichiometrical amounts compared to nucleosomes (Freidkin and Katcoff, 2001; Downs et al., 2003). Thus, it might be that the less compact chromatin structure in yeast is due to the low abundance of Hho1.

2.1.2 Chromatin dynamics and transcription

Although in general the nucleosomal structure is inhibitory to all DNA-dependent processes, chromatin is locally reorganised in response to cellular signals, allowing regulatory factors to access their cognate DNA elements. At least two mechanisms leading to chromatin rearrangements are well known. The first mechanism relies on ATP-dependent chromatin remodelling factors. These multiprotein complexes couple ATP hydrolysis to alterations of the chromatin structure at the level of the nucleosomal array (reviewed in Längst and Becker, 2004). The second mechanism involves post-translational modifications of the histone N-termini. The highly basic histone tails are less structured than the histone fold regions and are predicted to interact with the negatively charged DNA backbone or with other chromatin-associated proteins (Luger and Richmond, 1998; Wolffe and Kurumizaka, 1998; Hansen et al., 1998). The possibility to combine a multitude of these covalent modifications at the histone N-termini, led to the proposal of a "histone code" which is recognised and decrypted by other proteins initiating distinct downstream events (Strahl and Allis, 2000).

One example of posttranslational modifications of core histones is acetylation by histone acetyltransferases (HATs), which has been linked causally to transcriptional activation of genes. Accordingly, a large number of previously identified transcriptional co-activators were shown to be HATs (Sterner and Berger, 2000; Roth et al., 2001). The enzymatic acetylation of ε-amino groups of lysine residues reduces the overall positive charge of the histone tails. Thus it has been postulated that this modification decreases the affinity for the negatively charged DNA, thereby facilitating the binding of regulatory proteins to chromatin templates (Rice and Allis, 2001).

Initiation of transcription is prevented by the presence of nucleosomes at promoter regions *in vitro* and *in vivo* (Lorch et al., 1987; Knezetic and Luse, 1986; Han and Grunstein, 1988). Several studies revealed that the alterations in chromatin structure during transcriptional activation lead to the complete disassembly of nucleosomes at the promoter region of genes (Boeger et al., 2003; Reinke and Hörz, 2003; Adkins et al., 2004). It has been suggested that chromatin remodelling complexes and HATs act synergistically to establish a local chromatin structure that is permissive for the assembly of general transcription factors and thus, for transcription initiation (Fry and Peterson, 2001). Besides, the nucleosome represents also a barrier for transcription elongation *in vitro*. Thus, transcription of nucleosomal templates is slower *in vitro* than *in vivo* and a single nucleosome has the potential to stop elongating RNA polymerases (Lavelle, 2007;

Kulaeva et al., 2007). Interestingly, for some heavily transcribed genes in yeast, transcription-dependent nucleosome removal within the coding sequence has been reported *in vivo* (Kristjuhan and Svejstrup, 2004; Lee et al., 2004; Schwabish and Struhl, 2004). The results obtained until today suggest that nucleosomal histones are evicted partially or completely in front of elongating RNA polymerase II (Pol II), followed by subsequent rapid reassembly of nucleosomes after passage of the polymerase (Workman, 2006).

Numerous auxiliary factors were suggested to facilitate transcription through nucleosomes by histone exchange or displacement. One of these transcription elongation factors is represented by the FACT complex (Facilitates Chromatin Transcription; Orphanides et al., 1998). FACT was shown to assist Pol II to read through nucleosomal DNA during transcription elongation *in vitro* an *in vivo* by removing one H2A/H2B dimer (Orphanides et al., 1999; Belotserkovskaya et al., 2003; Mason and Struhl, 2003, 2005). Moreover, FACT was observed to contain histone chaperone activity (Belotserkovskaya et al., 2003), suggesting that this complex also promotes the reassembly of nucleosomes. Interestingly, a recent study indicated that FACT might also facilitate transcription of nucleosomal templates by Pol I and Pol III (Birch et al., 2009).

2.1.3 Chromatin dynamics and DNA replication

Besides transcription dependent chromatin dynamics, a dramatic chromatin re-organisation occurs when the genomic DNA gets duplicated during S phase. Therefore, eukaryotic cells evolved efficient nucleosome-assembly pathways and chromatin-maturation mechanisms that reproduce chromatin organisation during DNA replication (Groth et al., 2007). The ordered assembly of nucleosomes at the DNA double strand is facilitated by histone chaperones, termed nucleosome assembly factors (Philpott et al., 2000; Verreault, 2000). These proteins assist in nucleosome deposition by neutralising the positively charged histones and thereby prevent unspecific association with DNA (Tyler, 2002).

Replication coupled nucleosome assembly involves the transient disruption of histone-DNA interactions of pre-existing nucleosomes located ahead of replication forks and their transfer to nascent DNA (Sogo et al., 1986; Gasser et al., 1996). Studies using cell-free DNA-replication systems and *in vivo* density-labelling techniques led to the general view that the core histone octamer is disrupted into two H2A-H2B dimers and a histone H3-H4 tetramer (Corpet and Almouzni, 2009), but whether the histone H3-H4 tetramer remains

intact during transfer is still an open question (Annunziato, 2005). The H3-H4 tetramer is then randomly transferred onto one of the nascent DNA strands and either old H2A-H2B dimers are recycled or newly synthesised H2A-H2B dimers are assembled to complete the nucleosome (Groth et al., 2007). In principal, stochastic transfer of parental histones to both daughter strands enables the preservation of specific post-translational modifications during DNA replication which may then be propagated to newly synthesised histones. Many factors, including chromatin remodelling complexes and histone chaperones are implicated in disruption and recycling of parental nucleosomes. Interestingly, besides its function during transcription, FACT seems also to be implicated in nucleosome disruption during replication as it has been identified recently in complex with the replicative DNA helicase in yeast and human cells (Gambus et al., 2006; Tan et al., 2006).

Newly synthesised histones are assembled through a pathway known as replication-dependent *de novo* nucleosome deposition (Groth et al., 2007). Expression of canonical histones is tightly coupled to DNA synthesis and proper control of histone levels seems to be crucial for genome stability (Marzluff and Duronio, 2002; Marzluff et al., 2008). In accordance, the passage through S phase in the absence of histone expression or the over-expression of H2A–H2B relative to H3-H4 dimers, or *vice versa*, leads to cell death or causes increased frequency of chromosome loss in yeast, respectively (Kim et al., 1988; Meeks-Wagner and Hartwell, 1986). An evolutionary conserved histone chaperone involved in *de novo* replication coupled nucleosome assembly is the three-subunit chromatin assembly factor 1 (CAF-1) (Stillman, 1986; Kaufman et al., 1997). CAF-1 deposits newly synthesised H3-H4 and facilitates nucleosome assembly following DNA replication by interacting with proliferating cell nuclear antigen (PCNA), a component of the DNA replication machinery (Shibahara and Stillman, 1999). CAF-1 dependent histone deposition onto replicated DNA is assisted by anti silencing function 1 (Asf1), another H3-H4 histone chaperone (Tyler et al., 1999; Mello et al., 2002). Structural studies revealed that Asf1 binds H3-H4 dimers at the H3 interface blocking the formation of the H3-H4 tetramer (English et al., 2006; Natsume et al., 2007). However it is still unknown, whether both new histone H3-H4 dimers are provided by Asf1 and then deposited by CAF-1 onto DNA or whether additional chaperones are needed for efficient assembly of the H3-H4 tetramer (Corpet and Almouzni, 2009). After delivery of the H3-H4 tetramer to newly synthesised DNA, nucleosome assembly protein 1 (NAP-1) is suggested to assist in the subsequent addition of histones H2A-H2B (Zlatanova et al., 2007).

Incorporation of new H2A-H2B dimers, however, does not necessarily have to be tightly linked to DNA replication because substantial exchange of H2A-H2B dimers occurs also outside of S phase (Kimura and Cook, 2001). As mentioned above, nucleosome eviction occurs at the regulatory regions of many active genes and in general there is a strong correlation between nucleosome disassembly and the rate at which the gene is transcribed (Bernstein et al., 2004; Lee et al., 2004; Yuan et al., 2005). Interestingly, rapid reassembly of nucleosomes, independent of DNA replication, could be observed upon transcriptional shutdown (Schwabish and Struhl, 2004; Adkins et al., 2004; Schermer et al., 2005). The histone chaperone Spt6 was shown to mediate nucleosome reassembly at several promoters during transcriptional repression (Adkins and Tyler, 2006). Besides, the HIR (histone regulatory) complex and Asf1 are implicated in replication independent histone deposition, indicating that these proteins function together as a conserved eukaryotic pathway for histone replacement throughout the cell cycle (Green et al., 2005; Amin et al., 2011).

2.1.4 Chromatin dynamics and DNA repair

2.1.4.1 Nucleotide excision repair in yeast

There exist two different pathways of DNA repair that specifically remove lesions from DNA (Friedberg et al., 2005). Whereas base excision repair (BER) eliminates nucleotides containing small modifications like oxidised, deaminated or alkylated bases, nucleotide excision repair (NER) removes lesions that induce severe distortions of the DNA helix induced by UVB and UVC light (Ravanat et al., 2001). The most common DNA adducts and UV-photoproducts, removed by NER, represent cyclobutane pyrimidine dimers (CPDs) and pyrimidine-(6-4)-pyrimidone photoproducts (Lindahl and Wood, 1999).
The NER pathway involves several distinct steps: (1) recognition of the lesion, (2) incisions on both sides of the lesion in the damaged strand, (3) excision of the 25-30bp oligonucleotide containing the lesion, (4) filling the gap by DNA replication and (5) ligation of the newly replicated strand (Fig. 2-2). The process of NER itself can be subdivided into two further pathways: global genomic repair (GGR), which is responsible for the repair of non-transcribed DNA sequences and transcription coupled repair (TCR), which rapidly repairs the transcribed strand (TS) of actively transcribed genes (Hanawalt, 2000; Hoeijmakers, 2001). In general, DNA lesions are removed more efficiently by TCR than by GGR (Bohr et al., 1985; Mellon et al., 1986).

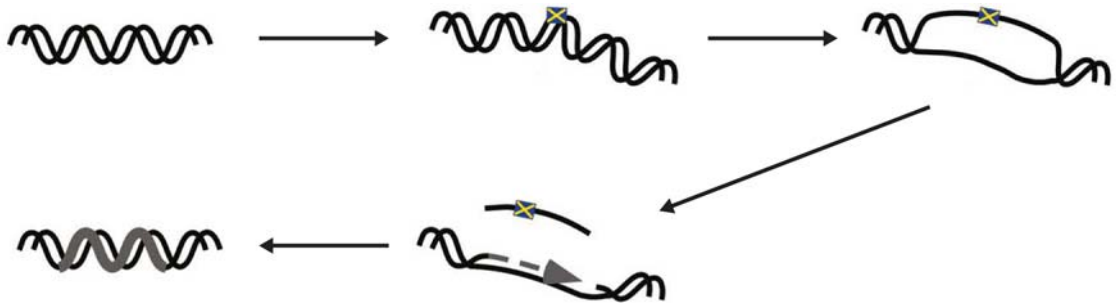

Figure 2-2. Schematic representation of Nucleotide excision repair (NER) steps.
UV photoproducts (indicated as yellow cross) induce a kink in the DNA. After damage recognition, the DNA is unwound. Then, single-strand incisions are made at both sides of the lesion and an oligonucleotide (25-30nt) containing the lesion is excised. Finally, the resulting gap is filled (repair DNA synthesis; grey arrow), using the opposite DNA strand as template and the newly synthesised strand is ligated by DNA ligase. (from Tremblay et al., 2009)

Except for the proteins implicated in DNA damage recognition, the majority of NER proteins participate in both subpathways. In yeast, the Rad1/10–Rad2 endonucleases, the Rad4/23 complex, the Rpa protein, the Rad14 DNA-damage recognition protein and TFIIH (comprised of the Rad3 and Rad25 helicases) form the core of the NER machinery. These proteins and protein complexes proved to be sufficient and necessary for incision of the damaged strand *in vitro* (Prakash and Prakash, 2000). Although strains that carry a deletion of the *RAD7* and *RAD16* genes exhibit only moderate sensitivity towards UV light, Rad7 and Rad16 proteins were shown to be essential for GGR *in vivo* (Guzder et al., 1995). TCR, however, is not affected in *rad7Δ* and *rad16Δ* cells (Verhage et al., 1994; Mueller and Smerdon, 1995). As its name implies, ongoing transcription is necessary for the removal of DNA lesions from the TS by TCR (Hoeijmakers, 2001). Accordingly, efficient repair of the TS of actively transcribed genes was abolished in Pol II temperature sensitive mutants at the restrictive temperature in yeast (Sweder and Hanawalt, 1992; Leadon and Lawrence, 1992). It was hypothesised that RNA polymerases stalled at damage sites serve as the recognition signal for the recruitment of NER proteins (Tornaletti and Hanawalt, 1999; Citterio et al., 2000; Sarker et al., 2005). In addition, stalled RNA polymerases must be displaced to make the DNA damage site accessible to repair enzymes (Tornaletti and Hanawalt, 1999; Citterio et al., 2000; Hanawalt, 2000; Mellon, 2005). In human cells, the product of the Cockayne syndrome B (CSB) gene (together with XPB, XPD and XPG) is involved in detection and eviction of stalled RNA polymerases (Troelstra et al., 1992; Le Page et al., 2000; Citterio et al., 2000; Lainé and Egly, 2006).

Rad26 represents the functional homolog of CSB in yeast (van Gool et al., 1994). As a result, mutants lacking the *RAD*26 gene are TCR deficient, similar to CSB cells. Interestingly, Rad26 and CSB belong to the Swi2/Snf2 family of chromatin remodelers and consequently could be involved in remodelling of protein-DNA interactions during TCR (Green and Almouzni, 2002; Ura and Hayes, 2002).

2.1.4.2 Nucleotide excision repair in chromatin

Like in all DNA dependent processes, chromatin structure has also a great impact on DNA repair (Smerdon and Conconi, 1999; Thoma, 1999). In a series of studies using human fibroblasts, nucleosome rearrangement during NER (Smerdon and Lieberman, 1978), the formation of nucleosomes after repair and the repositioning of nucleosomes at repaired regions were analysed (Smerdon et al., 1979; Smerdon and Lieberman, 1980; Hunting et al., 1985; Smerdon, 1986). These studies revealed that during the DNA synthesis step newly repaired DNA is not tightly bound to the surface of core histones. Accordingly, the structure of nucleosomes is altered during NER (Tremblay et al., 2009). Besides, it was shown that the DNA ligation step precedes nucleosome formation (Smerdon, 1986). These data led the authors to propose that nucleosomes are rearranged by sliding or unfolding during NER (Fig. 2-3).

Deeper insight in NER in the context of chromatin was gained by *in vitro* repair assays. One of these studies showed that repair of specific CPD sites in reconstituted mononucleosomes is strongly inhibited at many positions of the nucleosomal DNA (Liu and Smerdon, 2000). Besides, the excision of a UV photoproduct was also inhibited when present in linker DNA between reconstituted dinucleosomes (Ura et al., 2001).

In addition, the yeast system was used to study NER in chromatin *in vivo*. In general, these analyses revealed that DNA sequences occupied by nucleosomes are repaired slowly. Moreover, these analyses showed that repair is only modulated by chromatin in the non transcribed strand (NTS) of actively transcribed genes, whereas repair of the TS occurs always fast and uniform (Wellinger and Thoma, 1997; Tijsterman et al., 1999; Ferreiro et al., 2004). Another study, analysing CPD removal in an *URA3* gene inserted 2kb from the telomere, revealed that NER is inhibited at the promoter and coding sequence when the gene is fully silenced (Livingstone-Zatchej et al., 2003).

Considering the size of the NER machinery it was hypothesised that nucleosome rearrangements have to occur during repair to provide access to the DNA lesion. Besides histone modifications and chromatin remodelling could also play important roles

to restore the original chromatin state after repair. Indeed, there is evidence that covalent modifications of histones take place during NER (Teng et al., 2005; Yu et al., 2005) and that chromatin remodelling promotes NER (Yu and Waters, 2005; Zhang et al., 2009; Palomera-Sanchez and Zurita, 2011). In addition, the chromatin assembly factor CAF-1, which is implicated in replication-dependent chromatin assembly (Smith and Stillman, 1989), appears to assist in restoring the original structure of chromatin after DNA repair (Mello and Almouzni, 2001). Although, evidence exists that chromatin modification facilitates DNA repair, it is still unclear to what extent this process is needed for efficient NER in nucleosomes or if the intrinsic mobility of nucleosomes is sufficient to enable DNA repair (Thoma, 2005; Bucceri et al., 2006).

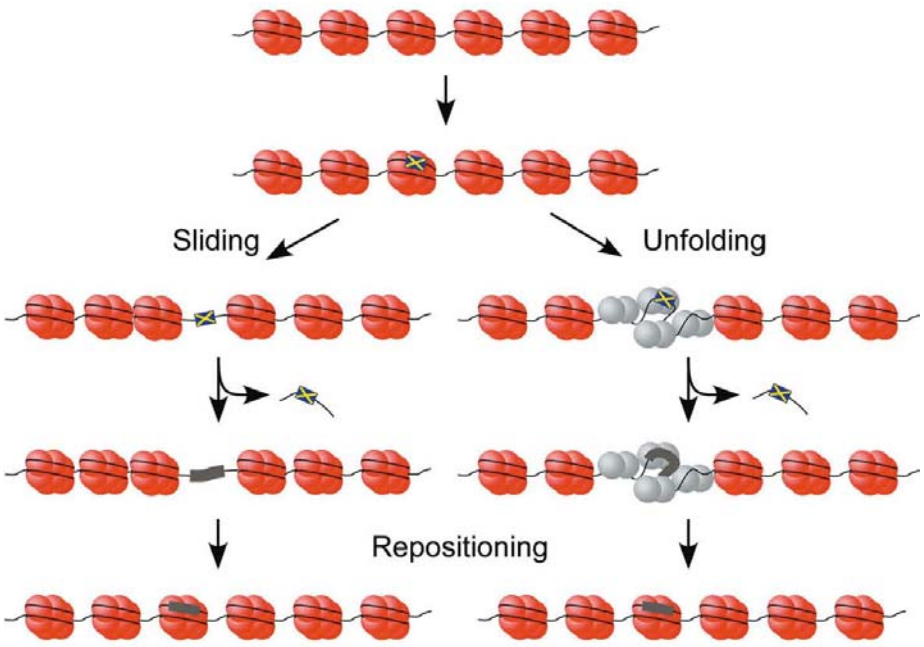

Figure 2-3. Possible models of NER in nucleosomal templates
A UV photoproduct (indicated as yellow cross) is introduced in DNA wrapped around a nucleosome (depicted as orange bubbles). Recognition of the DNA lesion is followed by nucleosome rearrangement (sliding or unfolding). This provides access of NER enzymes to the lesion. Repair DNA synthesis and ligation occur prior to repositioning of the nucleosome on the newly synthesised patch (grey region). (from Tremblay et al., 2009)

2.2 The ribosomal gene locus of *Saccharomyces cerevisiae*

Cells have evolved various mechanisms to satisfy the high demand for ribosomal RNAs. Thus, ribosomal DNA (rDNA) loci are arranged in multigene clusters in all eukaryotes. Due to its repetitive structure and the unique assembly of diverse genetic elements, the rDNA locus represents an ideal model system to study chromatin dynamics during processes such as transcription by all three RNA polymerases, replication, and recombination. As outlined below the rDNA locus has also served to investigate chromatin dynamics during DNA repair.

In proliferating yeast cells, ribosomal RNA (rRNA) genes are highly transcribed and, more than 60% of total transcription is due to RNA polymerase I (Pol I) activity (Warner, 1999). In fact, the only essential function of Pol I is the transcription of the 35S rRNA genes, yielding an rRNA precursor, which is further processed into the mature 25S, 18S and 5.8S rRNAs (Nogi et al., 1991). Moreover, ribosome synthesis is dependent on the activities of Pol II transcribing the genes encoding ribosomal proteins and Pol III, which is required for transcription of the 5S rRNA. In addition to structural components of the ribosome, more than 150 trans-acting ribosome biogenesis factors and about 100 small nucleolar RNAs (snoRNAs) participate in the complex maturation pathway of ribosomes (Kressler et al., 1999; Venema and Tollervey, 1999; Fatica and Tollervey, 2002; Tschochner and Hurt, 2003).

2.2.1 Cellular localisation and structure of the yeast rRNA gene locus

2.2.1.1 The nucleolus

In all eukaryotes, the rRNA genes are located within the most prominent nuclear substructure, the nucleolus. Ultrastructural analyses revealed that the nucleolus can be subdivided into three morphologically different compartments: fibrillar centers (FCs); dense fibrillar components (DFCs) and granular components (GCs) (Raska, 2003; Koberna et al., 2002) (Fig. 2-4). Protein and DNA localisation studies and the analysis of aberrant morphologies in conditional yeast mutants allowed assigning temporally different events of ribosome biogenesis to distinct nucleolar substructures (Oakes et al., 1998; Léger-Silvestre et al., 1999; Trumtel et al., 2000). These studies revealed that ribosomal DNA (rDNA) is localised to the FC, whereas Pol I is concentrated at the

boundary between the FC and the surrounding DFC, suggesting that this is also the site of rRNA gene transcription. This led to the model that nascent pre-rRNA spreads into the DFC, where first processing steps occur. Finally further maturation steps and assembly of ribosomal subunits occurs in the GC (Scheer and Hock, 1999).

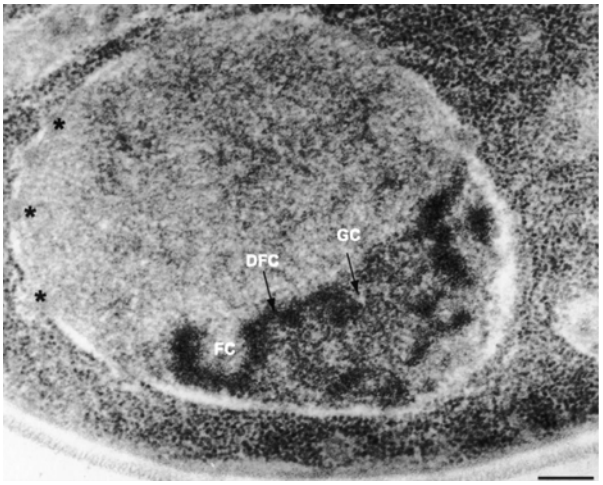

Figure 2-4. Nucleolar morphology of *Saccharomyces cerevisiae*
The electron micrograph depicts the morphology of a yeast nucleus after cryofixation and freeze-substitution. The nucleus is seen to be outlined by a double envelope with pores (asterisks). In the nucleolus, three distinct morphological compartments are identified: the fibrillar centres (FC) are detected near the nuclear envelope, surrounded by a dense fibrillar component (DFC) that extends as a network throughout the nucleolar volume. A granular component (GC) is dispersed throughout the rest of the nucleolus. Bar represents 200nm. (from Léger-Silvestre et al., 1999)

2.2.1.2 Structure of the yeast rDNA locus

In budding yeast 150–200 rDNA copies are tandemly arranged (head to tail) on the right arm of chromosome XII (Petes, 1979; Long and Dawid, 1980), representing about 10% of the entire yeast genome. Although the repetitive structure makes the rDNA locus prone to deletional recombination events an elaborate amplification system evolved to maintain a stable copy number in wild type cells (Kobayashi, 2006). Each rDNA repeat is 9.1kb in size and encodes the 35S rRNA gene transcribed by Pol I and the 5S rRNA gene transcribed by Pol III (Philippsen et al., 1978) (Fig. 2-5). The combination of these two different transcription units in one rDNA cluster in yeast is rather uncommon and in most species 5S rRNA genes are detached from the ribosomal RNA genes (Haeusler and Engelke, 2006).

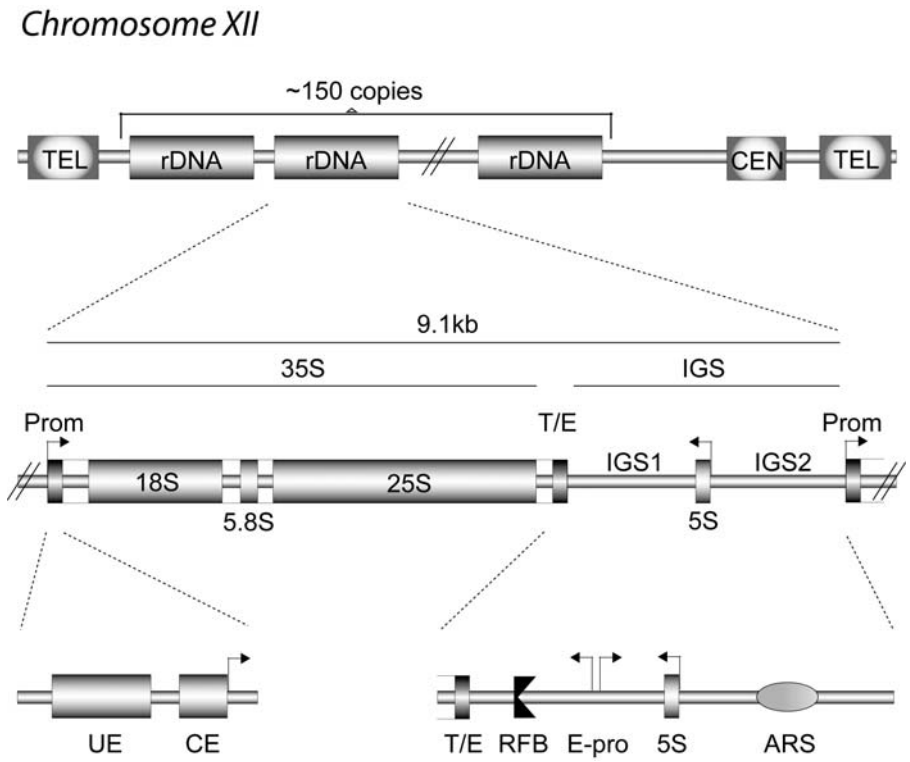

Figure 2-5. Schematic representation of the rRNA gene locus of *S. cerevisiae*
The position of the rDNA repeat cluster on chromosome XII with respect to the centromere (CEN) and telomeres (T) is shown. Each 9.1kb large rDNA repeat consists of the Pol I-transcribed 35S rRNA gene (precursor for the 18S, 5.8S and 25S rRNAs), the RNA Pol III-transcribed 5S rRNA gene and two intergenic spacer regions IGS1 and IGS2. Arrows mark transcription start sites and direction. The positions of several DNA elements are indicated. The upstream element (UE) and core element (CE) constitute the Pol I promoter (P). Termination occurs at the terminator (T) which is located within a region called the enhancer (E). The autonomous replication sequence (ARS), the bidirectional Pol II promoter E-Pro and the replication fork barrier (RFB) are depicted. (modified from Goetze et al., 2010)

The 35S rRNA is transcribed as a polycistronic precursor which is processed into the mature 18S, 5.8S, and 25S rRNAs. Different elements important for the regulation of rDNA transcription have been identified within the 35S rRNA genes (Kulkens et al., 1992; Musters et al., 1989). The bipartite upstream element (UE) and the core element (CE) are located at the 5' end of the 35S rDNA within the intergenic spacer region 2 (IGS2). These elements span about 170bp and constitute the 35S rDNA promoter. In addition, an element located at the 3' end of the 35S transcription unit has been identified and termed the enhancer. The enhancer element was shown to exhibit a stimulatory effect on RNA synthesis by Pol I in *in vitro* and *in vivo* experiments from Pol I reporter templates (Elion and Warner, 1986, 1984). Nevertheless, in later experiments it was demonstrated that a deletion of the enhancer does not impair rRNA production and hence, this DNA element is dispensable for 35S rRNA gene transcription *in vivo* (Wai et al., 2001). This result was rather surprising as the enhancer region contains two Pol I transcription

termination sites. Approximately 90% of all transcripts terminate at a T1 site located 93 nucleotides downstream of the 3' end of mature 25S rRNA. The remaining transcripts terminate at a T2 failsafe termination site composed of a thymine-rich DNA stretch located 250 nucleotides downstream of the 3' end of the mature 25S rRNA (Reeder et al., 1999). Apparently, efficient transcription termination at the proposed sites is not required for processing of rRNA to form functional ribosomes, because deletion of these terminator elements does not affect cell growth (Wai et al., 2001).

Several other *cis*-elements were identified in the IGS region and have been studied extensively. Each IGS2 harbours an autonomous replication sequence serving as origin of replication (Linskens and Huberman, 1988). Although replication starts bidirectional, the replication fork migrating in the direction of the 5S rRNA gene is stalled at the replication fork barrier (RFB) to prevent a collision between the replication and the Pol I transcription machinery (Brewer and Fangman, 1988; Brewer et al., 1992; Kobayashi et al., 1992). The protein Fob1 (fork blocking protein) which binds to the RFB site located in IGS1 is implicated in the inhibition of replication fork progression (Kobayashi and Horiuchi, 1996). In addition Fob1 is required for the expansion and contraction of rDNA copy number as part of an amplification system which is based on recombination between sister chromatids (Kobayashi et al., 1998). These recombination events are triggered by double strand breaks introduced into the rDNA by Fob1-dependent pausing of the DNA replication machinery at RFB sites (Kobayashi et al., 1998, 2004; Burkhalter and Sogo, 2004). In addition to the RFB, an adjacent region termed EXP was shown to be required for repeat expansion (Kobayashi et al., 2001). This region harbours a bi-directional Pol II promoter (E-pro) (Kobayashi and Ganley, 2005). Transcription at E-pro produces non-coding RNAs and promotes the dissociation of cohesin from neighbouring DNA regions. Cohesin association is suggested to stabilise the position of sister chromatids, suppressing sister chromatid-based changes in rDNA copy number (Kobayashi et al., 2004). Thus, transcription of E-pro regulates recombination by cohesin dissociation. Interestingly, Kobayashi and co-workers demonstrated that transcription from E-pro is regulated by the sirtuin Sir2 (silent information regulator 2; Kobayashi and Ganley, 2005). Sir2 is a protein with NAD^+ dependent histone deacetylase activity (Imai et al., 2000; Landry et al., 2000; Smith et al., 2000) that is reported to be required for transcriptional silencing of Pol II transcription at the silent mating type loci, the telomere regions and the rDNA locus (Gottschling et al., 1990; Imai et al., 2000; Bryk et al., 1997; Smith and Boeke, 1997).

2.2.2 Chromatin structure at the yeast rDNA locus

2.2.2.1 Chromatin structure at the 35S rRNA gene

The chromatin structure at actively transcribed rRNA genes has been a matter of debate since many years. Several biochemical studies indicated that transcriptionally active rRNA genes are partially or perhaps transiently associated with histone aggregates in the form of nucleosomes (Matsui and Busch, 1977; Higashinakagawa et al., 1977; Weintraub and Groudine, 1976; Reeves and Jones, 1976; Reeves, 1977, 1976; Piper et al., 1976; Mathis and Gorovsky, 1976; Gottesfeld et al., 1976). All these analyses were in accordance with the idea that the presence of nucleosomes at a DNA template does not necessarily exclude its transcription.

In contrast, evidence for a non-nucleosomal chromatin state of actively transcribed rRNA genes was gained by electron microscopy of Miller chromatin spreads (Miller and Beatty, 1969). When spread chromatin is visualised, actively transcribed rRNA-coding regions have a characteristic tree-like appearance, with a DNA "trunk" from which closely-packed ribonucleoprotein "branches" of increasing length extend (Mougey et al., 1993) (Fig. 2-6). Analyses of these so called “Miller trees” of various organisms revealed that transcriptionally active rRNA genes show an extended, non-nucleosomal conformation (Franke et al., 1976; Laird et al., 1976; Foe et al., 1976). Further studies using biochemical approaches suggested that nontranscribed regions are packed with nucleosomes, protected from nuclease digestion, whereas actively transcribed ribosomal genes are mostly depleted of nucleosomes (Ness et al., 1983; Davis et al., 1983). These results led to the hypothesis that in general the ribosomal RNA genes co-exist in two different chromatin states; one nucleosome depleted and transcribed by Pol I and the other nucleosomal and not transcribed. This hypothesis was supported by evidence from various eukaryotic systems (Scheer et al., 1984; Muscarella et al., 1987; Haaf et al., 1991). For example, MNase digestions of nuclei isolated from mouse culture cells showed a nucleosomal digestion pattern that was superimposed on a smear of fragments of heterogeneous sizes (Conconi, 1987).

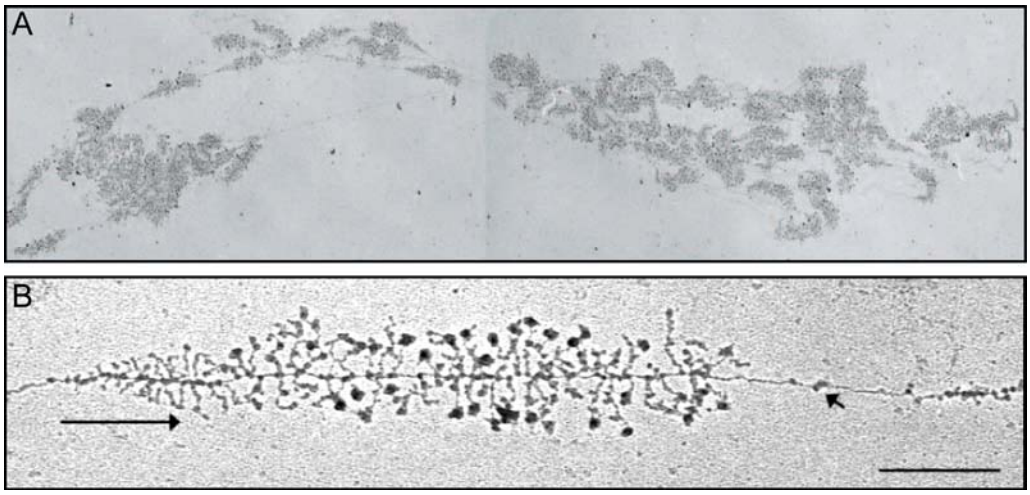

Figure 2-6 Single molecule analysis of rDNA by electron microscopy of Miller chromatin spreads

(A) Electron micrograph of spread yeast chromatin showing the entire rDNA. About 120 rDNA units are visible (from French et al., 2008). (B) Representative electron micrograph of one rDNA repeat after chromatin spreading. The long arrow indicates direction of Pol I transcription of the 35S rRNA gene. The short arrow indicates the structure frequently seen at the position of the 5S rRNA gene. Bar represents 400nm (from French et al., 2003).

Clear evidence for the existence of two different rDNA chromatin states *in vivo* resulted from photo-crosslinking experiments with psoralen (Conconi et al., 1989; Toussaint et al., 2005). Psoralen (4,5`,8-trimethylpsoralen, Fig. 2-7) is a three ringed furocoumarin found in many plants, serving as a defence against insects and fungi. The drug intercalates into double stranded nucleic acids and establishes covalent crosslinks between the two DNA strands upon irradiation with long-range UV light. Importantly, the integration of psoralen in double stranded DNA does not perturb the general structure of chromatin (Conconi et al., 1984; Gale and Smerdon, 1988). As a consequence, psoralen and its derivatives have been widely used to study the structure of DNA and chromatin (Parsons, 1980; Sinden et al., 1999). Besides, several studies demonstrated that incorporation of psoralen occurs preferentially in nucleosome free regions like promoters, origins of replication, enhancers and rDNA coding regions (Paule, 1999) or in linker DNA between nucleosomes (Hanson et al., 1976; Cech and Pardue, 1977). Consequently, nucleosomal and non nucleosomal DNA differ in their degree of psoralen incorporation The difference in psoralen accessibility provides also the molecular basis for distinguishing the two rDNA chromatin states by the psoralen crosslinking technique.

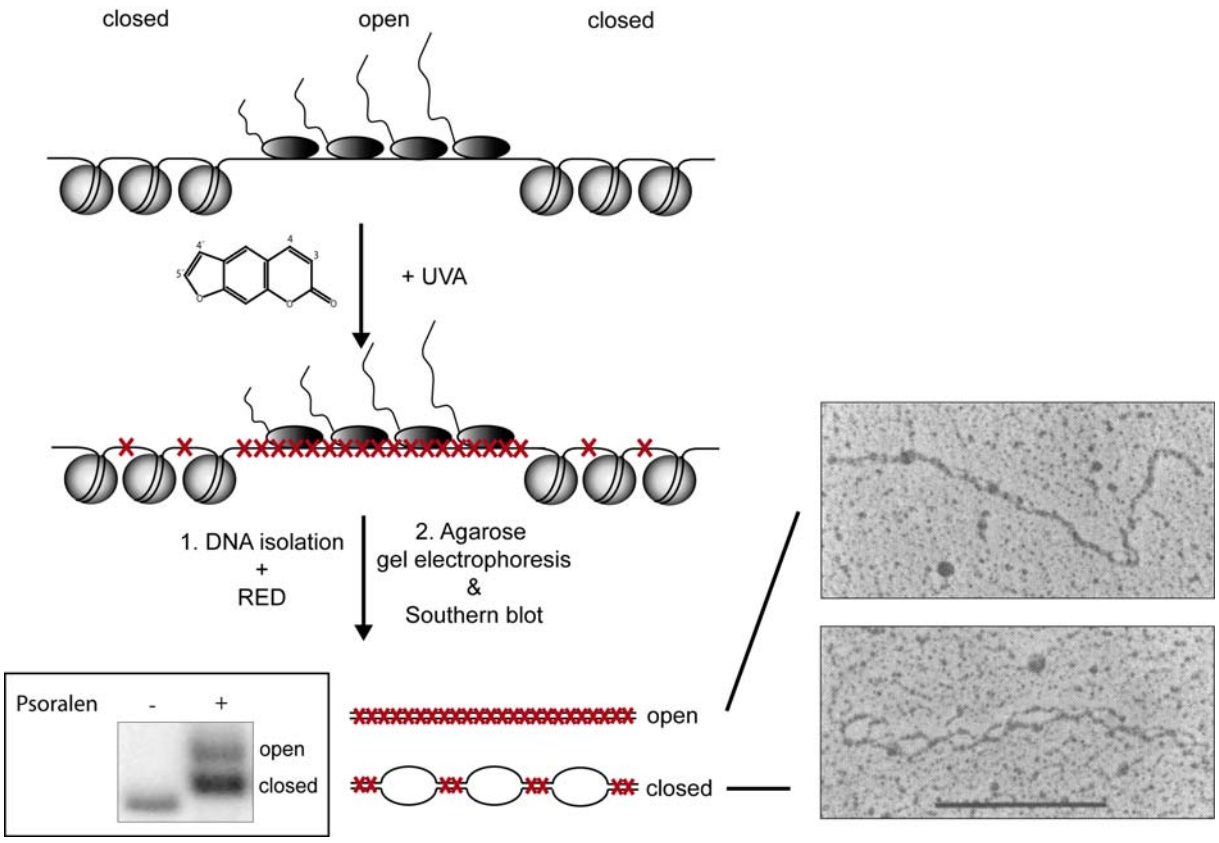

Figure 2-7. Schematic representation of a psoralen crosslinking analysis of 35S rRNA genes
Isolated nuclei are irradiated with long-range UV light in the presence of psoralen. Incorporation of psoralen preferentially occurs at DNA sequences devoid of nucleosomes. UVA irradiation induces the formation of covalent psoralen crosslinks between the DNA double strands. DNA is isolated and digested with a restriction enzyme (RED). (bottom left) After separation in a native agarose gel, DNA fragments are subjected to Southern blot analysis. After blotting, the membrane is hybridised with a probe detecting a fragment of the 35S rRNA genes. DNA fragments migrate according to the amount of incorporated psoralen molecules. The slow migrating band represents formerly nucleosome depleted (open) rRNA genes; the fast migrating band represents formerly nucleosomal (closed) rRNA genes. (right panel) Alternatively, the DNA can be purified after electrophoresis and analysed under denaturing conditions by electron microscopy. DNA from the closed chromatin state appears as rows of single-stranded bubbles. DNA from the open chromatin state shows a higher extent of psoralen crosslinking and appears with a rod like structure (from Dammann et al., 1993).

After DNA isolation and digestion with a restriction enzyme, psoralen crosslinked DNA is analysed by Southern blot after native agarose gel electrophoresis (Fig. 2-7). The migration of psoralen crosslinked DNA in agarose gel electrophoresis is dependent on the amount of psoralen incorporated into the double strand (Conconi et al., 1989; Sogo et al., 1984). In the absence of nucleosomes (termed “open” chromatin structure), DNA is accessible for psoralen and thus heavily crosslinked. As a result, DNA migrates slower in agarose gel electrophoresis because it is less flexible and has a higher molecular weight. Nucleosomal DNA (termed “closed” chromatin structure) allows only little psoralen

incorporation and migrates faster but still slower than DNA that has not been treated with psoralen. After psoralen crosslinking analysis, both bands representing the open and closed chromatin state can be observed when fragments of the Pol I transcribed 35S rRNA gene are investigated (Conconi et al., 1989) (see Fig. 2-7).

In addition, DNA was purified from an agarose gel after psoralen crosslinking and visualised by electron microscopy under denaturing conditions (Fig. 2-7, right). DNA-fragments derived from the band representing the closed chromatin structure showed single stranded bubbles of about 150bp size, presumably corresponding to nucleosomal DNA. In contrast, DNA derived from the band representing the open chromatin state appeared as a rod-like structure of heavily psoralen crosslinked DNA double strands (Dammann et al., 1993). Finally, nascent rRNA was found to be a component of the band representing the open chromatin state derived from mouse, *Xenopus* and yeast cells, indicating that only this chromatin state serves as the template for Pol I transcription (Conconi et al., 1989; Lucchini and Sogo, 1992).

Despite the above mentioned analyses the discussion about the nucleosomal nature of actively transcribed rDNA repeats is still ongoing (Birch and Zomerdijk, 2008; McStay and Grummt, 2008; Németh and Längst, 2008). A recent study using chromatin immunoprecipitation (ChIP) suggested that the 35S rRNA genes exist in a dynamic chromatin structure of unphased nucleosomes (Jones et al., 2007). However, by combining a technique called Chromatin Endogenous Cleavage (ChEC) with psoralen crosslinking analysis (termed ChEC/psoralen analysis), our laboratory provided further evidence that open rRNA genes are largely devoid of histone molecules but instead are associated with Hmo1 (Merz et al., 2008).

Hmo1 is a high mobility group (HMG) protein that was initially identified as a protein in yeast with a putative role in the maintenance of genome integrity, as *hmo1Δ* cells exhibited an enhanced plasmid loss rate and nuclease-sensitive chromatin (Lu et al., 1996). The discoveries that *HMO1* deletion is lethal in the absence of the Pol I subunit Rpa49 and that over-expression of Hmo1 suppresses the lethality of an *rpa49Δ* deletion at 25°C (Gadal et al., 2002), finally linked Hmo1 to the Pol I transcription machinery. Chromatin immunoprecipitation (ChIP) experiments showed that Hmo1 associates with the entire 35S rRNA gene sequence and that Hmo1 is enriched at the promoter and terminator regions (Hall et al., 2006; Kasahara et al., 2007; Berger et al., 2007). Importantly, one of these studies revealed that binding of Hmo1 to rRNA genes is dependent on Pol I transcription, as no association could be detected in a Pol I mutant strain, where Pol II transcribes rRNA from a helper plasmid (Kasahara et al., 2007).

Until recently, it has been unclear why eukaryotic cells maintain a fraction of their rRNA genes in the transcriptionally inactive, closed chromatin state. An analysis by Kobayashi and coworkers revealed that yeast strains carrying a reduced copy number of rRNA genes that are all actively transcribed become sensitive to DNA damage induced by mutagens (Ide et al., 2010). Thus, the fraction of nontranscribed rRNA genes appears to be important for the integrity of the ribosomal DNA locus.

Since it has been shown that the two different chromatin states stably co-exist throughout the cell cycle (Conconi et al., 1989), the mechanisms by which both chromatin states are maintained are object of current research. For metazoan cells, it has been suggested that covalent histone modifications or DNA methylation patterns contribute to the propagation of active rRNA genes (McStay and Grummt, 2008). In yeast, however, individual rRNA genes may change their transcriptional state stochastically such that, each new generation, the set of rRNA genes may be different from the set that was active the previous generation (Dammann et al., 1995). Accordingly, in experiments showing that the passage of the replication fork leads to nucleosome assembly at rRNA genes on both daughter strands, no strict correlation between the chromatin state of individual rRNA genes before and after replication could be observed (Lucchini and Sogo, 1995). More recent data based on transcript counting in single yeast cells and mathematical modelling indicated that the set of transcriptionally active rRNA genes changes independent of replication (Tan and van Oudenaarden, 2010). Nonetheless, the average ratio between the two chromatin states at yeast rRNA genes is faithfully transmitted to daughter cells during growth in exponential phase.

2.2.2.2 Chromatin structure at the intergenic spacer

Several studies demonstrated that the intergenic spacers flanking ribosomal genes are covered with nucleosomes (Ness et al., 1983; Sogo et al., 1984; Lucchini et al., 1987; Dammann et al., 1993). Accordingly, psoralen retardation analysis of a 2.4kb *Eco*RI fragment, containing the entire rDNA spacer region did not reveal the typical pattern of open and closed chromatin, usually observed for fragments derived from the 35S rRNA coding sequence (Dammann et al., 1993). Furthermore, ChEC analysis indicated that the IGS has a histone density similar to Pol II transcribed loci (Merz et al., 2008). Studies on rDNA chromatin using MNase digestion showed that five nucleosomes are well positioned in the IGS2 (Vogelauer et al., 1998). In contrast, positions of nucleosomal particles do not seem to be as strictly defined in the IGS1 (Vogelauer et al., 1998).

The combination of psoralen retardation assays and EM analyses enabled the analysis of rDNA spacer regions flanked either by actively transcribed or by transcriptionally inactive 35S rRNA genes. These analyses revealed, that the rDNA spacers between transcriptionally inactive 35S rRNA genes showed a regular size distribution of single stranded DNA bubbles as it is obtained for the bulk genomic DNA. Instead, the bubbles found within spacer regions surrounded by actively transcribed rRNA genes showed a size distribution intermediate to that expected for mono- and di-nucleosomes (Dammann et al., 1993). Besides, a structural link between the transcriptional state of rRNA genes and the neighbouring enhancer element was observed (Dammann et al., 1995). Open 35S rRNA genes were found to be flanked by non nucleosomal enhancer sequences, whereas closed genes showed enhancers at their 3' end with a regular nucleosomal pattern. The non-nucleosomal enhancer structure downstream of active genes was suggested to correlate with a function in replication termination (Dammann et al., 1995). Indeed, later studies revealed that initiation of replication starts at those rARS sequences placed immediately downstream of transcribing rRNA genes (Muller et al., 2000).
In contrast to the 35S rRNA genes, little is known about the chromatin structure of the yeast 5S rRNA gene. High-resolution *in vitro* and *in vivo* mapping of MNase digested yeast chromatin indicated the 5S rDNA region is completely covered by nucleosomes occupying alternative positions (Buttinelli et al., 1993). The influence of yeast 5S rRNA gene transcription by Pol III on its chromatin state, however, still remains to be determined. Nevertheless, a study using Miller chromatin spreading showed that the activity of 5S rRNA genes is largely independent of the activity of the neighbouring 35S rRNA genes and *vice versa* (French et al., 2008).

2.2.3 rRNA gene chromatin dynamics and RNA polymerase I transcription

Initiation of yeast Pol I transcription is dependent on four different transcription factors: the TATA binding protein (TBP), Rrn3, upstream activating factor (UAF) and core factor (CF). The CF contains three subunits, Rrn6, Rrn7 and Rrn11 and binds to the core element (CE) next to the transcriptional start site (Lalo et al., 1996; Lin et al., 1996; Keys et al., 1996). UAF comprises six subunits, Rrn5, Rrn9, Rrn10, Uaf30 and histones H3 and H4 (Keys et al., 1996; Keener et al., 1997; Siddiqi et al., 2001). UAF binds to an element situated upstream of the start site called the upstream element (UE) or upstream control element (Keys et al., 1996). TBP bridges UAF and CF by binding to Rrn9 and Rrn6 and is required for the UAF-dependent recruitment of CF to the promoter (Steffan

et al., 1996). Finally, Rrn3 associates with Pol I to form an initiation-competent Pol I complex (Yamamoto et al., 1996). Interestingly, psoralen crosslinking experiments using deletion mutants of several Pol I initiation factors or Pol I subunits indicate that Pol I transcription is indispensable for the establishment of the open chromatin state at the 35S rRNA genes (Hontz et al., 2008; Merz, 2008; Götze, 2010).

Two potential ways of Pol I transcriptional regulation have been previously suggested. On the one hand the number of genes used for Pol I transcription can be adapted according to the cellular demand for rRNAs. On the other hand rRNA production can be controlled by modulation of transcription initiation frequency and/or elongation from each open 35S rRNA gene. (Reeder, 1989; Schultz et al., 1992; Aprikian et al., 2001; French et al., 2003)

Surprisingly, yeast cells harbouring an rDNA locus with an artificially decreased copy number of ~42 or even ~25 do not exhibit a severe growth phenotype (French et al., 2003; Cioci et al., 2003). It was shown that in these strains almost all genes are transcribed by Pol I and that the reduced number of genes is compensated by an increase in polymerase loading (French et al., 2003). This led to the conclusion that rRNA production is rather controlled on the level of polymerase loading than by increasing the number of transcribed 35S rRNA genes. This hypothesis was corroborated by the observation that the number of actively transcribed rRNA genes changes only slightly when cells enter stationary phase, although rRNA transcription is reduced drastically (Fahy et al., 2005). Besides, in cells harbouring a deletion of the gene coding for the histone deacetylase Rpd3, 35S rRNA transcription is down-regulated in stationary phase but the number of transcribed rRNA genes is similar to the number of transcribed rRNA genes in exponential phase (Sandmeier et al., 2002). Interestingly, electron microscopy of Miller chromatin spreads revealed that the number of RNA polymerases transcribing each open gene in the *rpd3Δ* mutant was significantly reduced when cells grew past log phase (Sandmeier et al., 2002).

Biochemical studies revealed that down-regulation of rRNA transcription during stationary phase correlates with a reduction of the initiation-competent Pol I-Rrn3 complex (Milkereit and Tschochner, 1998). Treatment of yeast cells with rapamycin, a drug that inhibits the TOR (Target Of Rapamycin) pathway, mimics starvation. This leads to a state resembling stationary phase (Heitman et al., 1991; Barbet et al., 1996) and thus to a strong reduction of Pol I transcription (Zaragoza et al., 1998; Powers and Walter, 1999). Indeed, it was found that the decrease in the transcription rate of individual open genes, observed after rapamycin treatment and when cells enter

stationary phase is achieved by down-regulation of the Rrn3-dependent polymerase recruitment step (Claypool et al., 2004). Again, electron microscopy of Miller chromatin spreads showed that the number of genes being actively transcribed by Pol I remains unchanged under these conditions (Claypool et al., 2004).

2.2.4 rRNA gene chromatin dynamics and DNA repair

The first study describing DNA repair at rDNA was performed with UV-irradiated human diploid fibroblasts (Cohn and Lieberman, 1984). In a later study it was observed that CPD removal from ribosomal genes occurs much less efficient compared to the *DHFR* gene in hamster cells (Stevnsner et al., 1993). A study investigating NER at human rRNA genes corroborated these results by showing that little (or no) repair of UV photodimers occurs in either strand of human rDNA (Fritz et al., 1996). The results from Stevnsner et al. indicated that TCR does not occur at rRNA genes as the repair rate observed was similar to the rate determined for the whole genome (Bohr et al., 1985). Further analyses directly looking for TCR in CHO and human cells concluded that DNA lesions are removed from rRNA genes exclusively by GGR (Christians and Hanawalt, 1993, 1994). Moreover, a combination of immunoflourescent labelling and light microscopy explained the inefficient repair of photoproducts in the rDNA by the underrepresentation of NER proteins in the nucleoli (Balajee et al., 1999). However, in disagreement with this observation, it was shown that a fraction of cellular TFIIH resides within the nucleolus, at sites where rDNA is actively transcribed (Iben et al., 2002). The studies mentioned above neglected the fact that rRNA genes co-exist in two different chromatin states. Nevertheless, a study addressing this specific point by selectively releasing the active rDNA fraction from nuclei by restriction enzyme digest revealed that TCR is absent at the open rRNA genes (Fritz and Smerdon, 1995). However, repair at rRNA genes was almost non-existent in the mouse cell line investigated.

In growing yeast cells CPDs are efficiently removed by NER from the rDNA locus (Verhage et al., 1996; Conconi et al., 2000). In contrast to its homolog CSB in human cells, strand-specific repair of yeast rDNA is independent of Rad26 (Christians and Hanawalt, 1994; Verhage et al., 1996). Finally, the existence of TCR in Pol I-transcribed genes was directly demonstrated in wild type strains (Meier et al., 2002; Conconi et al., 2002). These studies released open rRNA genes by restriction enzyme digestion of nuclei and analysed removal of CPDs in both rDNA populations. The results clearly demonstrated that TCR occurs in nucleosome depleted 35S rRNA genes but not in the

nucleosomal fraction of rRNA genes. Interestingly, the NTS of open rRNA genes is repaired faster than either strand of closed rRNA genes. Since the NTS of active genes and both strands of inactive genes are repaired by GGR, these data suggest that open, non-nucleosomal rRNA genes are more accessible to GGR enzymes than nucleosomal, closed rRNA genes (Conconi, 2005; Tremblay et al., 2009). Furthermore, the Rad4 homolog Rad34 was found to participate in TCR of Pol I (den Dulk et al., 2005; Tremblay et al., 2008)

Interestingly, psoralen crosslinking analyses revealed further a transition of open to closed rRNA genes within minutes after UV irradiation (Conconi et al., 2005). In addition, chromatin reorganisation correlated with a strong reduction of Pol I transcription and occurred even in the absence of functional NER (Conconi et al., 2005), suggesting that UV-induced DNA lesions inhibit 35S rRNA transcription and induce the formation of the closed chromatin state. Moreover, the resumption of Pol I transcription during NER-dependent removal of CPDs correlated well with the reappearance of open rRNA genes. Nevertheless, it is still unclear whether solely the displacement of Pol I stalled at CPDs triggers the establishment of closed rRNA gene chromatin. It could also be that DNA lesions are preferentially packaged into nucleosomes and that this initial nucleosome deposition in turn leads to further nucleosome assembly at open rRNA genes. Indications for such a phenomenon were observed when DNA repair was reconstituted *in vitro* (Gaillard et al., 1997; Moggs et al., 2000).

2.3 Objectives

Psoralen crosslinking studies in various organisms revealed that rRNA genes adopt two discrete chromatin states reflecting their respective transcriptional activity (reviewed in Toussaint et al., 2005). These analyses led to a model in which psoralen-accessible (open) rRNA genes are actively transcribed and virtually free of nucleosomes, whereas psoralen-inaccessible (closed) rRNA genes are nontranscribed and nucleosomal (Dammann et al., 1993; Stancheva et al., 1997). Besides, it was demonstrated recently that the HMG box protein Hmo1 is part of the open chromatin state, characteristic of transcribed rRNA genes (Merz et al., 2008).

Although it was known that both chromatin states coexist throughout the cell cycle (Conconi et al., 1989) and that the passage of the replication fork leads to nucleosome assembly at rRNA genes on both daughter strands (Lucchini and Sogo, 1995), it was still an open question how these chromatin states are established and maintained in exponentially growing cells. Accordingly, one aim of this study was to investigate the molecular mechanisms leading to the formation of the open and closed 35S rRNA chromatin state in yeast cells. To this end, the dynamics of the rRNA gene chromatin states were investigated during the cell cycle and upon cell-cycle arrest by using the psoralen crosslinking technique. Furthermore, the protein composition of the 35S rRNA genes during prolonged cell-cycle arrest was analysed by Chromatin Endogenous Cleavage (ChEC) in combination with psoralen crosslinking (ChEC/psoralen, Merz et al., 2008) and Chromatin Immunoprecipiation (ChIP). To reveal the role of RNA polymerase I transcription and Hmo1 in the establishment and maintenance of the open rRNA genes, alterations of rRNA chromatin were analysed in conditional or deletion mutants, respectively.

As another example for rDNA chromatin dynamics the molecular basis for the conversion of open 35S rRNA genes to the closed chromatin state after DNA damage caused by UV irradiation of yeast cells has been investigated. To this end, the differential association of histone molecules, Pol I and Hmo1 with distinct rRNA chromatin states was analysed by ChEC/psoralen after DNA damage. To discriminate which of the compositional alterations have been caused by nucleotide excision repair (NER), analyses were performed in wild type yeast strains and NER-deficient mutants.

3 Results

In this work, alterations of the two 35S rRNA chromatin states were investigated during the cell cycle and after exposure of yeast cells to UV light. To this end, psoralen crosslinking, ChEC and ChEC/psoralen analyses have been employed amongst other techniques to monitor changes in the chromatin structure of yeast rRNA genes. To facilitate proper interpretation of Southern blot data the recognition sites of utilised restriction enzymes, the resulting rDNA fragments and the position of probes used to detect those fragments are depicted in Fig. 3-1.

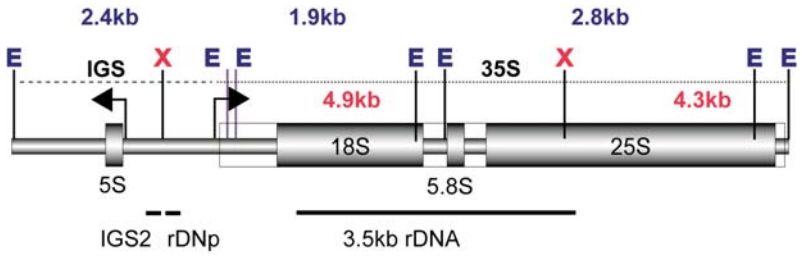

Figure 3-1. Cartoon of the yeast rDNA locus.
Schematic representation of the yeast rDNA locus containing the 35S, 25S, 18S, 5.8S, and 5S, rRNA-coding regions and the intergenic spacer region (IGS). *Eco*RI restriction sites are depicted in blue (E) and sizes of the analysed rDNA fragments emerging after digest are indicated in blue. *Xcm*I restriction sites are depicted in red (X) and sizes of the analysed rDNA fragments emerging after digest are indicated in red. Probes used for Southern blot analyses (IGS2, rDNp, 3.5kb rDNA) are displayed as black bars. Arrows indicate transcription start sites.

3.1 Establishment and maintenance of alternative 35S rRNA gene chromatin states

3.1.1 The ratio of open and closed 35S rRNA gene chromatin states varies during the cell cycle

To analyse if there are changes in 35S rRNA gene chromatin states during the cell cycle, psoralen crosslinking analysis was performed with yeast cells before, during and after release from G1 arrest with alpha factor. Alpha-factor is a peptide consisting of 13 amino acids which binds to a receptor found on *MATa* cells. As a result, treatment with alpha factor leads to inactivation of the G1 cyclin/Cdc28 kinase complex and to arrest in G1-phase (Futcher, 1999). Whenever cells were arrested in G1 with alpha factor, yeast

strains that carry a deletion of the gene *BAR1* were used. Bar1 is a protease that is secreted by *MATa* cells and cleaves and inactivates alpha factor and thereby releases cells from pheromone induced cell cycle arrest (Ciejek and Thorner, 1979; Futcher, 1999). By using *Δbar1* strains the amount of alpha factor needed to induce cell cycle arrest is reduced 100 to 1000 fold and the arrest is persisting longer than in wild type cells (Futcher, 1999).

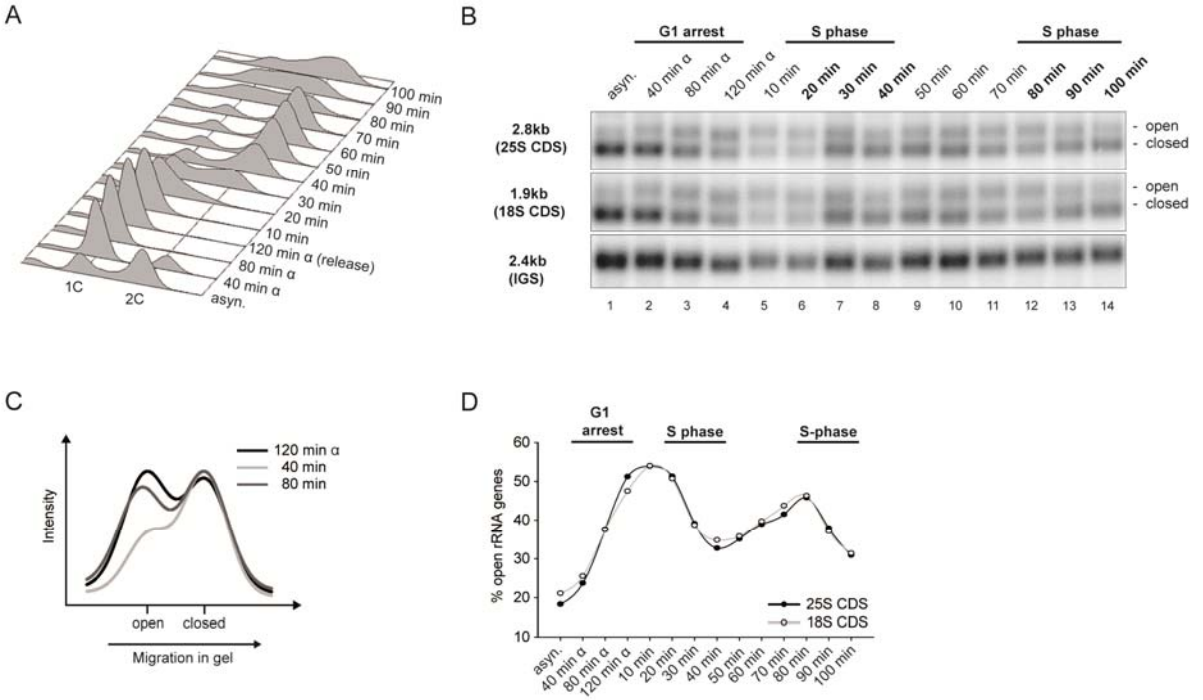

Figure 3-2. The ratio of open and closed rRNA genes varies during the cell cycle.
(A–D) Yeast strain y1757 was arrested in G1 by treatment with alpha factor and then released. Samples were taken from the exponentially growing asynchronous culture (asyn.) at the indicated times of G1 arrest (α) and at 10 min intervals after release. Cell aliquots were either fixed with ethanol for flow cytometry or formaldehyde for psoralen crosslinking analysis. (A) Flow cytometry. The cell number is plotted against the relative DNA content (1C, 2C) measured by Sytox Green incorporation. (B) Psoralen crosslinking analysis. Crude nuclei were prepared and treated with psoralen. DNA was isolated, digested with *Eco*RI and analysed by Southern blot with probes detecting fragments of the 18S and 25S rRNA coding sequence (CDS) and the intergenic spacer fragment (IGS). Fragments originating from open and closed rRNA genes are indicated. (C) Profile analysis of individual Southern blot lanes. Signal intensities of 25S rRNA CDS fragments derived from the samples indicated in the legend of the graph were normalised to peak values and plotted against the migration in the gel. The positions of bands derived from open and closed rRNA genes are indicated. (D) The percentage of open rRNA genes in individual samples taken during the experiment. After profile analysis, the peak areas obtained for open and closed rRNA genes of the 18S and 25S rRNA CDS fragments were determined from graphs as the ones presented in Fig. 3-2C and used to calculate the percentage of open rRNA genes. (modified from Wittner et al., 2011)

Cells for fixation with ethanol (flow cytometry) and formaldehyde (psoralen crosslinking) were taken before, during, and after release from G1. Flow cytometric analysis showed, that cells were progressively synchronised in G1 phase with 1C DNA content in the presence of alpha factor (Fig. 3-2A, samples asyn., 40min, 80min, and 120min α). Additionally, the histograms of flow cytometry indicate that cells entered S phase 20min after the release from alpha factor arrest and that DNA replication was completed after 40min. Almost all cells had a 2C DNA content (G2 and M-phase) between 50min and 70min and DNA replication started again 80min after release from G1 arrest (Fig. 3-2A). It has to be mentioned that after completing the first cell cycle, cells released from G1 arrest were no longer synchronously growing (samples 80-100min).

Southern blot analysis of samples derived from psoralen crosslinking revealed that the open/closed ratio of two different *Eco*RI fragments spanning the region coding for 18S rRNA and for 25S rRNA, respectively, varied during the cell cycle (Fig. 3-2B, upper two rows). In contrast, psoralen accessibility of an *Eco*RI rDNA fragment containing the IGS, migrating as one band, did not change in all samples taken in course of the experiment (Fig. 3-2B, bottom row). Remarkably, the fraction of open 35S rRNA genes decreased whenever cells entered S phase (Fig. 3-2B, upper two rows, samples 20-40min and 80-100min). Variation of the ratio of open and closed 35S rRNA genes in the different samples of this block and release experiment was also analysed by plotting the relative intensity of the radioactive signals against the migration in the gel (Fig. 3-2C, profile analysis; signal intensities were normalised to maxima). To quantitate the observed changes in the open/closed ratio, peak areas obtained for open and closed rRNA genes of the 18S and 25S rRNA CDS fragments were determined from graphs as the ones presented in Fig. 3-2C with PeakFit software (Systat Software Inc.) and used to calculate the percentage of open rRNA genes (Fig. 3-2D). Quantitation revealed that in average, the percentage of open 35S rRNA genes declined from 49% (120min α) to 34% (40min) during S phase. In G2 and M-phase there was again an increase in the percentage of open 35S rRNA genes to 46%. In general a steady increase of the percentage of open genes was always observed outside of S phase and during the G1 arrest (Fig. 3-2B). On the contrary, genes were closing during S phase, being in accordance with earlier reports indicating that all newly replicated 35S rRNA genes are assembled into an array of nucleosomes and become psoralen inaccessible (Lucchini and Sogo, 1995).

To examine replication-dependent nucleosome assembly at the 35S rRNA genes in an independent experiment, chromatin immunoprecipitation (ChIP) experiments were performed with extracts from cells expressing histone H4 with a C-terminal HA-epitope from its endogenous chromosomal location and the corresponding wild-type strain as an

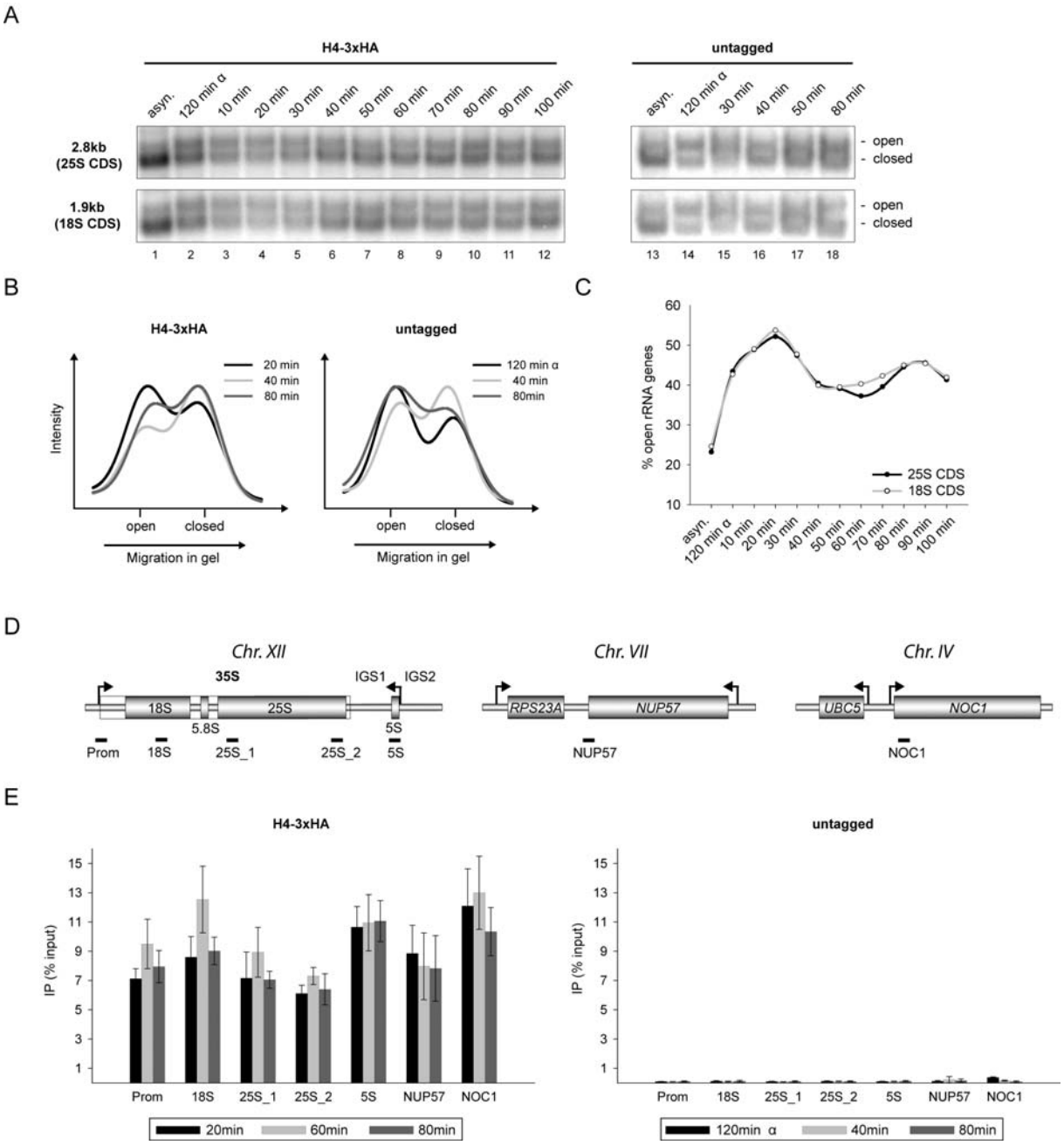

Figure 3-3. Histone occupancy at the rRNA genes increases during S phase

(A-E) Yeast strains y2122, or y1757 expressing histone H4 with a triple HA-tag, or a wild type copy of the gene were arrested in G1 by treatment with alpha factor and then released. Samples were taken from the exponentially growing asynchronous culture (asyn.) at 120min of G1 arrest (α) and at 10min intervals after release, and treated with formaldehyde. For strain y1757 only selected time points according to the experiment presented in Figure 3-2 were analysed. (A-B) Psoralen crosslinking analysis, and profile analysis were performed as described in the legend to Figure 3-2. (C) Determination of the percentage of open rRNA genes was carried out for strain y2122 as described in the legend to Figure 3-2. (D) Cartoons of the yeast rDNA locus on chromosome XII (see legend to Fig. 3-1 for details) and two unrelated genomic loci on chromosomes VII and IV show the position of DNA regions analysed by quantitative PCR (Prom, 18S, 25S_1, 25S_2, 5S, NUP57, NOC1). (E) The same samples as analysed in (B) were subjected to ChIP experiments. The graphs depict the percentage of the input of the respective DNA fragment coprecipitating with histone H4-3xHA-tagged fusion protein or from extracts of the untagged control strain. Error bars indicate standard deviation errors derived from three independent ChIP experiments, each analysed in triplicate qPCRs. (modified from Wittner et al., 2011)

untagged control (Fig. 3-3). First, psoralen crosslinking analysis was performed to verify that tagging of H4 does not influence chromatin structure at the rDNA during the cell cycle (Fig. 3-3A, left). Samples for formaldehyde fixation were taken from the exponentially growing asynchronous culture (asyn.) at 120min of G1 arrest (α) and at 10min intervals after release. For the wild type strain only selected time points according to the experiment presented in Fig. 3-2 were analysed (Fig. 3-3A, right). Samples that showed the largest difference in the percentage of open 35S rRNA genes before, during and after S phase were determined by profile and quantitative analyses (see Fig. 3-3B for individual profile analyses and Fig. 3-3C for graphical representation of the data) and subsequently used for ChIP analysis. Coprecipitation of DNA fragments from the Pol I promoter (Fig. 3-3D, Prom), three different regions within the 35S rRNA gene sequence (Fig. 3-3D, 18S, 25S_1, 25S_2), the 5S rRNA gene (Fig. 3-3D, 5S), and two unrelated genomic loci within an intergenic region close to the 3' end of the *NUP57* gene and within the open reading frame of the *NOC1* gene was analysed. In the untagged strain none of these DNA fragments was significantly enriched in ChIP experiments (Fig. 3-3E, right graph). With tagged histone H4 a slight but reproducible increase in coprecipitation of various DNA fragments including regions of the 35S rRNA-coding sequence was observed during S phase (Fig. 3-3E, left graph). In contrast, the three different reference loci in and outside the rDNA did not show this tendency (Fig. 3-3E, left graph; 5S, NOC1, NUP57). The observed increase in coprecipitation of 35S rRNA gene DNA fragments with histone H4 during S phase (factor of 1.3 in average) is in good correlation with the increase in the percentage of closed 35S rRNA genes observed in the psoralen crosslinking analysis in this condition (factor of 1.28 in average).

Next, it was analysed if the alterations observed in the alpha factor block and release experiment can also be seen when cells are released from an arrest in a different cell cycle stage. First, a yeast culture was arrested in late anaphase by inactivating Cdc15, a protein kinase which is required for the exit from mitosis (Futcher, 1999). Cells expressing the temperature sensitive *cdc15-2* allele (Schwab et al., 1997) were blocked by a temperature shift to 37°C for 3h and then released by lowering the temperature to 24°C. Samples for flow cytometry and psoralen crosslinking were taken from the exponentially growing asynchronous culture at 24°C (asyn.), 90min and 180min during arrest in late anaphase at the restrictive temperature (37°C) and at 15min intervals after release. Histograms of flow cytometry show that a vast majority of cells is arrested with 2C DNA content during the 3h temperature shift to the restrictive temperature (Fig. 3-4A, samples asyn., 90min and 180min α). According to Futcher *cdc15-2* cells do not complete cell separation (especially in W303 genetic background), compromising the

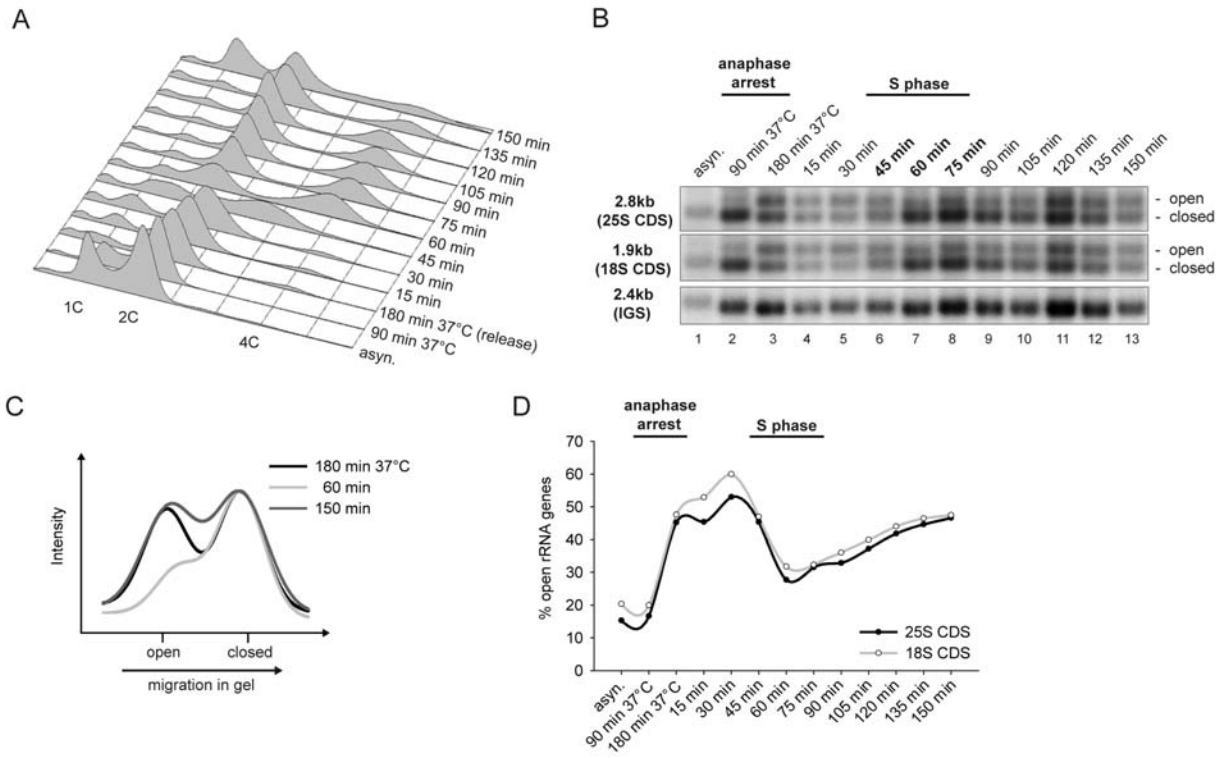

Figure 3-4. Variation of open/closed ratio of rRNA genes analysed after release from an anaphase arrest.

(A-D) Yeast strain y1925 expressing a temperature sensitive *cdc15-2* allele (Schwab et al., 1997) was arrested in late anaphase by temperature shift to 37°C and then released by further incubation at 24°C. Samples were taken from the exponentially growing asynchronous culture at 24°C (asyn.), at the indicated times of late anaphase arrest at the restrictive temperature (37°C) and at 15min intervals after release. Cell aliquots were either fixed with ethanol for flow cytometry or formaldehyde for psoralen crosslinking analysis. Flow cytometry (A), psoralen crosslinking analysis (B), profile analysis (C) and determination of the percentage of open rRNA genes (D) were performed as described in the legend to Figure 3-2. (from Wittner et al., 2011)

assessment of cell cycle progression (Futcher, 1999). Accordingly, in flow cytometry, cells with a DNA content between 2C and 4C can be detected during S-phase in addition to the usual cell population with a DNA content between 1C and 2C (Fig. 3-4A, samples 45min, 60min and 75min). Besides, after completion of DNA replication cells with a DNA content of 2C and 4C are observed (Fig. 3-4A, samples 45min, 60min and 75min). Southern blot analysis of psoralen crosslinked samples again revealed that the open/closed ratio of the two *Eco*RI fragments analysed varied during the experiment (Fig. 3-4B, upper two rows). Similar to the experiment shown in Fig. 3-2B, psoralen accessibility of an *Eco*RI rDNA fragment containing the IGS, did not change in all samples taken in course of the experiment (Fig. 3-2B, bottom row). Profile and quantitative analyses showed that rRNA genes were continuously opening during late anaphase arrest, right after the release and after completion of DNA replication (Figs. 3-4C and 3-4D). On the other hand, closing of rRNA genes was observed exclusively in

the samples collected during S phase, affirming the results obtained in the G1 arrest and release experiment (Fig. 3-2).

In a third approach to investigate 35S rRNA gene chromatin during the cell cycle, cells were arrested at prometaphase by addition of nocodazole. The drug nocodazole inhibits polymerisation of microtubule and by this, interferes with the formation of mitotic spindles (Futcher, 1999). Samples for flow cytometry and psoralen crosslinking were taken from the exponentially growing asynchronous culture (asyn.), 45min and 90min during G2/M arrest by nocodazole (N) and at 10min intervals after release. Analysis of DNA content by flow cytometry proved that the cell population was arrested with 2C DNA content during 90min nocodazole treatment (Fig. 3-5A, samples asyn., 45min and 90min N). Overall it can be observed that the synchrony of cells after release from the metaphase block was poor. Nevertheless, according to the flow cytometric histograms the samples

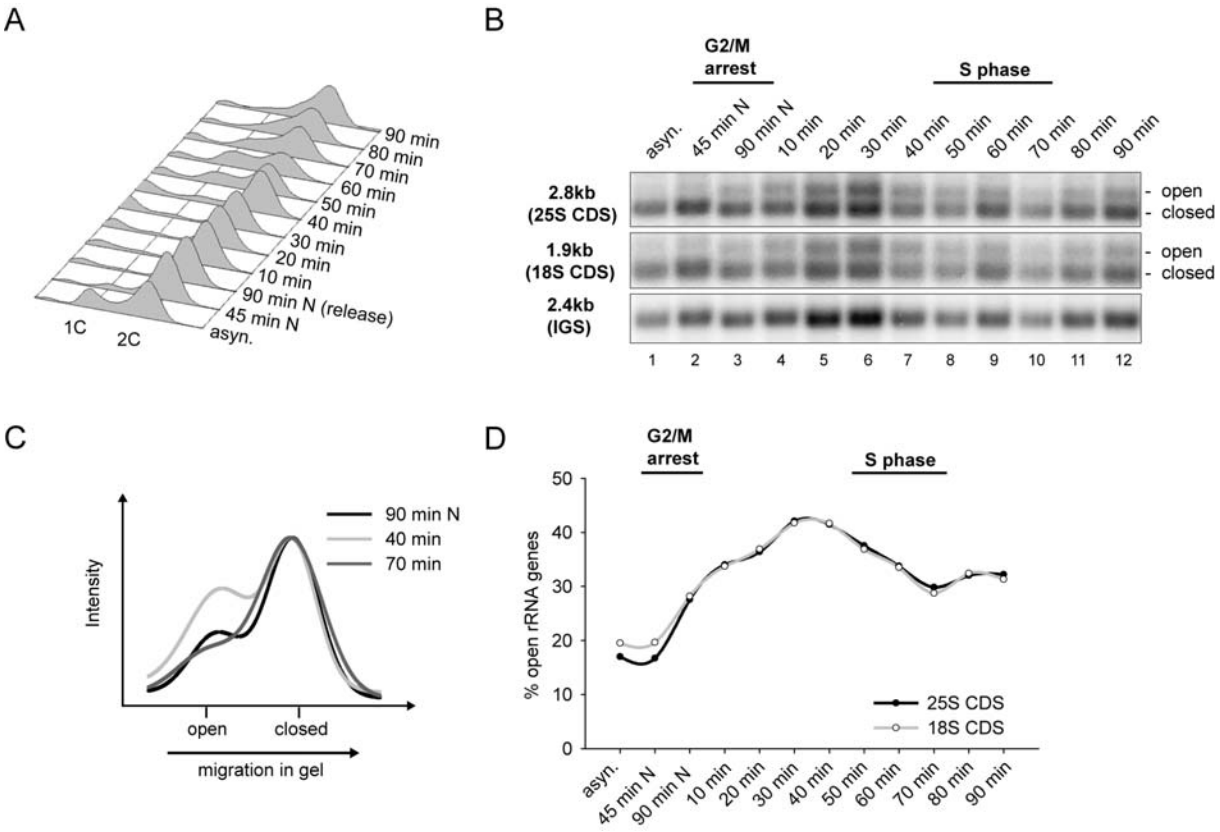

Figure 3-5. Variation of ratio of open and closed rRNA genes analysed after release from a metaphase arrest.

Yeast strain NOY505 (Nogi et al., 1991) was arrested by the addition of nocodazole and then released from the G2/M block by washing the cells and further incubation in YPAD. Samples were taken from the exponentially growing asynchronous culture (asyn.), at the indicated times of G2/M arrest by nocodazole (N) and at 10min intervals after release. Cell aliquots were either fixed with ethanol for flow cytometry or formaldehyde for psoralen crosslinking analysis. Flow cytometry (A), psoralen crosslinking analysis (B), profile analysis (C) and determination of the percentage of open rRNA genes (D) were performed as described in the legend to Figure 3-2. (from Wittner et al., 2011)

containing the largest fraction of cells in S phase were collected 50-70min after release (Fig. 3-5A). Analysis of psoralen crosslinked samples by Southern blot indicates that the open/closed ratio of the two *Eco*RI fragments analysed changed also in this experiment (Fig. 3-5B, upper two rows). Again, psoralen accessibility of an *Eco*RI rDNA fragment containing the IGS, did not change in all samples taken during the experiment (Fig. 3-5B, bottom row). Profile and quantitative analysis showed that rDNA genes were continuously opening during the arrest in metaphase and right after the release, whereas closing of rRNA genes was observed in the samples containing the largest cell population in S phase (Figs. 3-5C and 3-5D). Although in this experiment cells are not synchronised with the same quality as after arrest with alpha factor (Fig. 3-2) and after inactivation of Cdc15 (Fig. 3-4), the same conclusions can be drawn from the results. In the course of DNA replication 35S rRNA genes adapt the closed chromatin state whereas opening of genes occurs at all cell cycle stages outside of S phase.

In another experiment rRNA gene chromatin structure was analysed during and after release from a G1 arrest with alpha factor in a strain carrying a reduced number of approximately 25 rDNA repeats (Cioci et al., 2003). By electron microscopic inspection of Miller spreads derived from the ~25 copy strain, it was shown that in these cells almost all 35S rRNA genes are actively transcribed by Pol I (Cioci et al., 2003). The results of the flow cytometric analysis during the G1 arrest and release experiment of such a strain were almost identical to those obtained with a strain harbouring a wild type rDNA copy number (compare Figs. 3-6A and 3-2A). Yeast cells were continuously arrested in G1 phase with 1C DNA content during alpha factor treatment (Fig. 3-6A, samples asyn., 40min, 80min and 120min α). Histograms of flow cytometry indicate that DNA replication occurred 20-40min after the release from G1 arrest. Most cells were in G2- and M-phase between 50-70min and DNA replication started again 80min after release from G1 arrest (Fig. 3-6A). Results of psoralen crosslinking were analysed by Southern blot (Fig. 3-6B). Although it was described that in the ~25 copy strain all 35S rRNA genes are actively transcribed, a band representing the closed, nucleosomal chromatin state can be seen in all samples of this analysis (Fig. 3-6B). However, whereas the former analysis relied on single cell analysis by electron microscopy (Cioci et al., 2003), in this study the entire cell population is analysed by psoralen crosslinking. Furthermore, the presence of closed genes could be missed in electron microscopic analyses of Miller spreads because this technique only allows identifying actively transcribed rRNA genes. Profile and quantitative analysis revealed that there are substantial changes in the ratio of open to closed 35S rRNA genes during the cell cycle (Figs. 3-6C and 3-6D). Although the utilised strain contains a reduced number of rDNA repeats, opening of 35S rRNA genes could be

observed during the G1 arrest, before and after DNA replication (Fig. 3-6D). In contrast to the results obtained with the wild type copy number strain, closing of genes can only be observed 20 and 30min after release from alpha factor arrest and reopening occurs with faster kinetics (compare Figs. 3-6D and 3-2D). Apparently, the reduction in rDNA copy number reduces the time needed to replicate rDNA, which in turn leads to faster conversion to the open chromatin state in comparison to a wild type copy number strain. Alternatively, the faster kinetics of reopening may also be attributed to a higher pool of available transcription factors required for transcription initiation for Pol I.

With the experiments shown in this paragraph, a detailed analysis of alterations in 35S rRNA gene chromatin states during the cell cycle was performed. The results obtained all indicate that the ratio of open to closed 35S rRNA genes varies during the cell cycle and suggest that DNA replication is required to establish the closed chromatin state at 35S rRNA genes in proliferating yeast cells.

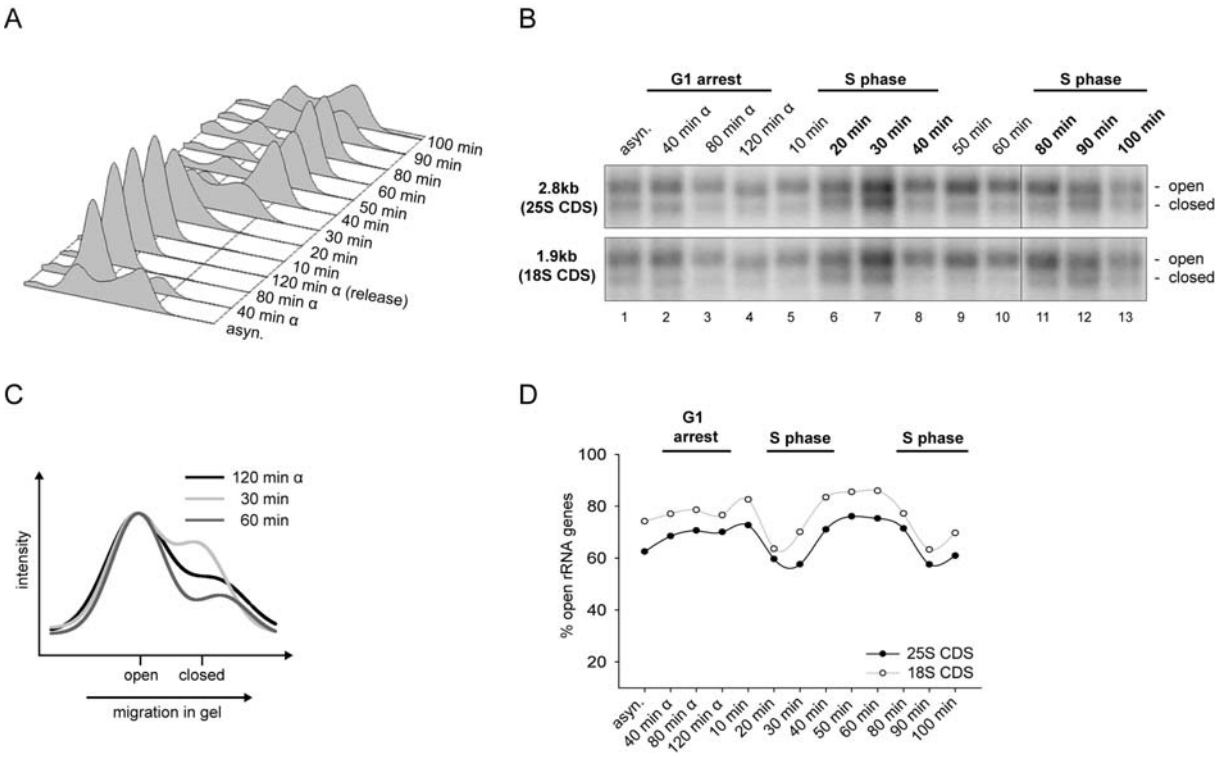

Figure 3-6. Variation of ratio of open to closed rRNA genes analysed in a strain harbouring a modified rDNA locus with only about 25 rDNA repeats.

Yeast strain y1759 carrying a modified rDNA locus with only about 25 rDNA repeats was arrested in G1 by treatment with alpha factor and then released. Samples were taken from the exponentially growing asynchronous culture (asyn.), at the indicated times of G1 arrest (α) and at 10min intervals after release. Cell aliquots were either fixed with ethanol for flow cytometry or formaldehyde for psoralen crosslinking analysis. Flow cytometry (A), psoralen crosslinking analysis (B), profile analysis (C) and determination of the percentage of open rRNA genes (D) were performed as described in the legend to Figure 3-2. (from Wittner et al., 2011)

3.1.2 35S rRNA gene chromatin continuously opens in the absence of replication

Analysis of 35S rRNA gene chromatin during the cell cycle revealed that DNA replication is required for the establishment of the closed chromatin state. Thus, it was investigated to which extent the fraction of open 35S rRNA genes can be increased when entry into S phase and thus initiation of DNA replication is blocked. Cells were arrested in different stages of the cell cycle. G1 arrest was induced by alpha factor treatment (Fig. 3-7A). To block cells at the G1/S transition cells expressing the temperature sensitive allele *cdc7-1* (Moll et al., 1991) were shifted to the restrictive temperature (Fig. 3-7B). Cdc7 is the catalytic subunit of the Dbf4-dependent kinase (DDK) and required for origin firing and replication fork progression (reviewed in Bell and Dutta, 2002). Additionally, *cdc15-2* cells

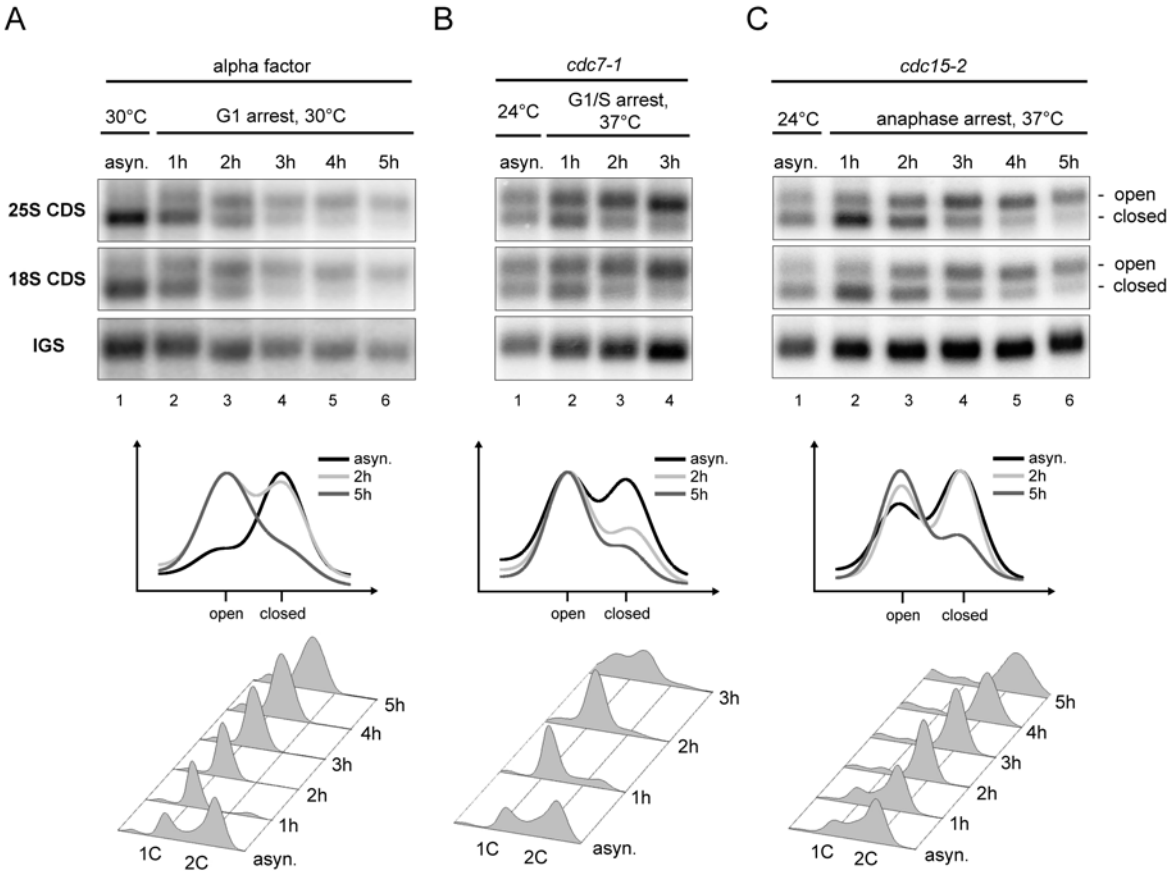

Figure 3-7. Arrest at different cell-cycle stages leads to opening of rRNA genes
(A) Cell-cycle arrest of yeast strain y1757 in G1 by treatment with alpha factor. (B) Cell-cycle arrest of yeast strain y1867 expressing a temperature-sensitive *cdc7-1* allele (Moll et al., 1991) at the G1/S transition after growth at 24°C and temperature shift to 37°C. (C) Cell-cycle arrest of yeast strain y1925 expressing a temperature-sensitive *cdc15-2* allele (Schwab et al., 1997) in late anaphase after growth at 24°C and temperature shift to 37°C. Samples were taken from the exponentially growing asynchronous culture (asyn.) or at the indicated times of cell-cycle arrest. Samples were analysed by psoralen crosslinking and flow cytometry, as described in the legend to Figure 3-2. (from Wittner et al., 2011)

were analysed during prolonged arrest in anaphase (Fig. 3-7C). Southern blot analysis of samples derived from psoralen crosslinking showed that in all cell cycle arrest situations the fraction of open 35S rRNA genes increased substantially (Figs. 3-7A–3-7C, upper two rows, see graphs for profile analysis). In contrast, psoralen accessibility of an IGS fragment remained unaltered (Figs. 3-7A–3-7C, bottom row).
These experiments demonstrate that almost the entire 35S rRNA gene population can adopt the open chromatin state in the absence of DNA replication.

3.1.3 Opening of 35S rRNA genes leads to histone depletion and Hmo1 recruitment

The open chromatin state of 35S rRNA genes has been linked to Pol I transcription, the presence of the HMG box protein Hmo1, and the absence of histone molecules (Dammann et al., 1993; Merz et al., 2008). To define the rDNA chromatin states of cells during prolonged G1 arrest on a molecular level, protein composition of open and closed rRNA genes was analysed by a combination of chromatin endogenous cleavage (ChEC, (Schmid et al., 2004) and psoralen crosslinking (ChEC/psoralen, (Merz et al., 2008; Goetze et al., 2010). The ChEC assay is based on genetic modification of the chromosomal locus of interest. The corresponding gene product is expressed as a fusion protein with a C-terminal Micrococcal Nuclease (MNase) (see Fig. 3-8A for a general outline of the ChEC assay). MNase is an endonuclease that requires calcium as co-factor (Telford and Stewart, 1989). Importantly, the MNase fused to the target protein is inactive in yeast cells, because the concentration of calcium is low in both cytoplasm and nucleoplasm. Thus, to determine the composition of rDNA chromatin, cells are first treated with formaldehyde to crosslink the MNase-tagged protein to its chromosomal binding sites. Then nuclei are isolated and incubated in a buffer containing calcium, which activates the MNase. The active MNase introduces nicks and DNA double strand cuts in the proximity of its binding site. The cleavage sites can be mapped to any locus and at high resolution by agarose gel electrophoresis and Southern blot (Schmid et al., 2004) or by primer extension (Schmid et al., 2006). In ChEC/psoralen experiments, psoralen photocrosslinking is performed with nuclei after ChEC (see Fig. 3-8B for a general outline of the ChEC/psoralen assay). As a result, either the open or closed 35S rRNA genes are preferentially degraded, depending on the specific association of the MNase fusion protein.

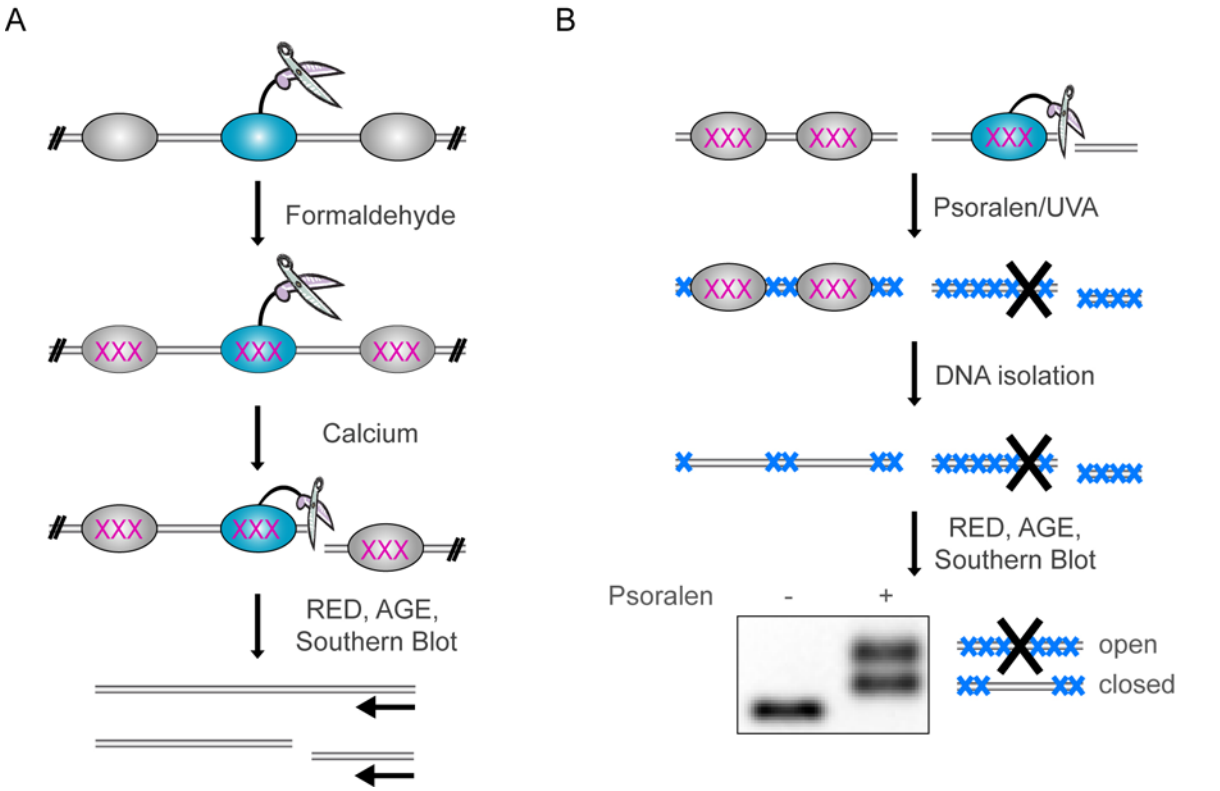

Figure 3-8. Schematic representation of ChEC and ChEC/psoralen analyses
(A) Exponentially growing yeast cells expressing a MNase fusion protein (MNase indicated as scissors) are treated with formaldehyde to crosslink proteins to DNA (crosslinks indicated as pink crosses). Nuclei are prepared and the MNase is activated by the addition of calcium. The DNA is cut in the proximity of the binding site of the MNase fusion protein. The reaction is stopped by the addition of EDTA. DNA is isolated and linearised with restriction enzymes (RED, restriction enzyme digest). After agarose gel electrophoresis (AGE), the DNA is transferred to a nylon membrane by Southern blotting. Cleavage events mediated by the MNase fusion proteins are detected by indirect end-labelling (probes are indicated as black arrows). (B) For ChEC/psoralen analysis, ChEC is performed as described in (A). Before DNA isolation, nuclei are treated with psoralen. Incorporation of psoralen preferentially occurs at DNA sequences devoid of nucleosomes. Upon irradiation with UVA light, psoralen forms covalent bonds between the two DNA strands (psoralen crosslinks are indicated by blue crosses). DNA is isolated and digested with a restriction enzyme (RED). After separation in a native agarose gel, the open (nucleosome depleted) and closed (nucleosomal) DNA fragments originating from the 35S rDNA are analysed by Southern blot. In the scheme, the MNase fusion protein cut in the open 35S rDNA. Therefore, the upper band representing the nucleosome depleted rDNA genes will disappear in the time course of the ChEC/psoralen analysis (indicated by black cross).

ChEC/psoralen experiments have been performed with yeast strains expressing either histone proteins H2A or H3, Pol I subunits A190 or A43 or Hmo1 as MNase fusion proteins from their endogenous chromosomal loci. Cells were crosslinked with formaldehyde before and after 2h and 4h of G1 arrest. First, it was confirmed that open 35S rRNA genes were depleted of histone molecules and thus resistant to histone-MNase cleavage before and during prolonged G1 arrest (Figs. 3-9A and 3-9B).

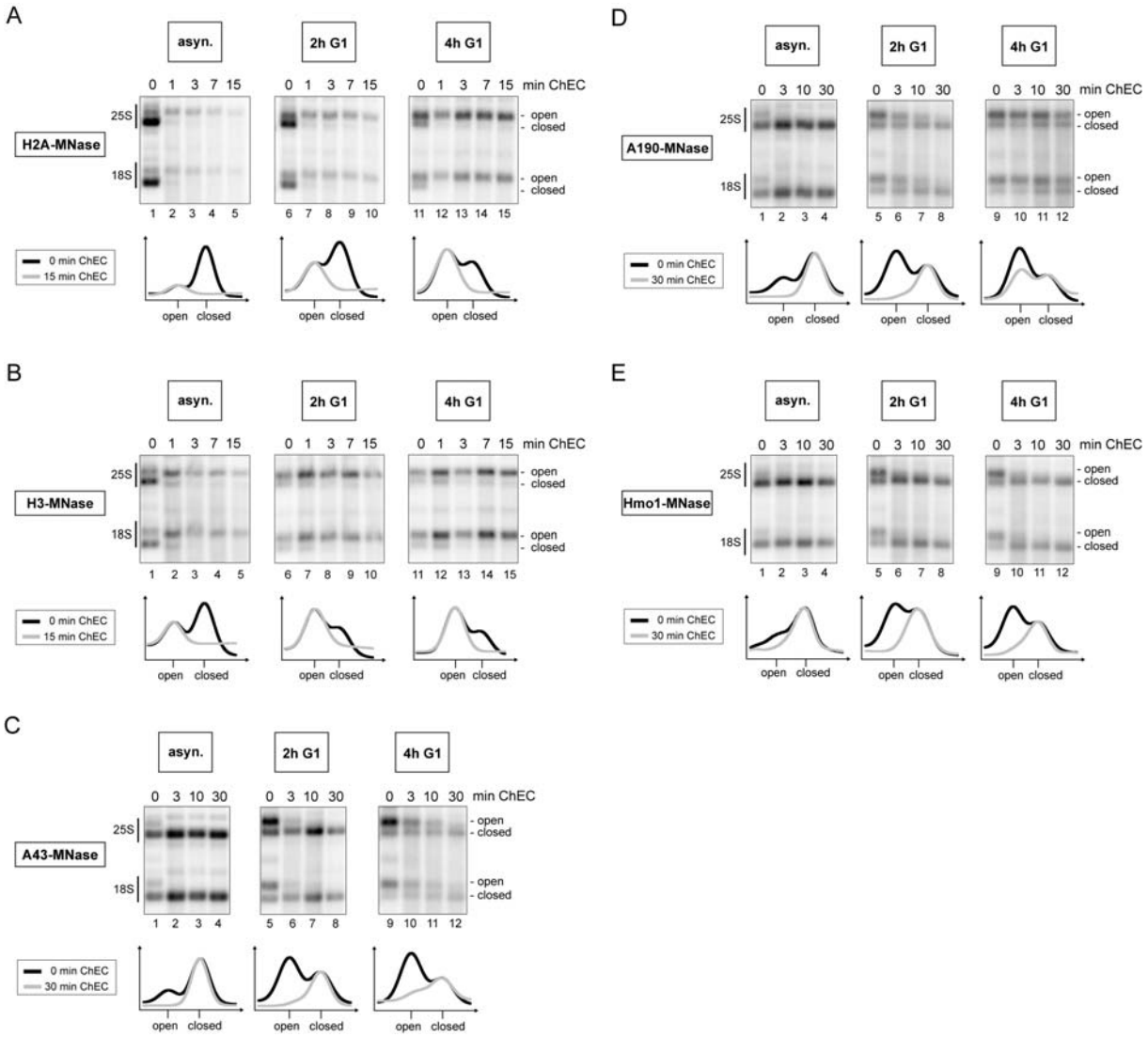

Figure 3-9. Prolonged G1 arrest leads to decreased Pol I association with open rRNA genes, which are devoid of histone molecules and bound by Hmo1

(A–E) Yeast strains y2116, y1995, y1704, y1717, or y1761 expressing histones H2A and H3 and the Pol I subunits A43, A190, or Hmo1 as MNase fusion proteins, respectively, were arrested in G1 by treatment with alpha factor. Samples were taken from the exponentially growing asynchronous culture (asyn.) or at the indicated times of G1 arrest and were treated with formaldehyde. Crude nuclei were subjected to ChEC for the times indicated above each lane. After ChEC, nuclei were treated with psoralen and DNA was analysed in a Southern blot as described in the legend to Figure 3-2B. Profile analysis of individual Southern blot lanes was performed as described in the legend to Figure 3-2C, with one exception: the peak value of fragments derived from open rRNA genes was used for normalisation when histone-MNase expressing strains were analysed, whereas the peak value of fragments derived from closed rRNA genes was used for normalisation when Pol I- or Hmo1-MNase expressing strains were analysed. (from Wittner et al., 2011)

The closed 35S rRNA genes were nucleosomal and thus fully degraded by histone-MNase fusion proteins (Figs. 3-9A and 3-9B, see graphs for profile analysis). In contrast, Pol I-and Hmo1-MNase fusion proteins degraded selectively the open 35S rRNA genes (Figs. 3-9C – 3-9E, see graphs for profile analysis). Remarkably, the degradation kinetics of open 35S rRNA genes mediated by the different Pol I-MNase fusion proteins became

significantly slower with prolonged G1 arrest (Figs. 3-9C and 3-9D, compare panels asyn, 2h G1, and 4h G1). This suggests that the density of Pol I-MNase fusion proteins on open 35S rRNA genes decreased during prolonged G1 arrest. An alternative explanation for this phenomenon could be that only a subpopulation of rRNA genes is actively transcribed under these conditions. Importantly, the reduced Pol I association with the rRNA genes does not affect the maintenance of the open chromatin state. Contrary to Pol I-MNase fusion proteins, Hmo1-MNase-mediated degradation of open 35S rRNA genes followed similar kinetics in nuclei from asynchronously growing cells and cells after 2h and 4h arrest in G1 (Fig. 3-9E).

These analyses indicate that reduced Pol I association with rRNA genes does not affect the stability of the open chromatin state. In addition, they confirm the previous observation made in our laboratory that Hmo1 is a component of the open 35S rRNA gene chromatin state being largely depleted of histone molecules (Merz et al., 2008).

To verify these results in an independent experiment, ChIP experiments were performed with extracts from cells expressing histone H3, the Pol I subunit A190 or Hmo1 as fusion proteins with a C-terminal HA-epitope from their endogenous chromosomal loci. As a control the corresponding wild-type strain was included. Coprecipitation of the same DNA fragments as in the ChIP experiment shown above was analysed (Fig. 3-3D). None of these DNA fragments was significantly enriched when ChIP experiments were performed in the untagged strain (Fig. 3-10, graph ‘‘untagged’’).

The observed decrease in coprecipitation of 35S rRNA gene fragments with the tagged histone H3 molecule during G1 arrest (Fig. 3-10, graph “H3”) correlates well with the increase in the number of open rRNA genes and the results of the ChEC/psoralen analyses (Figs. 3-9A and 3-9B). Remarkably, DNA fragments including the 5S rRNA gene or the *NOC1*-coding sequence were also less efficiently enriched during prolonged G1 arrest, although the observed decrease in coprecipitation with the tagged histone molecule was considerably smaller than the decrease in coprecipitation of 35S rRNA gene fragments. It is important to note that the analysed 5S rRNA gene and *NOC1* DNA fragments include genomic regions, which are potentially transcribed under these experimental conditions. Coprecipitation of the intergenic fragment close to the 3’ end of *NUP57* with tagged histone H3 instead got slightly more efficient in course of the arrest. Again, in good correlation with the increase in the number of open rRNA genes and the results of the ChEC/psoralen analyses (Fig. 3-9E), a strong increase in the coprecipitation of 35S rRNA gene fragments with tagged Hmo1 in the course of the G1 arrest was found (Fig. 3-10, graph “Hmo1”). A slight increase in coprecipitation of the DNA fragment including the 5S rRNA gene was also observed, correlating with the

modest decrease in coprecipitation of this fragment with tagged histone H3 (Fig. 3-10, graph “H3”). DNA fragments spanning the other genomic loci investigated were not substantially enriched after precipitation of tagged Hmo1. All together, these results are in full agreement with an anti-correlation of histone and Hmo1 association with 35S rRNA genes (Merz et al., 2008). Unlike the results obtained with tagged Hmo1, coprecipitation of 35S rRNA gene fragments with the tagged Pol I subunit A190 rather decreased during G1 arrest (Fig. 3-10, graph “A190”), although an increase of the number of open 35S rRNA genes is observed in these conditions in the same strain (Fig. 3-9D, lanes 1, 5 and 9). This is consistent with the results of the ChEC/psoralen experiments with Pol I-MNase fusion proteins during prolonged G1 arrest (Figs. 3-9C and 3-9D). Again, this experiment indicates that an increase in the number of open 35S rRNA genes does not necessarily result in an increased association of Pol I with these genomic loci.

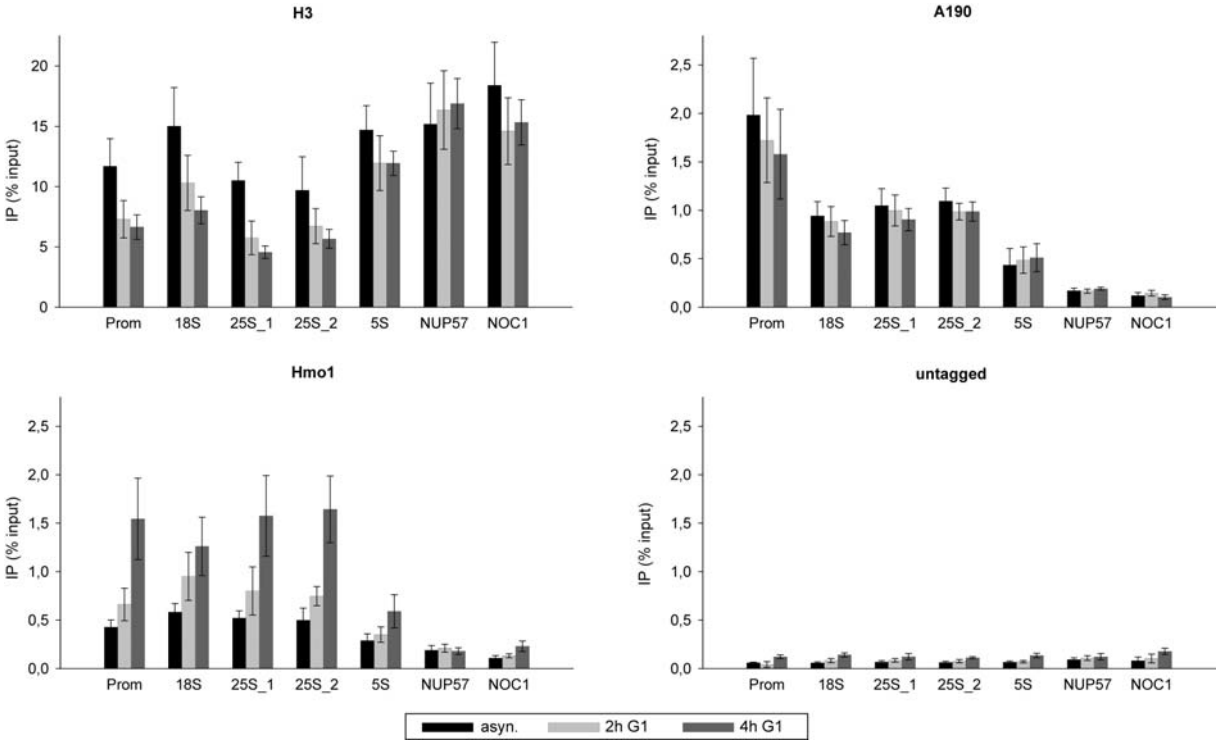

Figure 3-10. Prolonged G1 arrest leads to histone eviction and recruitment of Hmo1 at rRNA genes

Yeast strains y1995, y1761, or y1717 expressing histone H3, Hmo1, or the Pol I subunit A190 as fusion protein with a triple HA-tag, respectively, were arrested in G1 by treatment with alpha factor. The corresponding wild-type yeast strain y1757 was treated identically as an untagged control. Samples were taken from the exponentially growing asynchronous culture (asyn.) or at the indicated times of G1 arrest and were treated with formaldehyde. (B) The graphs depict the percentage of the input of the respective DNA fragment co-precipitating with the indicated HA-tagged fusion protein or from extracts of the untagged control strain. Note that there is a different scale for the y axis of the graph displaying the results of ChIP experiments with tagged histone H3. Error bars indicate standard deviation errors derived from six independent ChIP experiments, each analysed in triplicate qPCRs. (modified from Wittner et al., 2011)

Taken together, opening of rRNA genes in the absence of replication correlated with the depletion of histones (Figs. 3-9A and 3-9B and Fig. 3-10) and with the recruitment of Hmo1 (Fig 3-9E and Fig. 3-10). Nevertheless, a high Pol I occupancy does not seem to be required to maintain the open chromatin state (Figs. 3-9C and 3-9D and Fig. 3-10).

3.1.4 Maintenance of open rRNA gene chromatin requires Pol I transcription in replicating cells

To investigate the contribution of Pol I transcription to the maintenance of open rRNA gene chromatin, psoralen crosslinking analysis was performed with a strain expressing a temperature-sensitive allele of *RRN3* (*rrn3-ts*). *RRN3* encodes a factor that is involved in the recruitment of Pol I to the 35S rRNA gene promoter and therefore is essential for Pol I transcription initiation (Peyroche et al., 2000; Yamamoto et al., 1996). In the *rrn3-ts* strain, the ratio between open and closed 35S rRNA genes remained constant when the cells were cultured in exponential phase at the permissive temperature (Fig. 3-11A, lanes 1–6). Instead, a conversion from the open to the closed 35S rRNA gene chromatin state was observed when the *rrn3-ts* mutant was cultured at the restrictive temperature for more than 1h (Fig. 3-11A, lanes 7–12).

Again, the result was verified in an independent approach. ChIP experiments were performed with strains expressing histones H4 and H2B with a C-terminal HA tag. Coprecipitation of the same DNA fragments as in the ChIP experiment shown above was analysed (Fig. 3-3D). In accordance with the results obtained in the psoralen crosslinking analysis, a slight increase in the coprecipitation of DNA fragments spanning regions of the 35S rRNA gene was observed with tagged histones H4 and H2B molecules after shutdown of Pol I transcription (Fig. 3-11B, graphs “H4” and “H2B”). Importantly, three different reference loci in and outside the rDNA did not show this tendency (Fig. 3-11B, graphs “H4” and “H2B”; 5S, NOC1, NUP57). Again, the corresponding wild-type strain was included as an untagged control. None of the DNA fragments analysed was significantly enriched when ChIP experiments were performed in this strain (Fig. 3-11B, graph ‘‘untagged’’).

However, there was still a fraction of open 35S rRNA genes detectable, even 5h after inactivation of Pol I transcription (Fig. 3-11A, see profile analysis on the right). To investigate if Hmo1 is still part of rRNA gene chromatin in the absence of Pol I transcription, ChEC analysis was performed with an *rrn3-ts* strain expressing Hmo1 as a MNase fusion protein. Samples for formaldehyde fixation were taken before and after

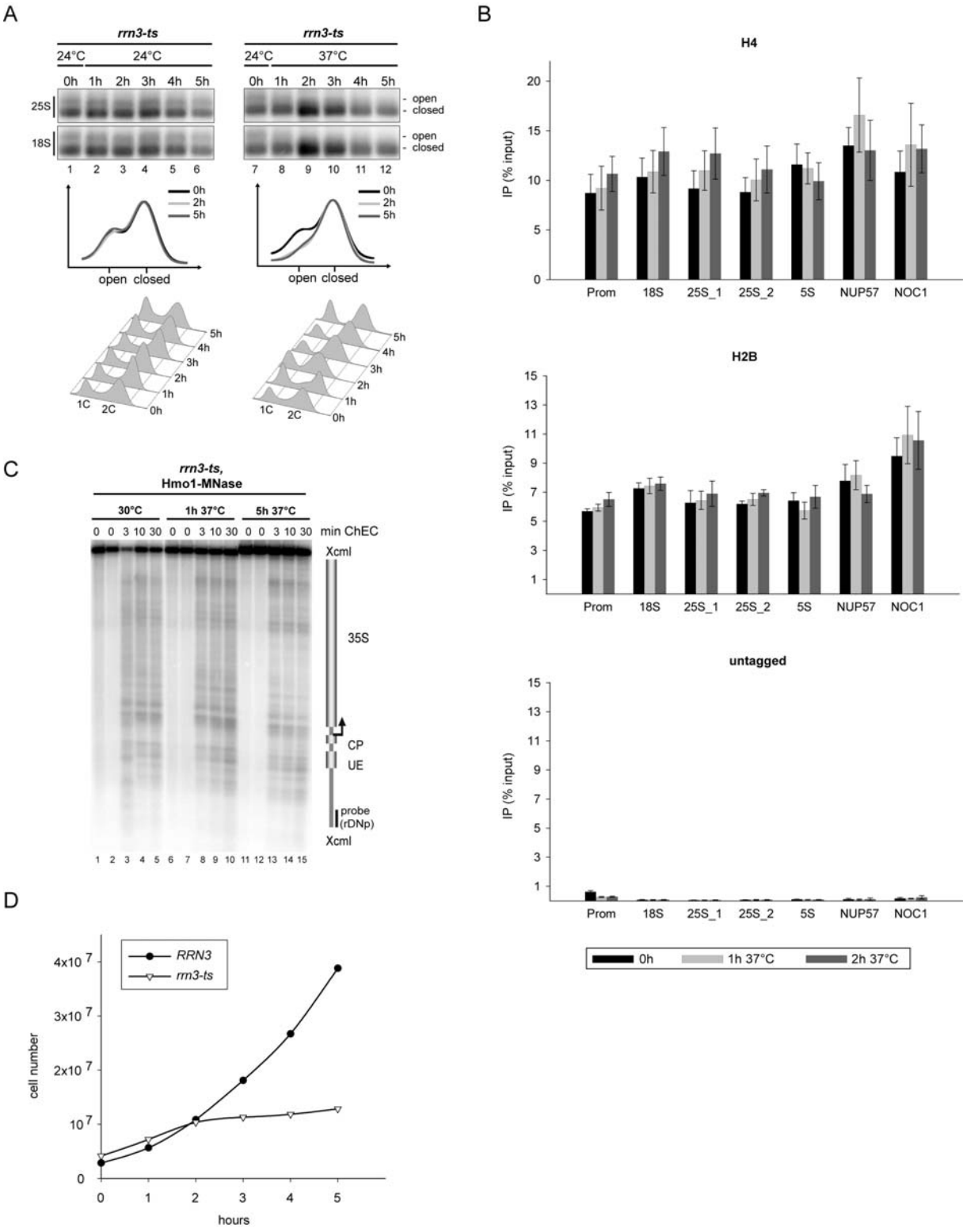

Figure 3-11. Pol I transcription is required for the maintenance of the open rRNA gene chromatin state in replicating cells.

(A) Yeast strain y2022 expressing a temperature-sensitive allele of the Pol I initiation factor Rrn3 (*rrn3-ts*) was cultured at 24°C to exponential phase and either further grown at the permissive temperature (24°C) or shifted to the restrictive temperature (37°C). Samples were taken from the exponentially growing culture in permissive conditions (0h) or at the indicated times of incubation at the respective temperature. Samples were analysed by psoralen crosslinking and flow cytometry, as described in the legend to Figure 3-2. (B) Inhibition of Pol I transcription leads to nucleosome assembly at rRNA genes

in replicating cells. Yeast strains y2022, y2021 or y2120, all expressing a temperature sensitive allele of the Pol I initiation factor Rrn3 (*rrn3-ts*) and histone H4, or H2B with a triple HA-tag, or wild type copies of these genes were cultured at 30°C to exponential phase and shifted to the restrictive temperature (37°C). Samples were taken before (0h) or at the indicated times after temperature shift and treated with formaldehyde. Samples were analysed in ChIP experiments as described in the legend to Figure 3-3. Average and standard deviation errors are derived from three independent ChIP experiments, each analysed in triplicate qPCRs. Note that there is a different scale for the y-axis of the graph displaying the results of ChIP experiments with tagged histone H4. (C) Hmo1 is still bound to 35S rRNA genes after shutdown of Pol I transcription. Yeast strain y2119 expressing a temperature-sensitive allele (*rrn3-ts*) and Hmo1 as MNase fusion protein was cultured at 30°C to exponential phase. Pol I transcription was shut down by shifting the culture to the restrictive temperature (37°C). Samples were taken at the permissive temperature or at the indicated times of temperature shift and were treated with formaldehyde. Crude nuclei were subjected to ChEC for the times indicated above each lane. DNA was isolated after ChEC, digested with *Xcm*I, and analysed in a Southern blot by indirect end labelling. The cartoon on the right shows a map of the fragment analysed by indirect end labelling (see legend to Figure 3-1 for details). The position of the radioactive probe used for the analysis is indicated (rDNp). (D) Inhibition of Pol I transcription severely impairs cell proliferation. Yeast strains y2022, or y1757 expressing the *rrn3-ts* allele or wild type *RRN3*, respectively, were cultured at 30°C to exponential phase and shifted to 37°C. Samples were taken before (0h) or at the indicated times after temperature shift. Cell number was determined and plotted against hours after temperature shift. (modified from Wittner et al., 2011)

shutdown of Pol I transcription by shifting the yeast culture to the restrictive temperature. Similar to results published before (Merz et al., 2008), Hmo1 MNase still cleaved rDNA 1h and even 5h after shift to 37°C (Fig. 3-11C). Accordingly, Hmo1 stays a component of 35S rRNA gene chromatin in the absence of transcribing Pol I, suggesting that not all of the 35S rRNA genes have undergone replication-dependent nucleosome assembly after shutdown of Pol I transcription. In support to this notion, cell division ceased 2h after temperature shift of the *rrn3-ts* mutant (Fig. 3-11D).

These results indicate that Pol I transcription is important for maintaining the open 35S rRNA genes in proliferating cells, presumably because it is required for re-establishment of the open chromatin state after replication.

3.1.5 RNA polymerase I transcription is required to establish open 35S rRNA gene chromatin

To investigate if Pol I transcription is directly involved in the opening of 35S rRNA gene chromatin, the open/closed ratio of 35S rRNA genes was monitored after Pol I shutdown during cell cycle arrest. The *rrn3-ts* strain was arrested in G1 with alpha factor and simultaneously shifted to the restrictive temperature or kept at the permissive temperature as a control. G1 arrest of the strain grown at the permissive and at the

restrictive temperatures was confirmed by flow cytometry (Fig. 3-12, histograms). Whereas almost all 35S rRNA genes opened during the arrest under permissive conditions (Fig. 3-12, lanes 1–6, see profile analysis for quantitation), the ratio of open to closed 35S rRNA genes first increased and then remained constant 2h after shutdown of Pol I transcription initiation (Fig.3-12, lanes 7–12, see profile analysis for quantitation). To exclude that the temperature shift interfered with opening of rRNA genes, a corresponding *RRN3* wild-type strain was treated identically. In this strain, almost the entire 35S rRNA gene population became psoralen accessible during 5h of G1 arrest at 37°C (Fig. 3-12, lanes 13–18, see profile analysis for quantitation).

These data indicate that Pol I transcription is required to convert 35S rRNA genes from the closed to the open chromatin state. Interestingly, open 35S rRNA genes are stably maintained when both rDNA transcription and replication (entry into S phase) are blocked (Fig. 3-12, lanes 7–12, see profile analysis for quantitation).

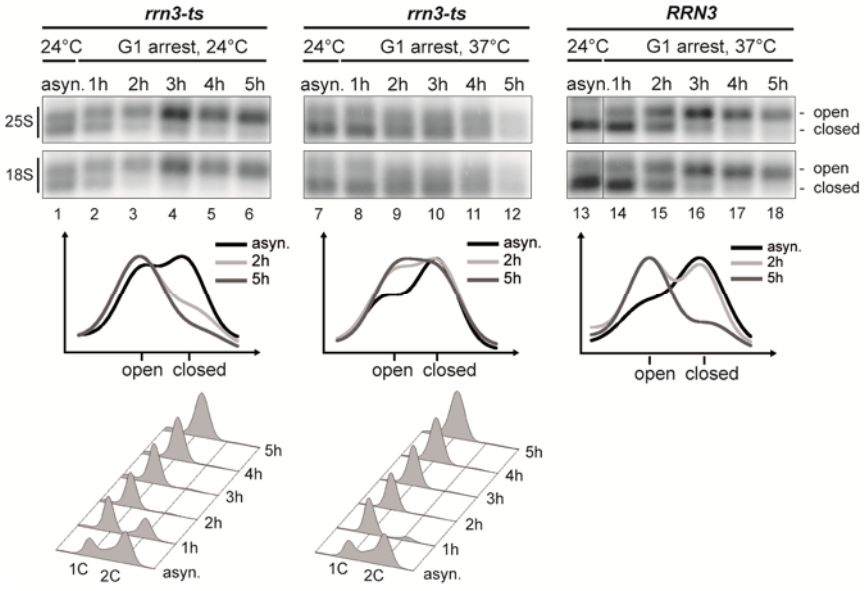

Figure 3-12. Inhibition of Pol I transcription prevents opening of rRNA genes during G1 arrest. Yeast strains y2022 or y1757 expressing the *rrn3-ts* allele or wild-type *RRN3*, respectively, were cultured at 24°C to exponential phase, arrested in G1 by treatment with alpha factor, and either further grown at 24°C or shifted to 37°C. Samples were taken from the exponentially growing asynchronous culture (asyn.) or at the indicated times of G1 arrest at the respective temperature. Samples were analysed by psoralen crosslinking and flow cytometry, as described in the legend to Figure 3-2. (modified from Wittner et al., 2011)

3.1.6 Hmo1 is a component of open 35S rRNA gene chromatin in the absence of Pol I transcription and replication

To explore the molecular basis of the maintenance of open rRNA gene chromatin in the absence of Pol I transcription and replication in more detail, ChEC/psoralen analyses were performed using *rrn3-ts* strains expressing A190- or Hmo1-MNase fusion proteins. Strains were arrested in G1 with alpha factor and simultaneously shifted to the restrictive temperature. As expected, degradation of open rRNA genes by A190-MNase was negligible after 1h of temperature shift and G1 arrest and undetectable after 5h (Fig. 3-13A, lanes 9–12 and 17–20, see graphs for quantitation). In contrast, Hmo1-MNase efficiently degraded open rRNA gene chromatin, even after 5h temperature shift and G1 arrest (Fig. 3-13A, lanes 21–24, see profile analysis for quantitation). In addition, cleavage events mediated by either Pol I- or Hmo1-MNase fusion proteins within the 35S rRNA gene-coding sequence before and after temperature shift and concomitant G1

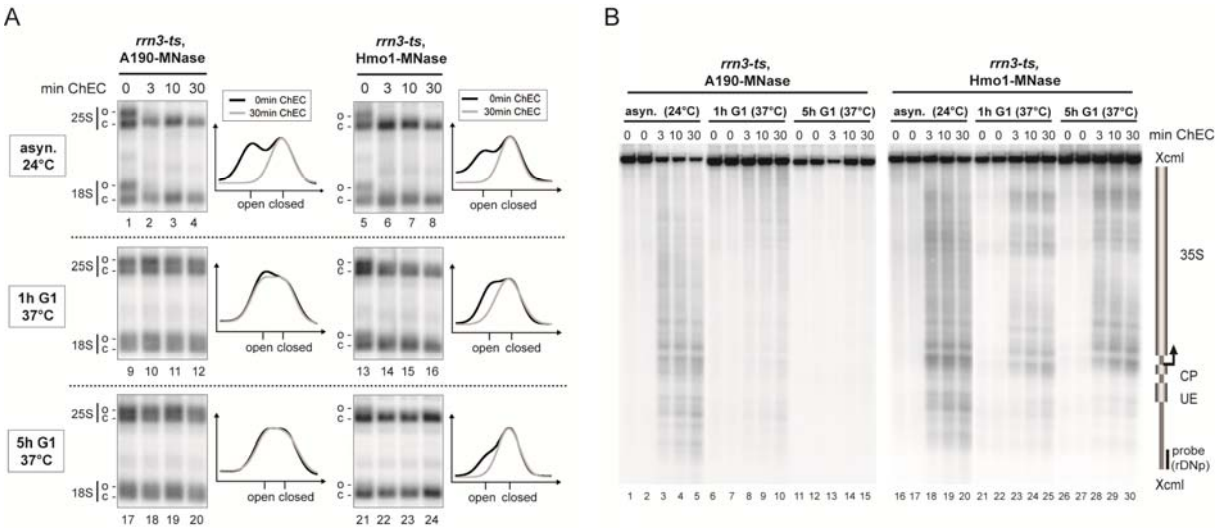

Figure 3-13. Hmo1 is a component of open rRNA gene chromatin in the absence of Pol I.
(A and B) Yeast strains y2123 or y2119, both expressing a temperature-sensitive allele (*rrn3-ts*) and the Pol I subunit A190 or Hmo1 as MNase fusion proteins, respectively, were cultured at 24°C to exponential phase. Cells were simultaneously arrested in G1 by treatment with alpha factor and shifted to the restrictive temperature (37°C). Samples were taken from the asynchronous culture (asyn.) or at the indicated times of G1 arrest and were treated with formaldehyde. Crude nuclei were subjected to ChEC for the times indicated above each lane. (A) After ChEC, nuclei were treated with psoralen, and isolated DNA was analysed in a Southern blot as described in the legend to Figure 3-9. o and c, fragments derived from open and closed rRNA genes. (B) DNA was isolated from crude nuclei after ChEC without subsequent psoralen crosslinking, digested with *Xcm*I, and analysed in a Southern blot by indirect end labelling. The cartoon on the right shows a map of the fragment analysed by indirect end labelling (see legend to Figure 3-1 for details). The position of the radioactive probe used for the analysis is indicated (rDNp). (modified from Wittner et al., 2011)

arrest were analysed. To this end, ChEC experiments without subsequent psoralen treatment were performed and the purified DNA was analysed by Southern blot and indirect end labelling. Consistent with the interpretation of the ChEC/psoralen experiments, only weak Pol I-MNase cleavage events within the 35S rRNA-coding sequence were detectable 1h after G1 arrest at the restrictive temperature and were absent after 5h (Fig. 3-13B, lanes 6–10 and 11–15). In contrast, substantial Hmo1-MNase-mediated cleavage was observed even 5h after G1 arrest at 37°C (Fig. 3-13B, lanes 26–30).

There was a noticeable decrease in the fraction of open 35S rRNA genes with prolonged G1 arrest at 37°C in the Hmo1-MNase expressing strain, whereas this fraction remained constant in the Pol I-MNase-expressing strain (Fig. 3-13A, compare lanes 13 with 21 and 9 with 17, see profile analysis for quantitation). One possible explanation for this phenomenon could be that Hmo1 is needed to stabilise the open 35S rRNA gene chromatin in the absence of Pol I transcription and that the Hmo1-MNase fusion protein is partly impaired in this function.

3.1.7 Hmo1 prevents replication-independent nucleosome assembly at open 35S rRNA genes

To test if Hmo1 is required to stabilise open 35S rRNA gene chromatin in the absence of Pol I transcription, the fate of the open chromatin state was investigated during G1 arrest in the absence of Hmo1. First, *HMO1* wild-type and *hmo1Δ* deletion strains were arrested in G1 for different periods (see Fig. 3-14A for an outline of the experiment). As observed before (see above Fig. 3-12, lanes 13–18), the 35S rRNA gene chromatin in the *HMO1* wild-type strain opened almost completely during alpha factor treatment (Fig. 3-14B, lanes 1–6, see profile analysis for quantitation). Opening of 35S rRNA genes, however, was compromised in the *hmo1Δ* strain (Fig. 3-14B, lanes 7–12, see profile analysis for quantitation). One explanation for the reduced kinetics of rRNA gene opening might be the prolonged generation time observed in this deletion background (Lu et al., 1996; Gadal et al., 2002). Thus, Hmo1 is not required to open 35S rRNA gene chromatin. Nevertheless this observation is still consistent with a role for this HMG box protein in the stabilisation of open 35S rRNA gene chromatin.

To further test this hypothesis, the stability of open 35S rRNA gene chromatin was investigated after shutdown of transcription in *rrn3-ts* strains being either deleted in *HMO1* or carrying a wild type copy of the gene. Cells were arrested in G1 for 1.5h prior

to shifting the cultures to the restrictive temperature. In both strains, 35S rRNA genes opened upon G1 arrest at the permissive temperature (Fig. 3-14C, compare lanes 1 with 2 and 7 with 8). As observed before (see above Fig. 3-12, lanes 7–12), inactivation of Pol I transcription led to a constant ratio of open to closed 35S rRNA genes after 2h of temperature shift in the *HMO1, rrn3-ts* strain (Fig. 3-14, lanes 3–6, see profile analysis for quantitation). In contrast, a conversion from the open to the closed 35S rRNA gene chromatin state was observed in the *hmo1Δ*, *rrn3-ts* strain under these conditions (Fig. 3-14, lanes 9–12, see profile analysis for quantitation).

These results suggest that the presence of Hmo1 stabilises the open 35S rRNA gene chromatin state in the absence of Pol I transcription, likely interfering with replication-independent nucleosome assembly.

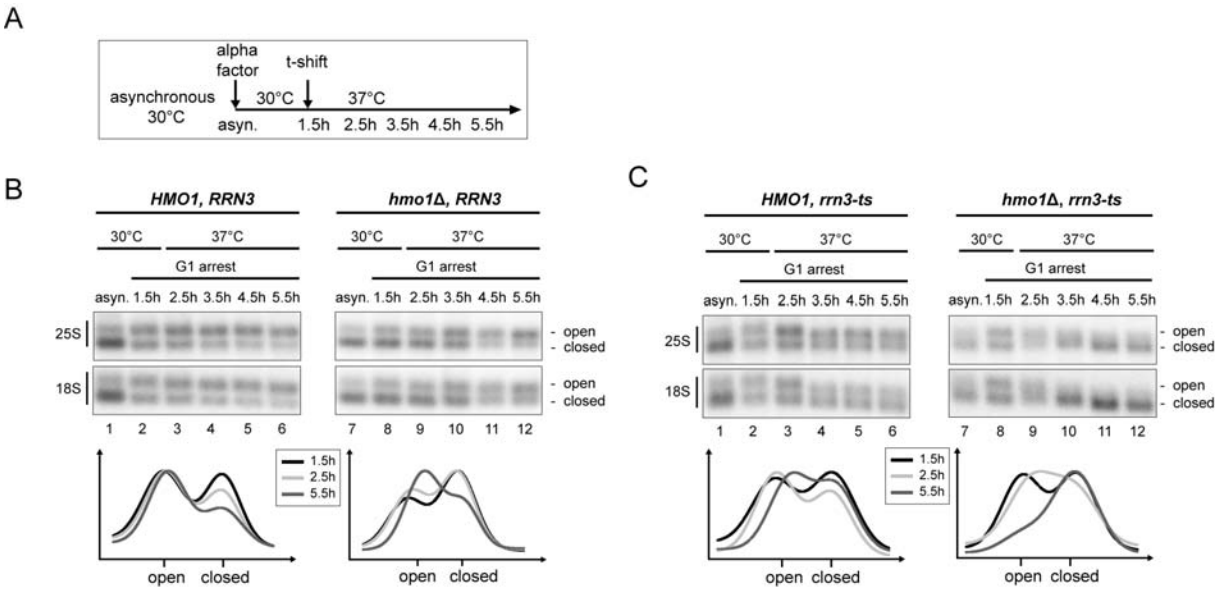

Figure 3-14. Hmo1 stabilises open rRNA gene chromatin upon G1 arrest in the absence of transcription

(A) Outline of the experiment. (B and C) Yeast strains expressing either wild-type *RRN3* (B) or the *rrn3-ts* allele (C) and being either wild-type in *HMO1* or carrying a complete deletion of the gene (*hmo1Δ*) were cultured at 30°C to exponential phase and arrested in G1 with alpha factor for 1.5 hr. G1 arrest was continued at 37°C (restrictive temperature for *rrn3-ts*) for another 4h. Samples were taken from the asynchronous culture (asyn.) or at the indicated times of G1 arrest and were treated with formaldehyde. Samples were analysed by psoralen crosslinking, as described in the legend to Figure 3-2. (from Wittner et al., 2011)

3.2 Chromatin dynamics at 35S rRNA genes after UV irradiation

In 2005, a study of the Smerdon laboratory showed that 35S rRNA gene chromatin structure changes substantially after irradiation of yeast cells with UVC light (Conconi et al., 2005). By using three independent assays (psoralen crosslinking, restriction enzyme accessibility and MNase sensitivity), they suggested that nucleosomes assemble at the open rRNA genes after UV irradiation and that the resulting decrease in the fraction of open genes does not depend on DNA repair by the NER machinery. In addition, the observed changes in rDNA chromatin structure correlated well with a strong reduction in Pol I transcription (Conconi et al., 2005).

3.2.1 Opening of 35S rRNA gene chromatin after UV irradiation occurs gradually from the 5' to the 3' end of the gene

In this work, the molecular basis of the compositional changes in 35S rRNA gene chromatin in response to UV irradiation was analysed in collaboration with the laboratory of Antonio Conconi. First, results of psoralen photocrosslinking experiments were reproduced with cells irradiated in our laboratory. Irradiation of yeast cells with UV light was performed as reported (Conconi et al., 2005; Tremblay et al., 2008). In brief, a yeast culture grown to early exponential phase was harvested, washed, resuspended in PBS and exposed to 180J/m^2 UV light (254nm) (see Fig. 3-15A for an outline of the experiment). At this dose, approximately 1.5 CPDs in average are formed within the transcribed strand of the 2.8kb *Eco*RI fragment derived from the 35S rRNA gene (Conconi et al., 2005). After irradiation, cells were collected by centrifugation, resuspended in fresh medium and incubated in the dark. Under these conditions DNA lesions can be repaired by NER but repair by photolyase is prevented. Samples were taken before (-UV), immediately after (0h) and at the indicated times after irradiation and were fixed with formaldehyde for psoralen crosslinking analysis and ethanol for flow cytometry. To monitor chromatin alterations early after UV irradiation, the study mentioned above was extended by taking additional samples 5 and 15min after UV treatment. Moreover, two *Eco*RI fragments derived from the 35S rRNA gene were probed (Fig. 3-1, 1.9kb and 2.8kb fragments), whereas in the former study only the 2.8kb fragment was analysed.

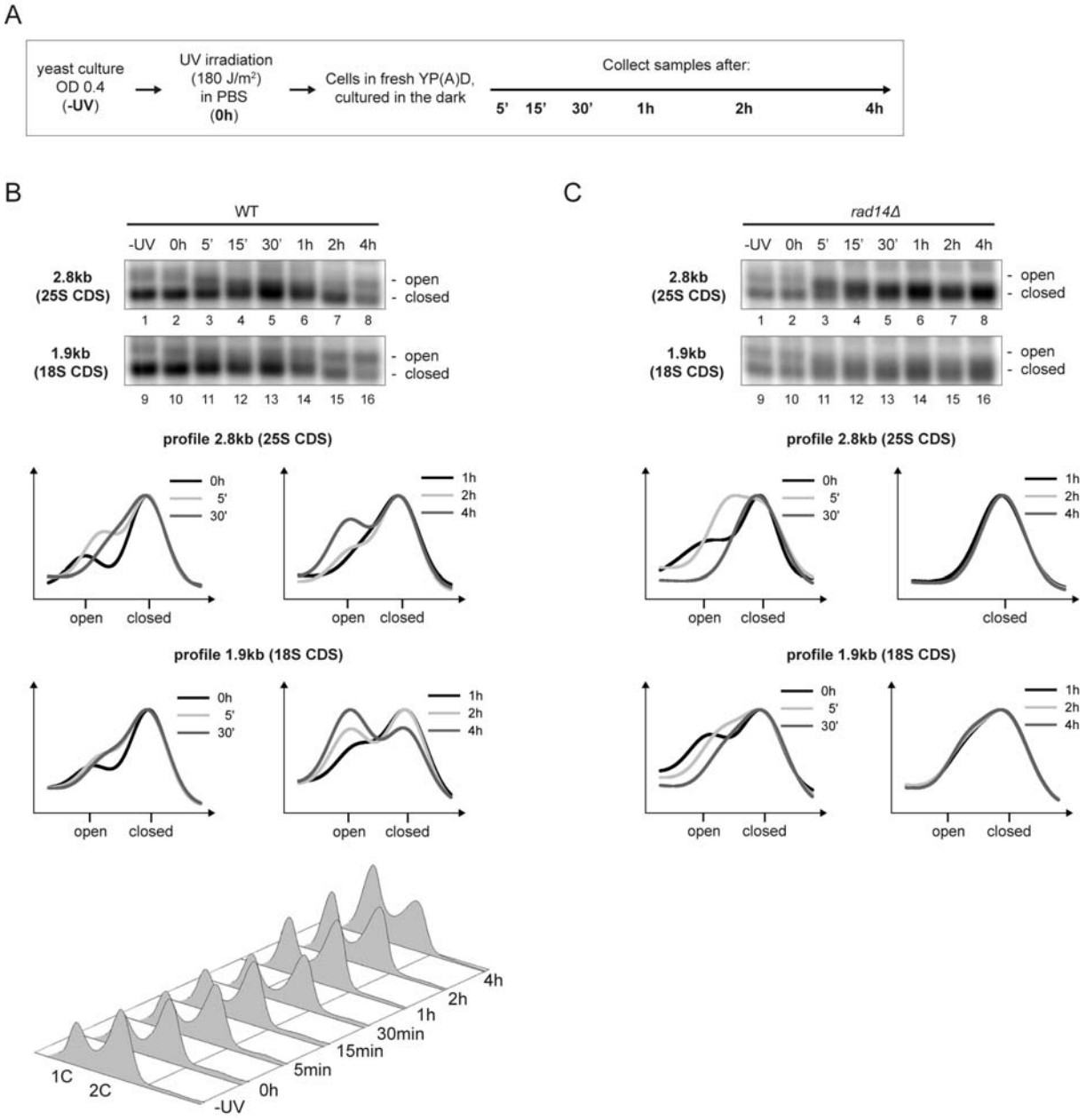

Figure 3-15. The percentage of closed rRNA genes increases during NER.
(A) Outline of the experiment. (B and C) Yeast strain JS311 (Smith et al., 1999) (B) and a strain carrying a complete deletion of *RAD14* (*rad14Δ*) (C) were cultured at 30°C to exponential phase, irradiated and further cultured at 30°C. Samples were taken before (-UV) and at the indicated times after irradiation and were fixed with formaldehyde for psoralen crosslinking analysis and ethanol for flow cytometry (only B). Samples were analysed by psoralen crosslinking and flow cytometry as described in the legend to Figure 3-2, with the exception that profile analyses were performed for the fragments derived from the 25S and 18S rRNA CDS.

Initially, changes in 35S rRNA chromatin structure were analysed by psoralen crosslinking in a wild type strain (Fig. 3-15B). Southern blot analysis revealed that the ratio of open/closed 35S rRNA genes remained unchanged immediately after irradiation (Fig. 3-15B, compare lane 1 with 2 and 9 with 10). Psoralen accessibility of the *Eco*RI

fragment derived from the 25S coding sequence (25S CDS) progressively decreased in the samples taken 5min and 15min after UV irradiation (Fig. 3-15B, lanes 3 and 4). This resulted in a smear migrating with slightly lower mobility than the band derived from the closed 35S rRNA genes 30min and 1h after irradiation (Fig. 3-15B, lanes 5 and 6, see also profile analysis). Psoralen accessibility of the 25S CDS fragment increased only slightly after 2h but was even enhanced after 4h if compared to the sample taken immediately after UV irradiation (Fig. 3-15B, lanes 7 and 8, compare lane 2 with 8, see also profile analysis). Taken together, these results confirmed the earlier observations (Conconi et al., 2005).

Psoralen accessibility of the *Eco*RI fragment derived from the 18S coding sequence (18S CDS) was also reduced 5min after irradiation but stayed largely constant up to 30min after UV treatment (Fig. 3-15B, lanes 11-13, see also profile analysis). Remarkably, establishment of the closed chromatin state was less pronounced during the first 30min when compared with the 25S CDS fragment (Fig. 3-15B, compare lanes 3-5 with 11-13, see also profile analysis) and reopening could be observed already 1h after UV irradiation (Fig. 3-15B, lane 14, see also profile analysis). Strong differences in psoralen accessibility between the 25S and 18S CDS fragments could also be detected 2h and 4h after irradiation (Fig. 3-15B, compare lanes 7-8 with 14-15, see also profile analysis). The percentage of open 18S CDS fragments after 2h was already higher than in the sample taken immediately after irradiation and a majority of the fragments were in the open chromatin state 4h after irradiation (Fig. 3-15B, compare lane 10 with 15 and 16, see also profile analysis).

Thus, the kinetics and the extent of closing and reopening observed for the 18S and 25S CDS fragments differed significantly after exposure to UV light, suggesting that chromatin alterations occur in a 5'-3' gradient at the 35S rRNA gene. Interestingly, psoralen crosslinking of both fragments showed a continuous increase of the open chromatin structure during late repair timepoints, leading to an open/closed ratio that was even higher than before or immediately after irradiation.

The steady opening observed 2h and 4h after UV irradiation strongly resembles the situation upon cell cycle arrest, when replication is prevented (see 3.1.2). In fact it has been reported that DNA damage may lead to cell cycle arrest at different checkpoints at G1/S, S and G2/M (Hartwell and Weinert, 1989, 1989; Russell, 1998; Willis and Rhind, 2009). This surveillance mechanism leads to the inhibition of DNA replication, allowing efficient DNA repair (Boye et al., 2009). To investigate if cells arrest in the cell cycle under our experimental conditions the DNA content of cells before and at different time

points after irradiation with UV light was measured by flow cytometry (Fig. 3-15B, histogram at the bottom). This revealed that the population of cells containing 1C and 2C DNA content was largely constant in the samples taken before (-UV), immediately after (0h) and 5min and 15min after irradiation (Fig. 3-15B, histogram at the bottom). In the 30min, 1h, 2h and 4h samples a gradual increase of the cell population harbouring 1C DNA content can be observed (Fig. 3-15B, histogram at the bottom). This indicates that some cells are still capable to complete mitosis during NER whereas the entry into or further progression in early S phase seems to be impaired.

As mentioned above, Conconi et al. further showed that NER is not required for the transition from open to closed 35S rRNA gene chromatin (Conconi et al., 2005). Their conclusions were derived from a yeast strain deleted in *RAD14*. Rad14 participates in the recognition of DNA lesions and is required for the recruitment of the endonucleases Rad1-Rad10 to the damaged site (Prakash and Prakash, 2000; Guzder et al., 2006). Thus, dual incision of the damaged DNA strand and consequently, the repair dependent DNA synthesis step are prevented in the absence of Rad14. Transition to the closed rRNA gene chromatin state after UV irradiation in a *rad14Δ* strain occurs with similar kinetics when compared to a wildtype strain; however, subsequent reopening of rRNA genes was not observed (Conconi et al., 2005).

To reproduce the published results, a strain being deleted in *RAD14* was irradiated with UV light and psoralen crosslinking analysis was performed as outlined above (Fig. 3-15A). Southern blot analysis confirmed that both rDNA populations are present in non-irradiated cells (Fig. 3-15C, lanes 1 and 9, see also profile analysis) and immediately after UV irradiation (Fig. 3-15C, lanes 2 and 10, see also profile analysis). After 5min incubation in the dark, psoralen accessibility of open rDNA chromatin decreased (Fig. 3-15C, lanes 3 and 11, see also profile analysis). 15min after UV irradiation, the band representing open chromatin was transformed into a smear migrating with slightly lower mobility than the band derived from the closed 35S rRNA genes (Fig. 3-15C, lanes 3-8 and 11-16, see also profile analysis). As described earlier (Conconi et al, 2005) re-establishment of open 35S rRNA chromatin did not occur in *rad14*Δ cells. Interestingly, although psoralen accessibility of both *Eco*RI fragments analysed was decreased after irradiation, the decrease seemed to be less pronounced for the fragment derived from the 18S coding sequence. Even 4h after irradiation a substantial fraction of the *Eco*RI fragments derived from the 18S CDS was still psoralen accessible migrating as a smear with slightly lower mobility than the band derived from the closed 35S rRNA genes (Fig. 3-15, lanes 14 to 16, see also profile analysis).

In summary, the results of the study of the Smerdon laboratory could be reproduced. The analysis of two different rRNA gene fragments further extended the earlier observations. It was found that the UV irradiation induced changes in psoralen accessibility of the 5' and 3' regions of the 35S rRNA gene differ from each other. Thus, reopening of rRNA gene chromatin in the course of NER occurs gradually, starting 5' of the gene followed by spreading to the 3' end. Moreover, it could be shown that reopening of 35S rRNA genes during DNA repair results in a higher open/closed ratio of both 35S rRNA gene fragments than before or immediately after irradiation with UV light. In good correlation with other results (see 3.1.2), this opening might be due to the absence of replication since flow cytometry indicated that cells arrest in the cell cycle under these experimental conditions (see Fig. 3-15, histogram at the bottom). Furthermore, it was confirmed that the transition to the closed 35S rRNA gene chromatin state does not depend on assembly of the NER machinery at damage sites.

3.2.2 Histones associate with the open rRNA genes after UV irradiation

To correlate the transition from the open to the closed rRNA gene chromatin state upon UV irradiation with nucleosome assembly at the open 35S rRNA genes, ChEC/psoralen analyses were performed with yeast strains expressing histones H2A and H3 as MNase fusion proteins, respectively. Yeast cells were crosslinked with formaldehyde before (-UV), immediately after irradiation with UV light (0h) and during incubation in the dark (30min, 1h, 2h, 4h).

In the samples taken before and instantly after UV irradiation the closed 35S rRNA genes were rapidly degraded by the histone MNase fusion proteins whereas open, nucleosome depleted rDNA persisted cleavage by the MNase fusion proteins (Figs. 3-16A and 3-16B, samples -UV and 0h, see graphs for profile analysis). Nevertheless, it has to be mentioned that in the JS311 background (Smith et al., 1999), degradation of the band representing the closed 25S CDS fragment by histone MNase fusion proteins was never complete in all analyses. The reason for this phenomenon is still unknown. As described in the psoralen analysis above (Fig. 3-15B), 30min after irradiation the 25S CDS fragment derived from open rRNA genes was transformed into a smear migrating with slightly lower mobility than the band derived from the closed 35S rRNA genes (Figs. 3-16A and 3-16B, lanes 9). In this sample, almost the complete 25S *Eco*RI fragment got degraded by H2A- and H3-MNase, except a small subpopulation, exhibiting the highest psoralen accessibility and thus migrating on top of the smear (Figs. 3-16A and 3-16B,

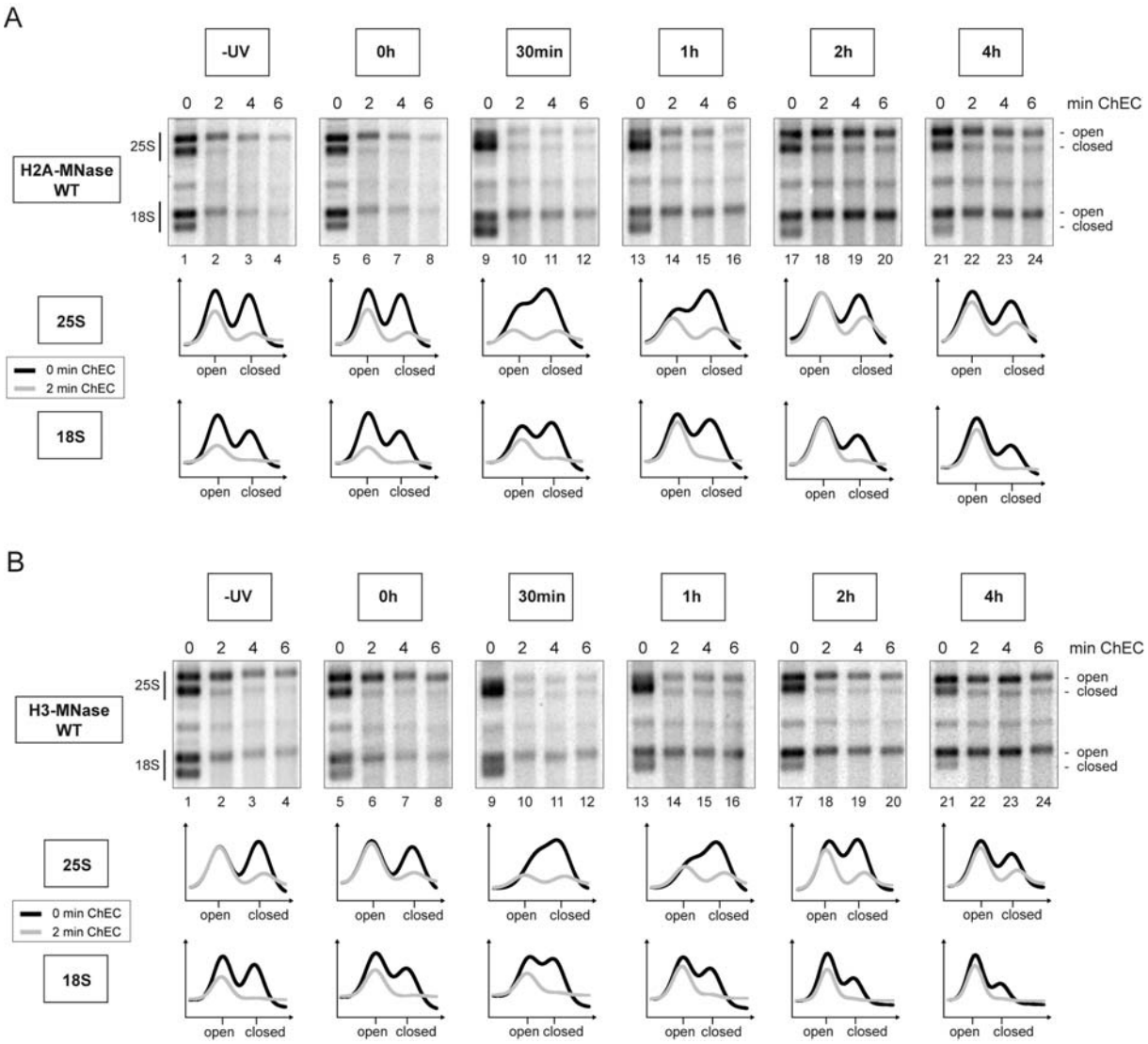

Figure 3-16. Histones associate with the open rRNA genes after UV irradiation.
(A and B) Yeast strains y2163 and y2164 expressing histones H2A and H3 as MNase fusion proteins, respectively, were cultured at 30°C to exponential phase, irradiated with UV light and further cultured at 30°C. Samples were taken before (-UV) and at the indicated times after irradiation and were treated with formaldehyde. Crude nuclei were subjected to ChEC for the times indicated above each lane. After ChEC, nuclei were treated with psoralen and DNA was analysed in a Southern blot as described in the legend to Figure 3-2B. Profile analysis of individual Southern blot lanes was performed as described in the legend to Figure 3-2C, with the exception, that values were normalised to background instead of using the peak value of fragments derived from closed rRNA genes.

samples 30min, 25S, see graphs for profile analysis). One explanation for the existence of this histone-MNase resistant subpopulation could be that it represents 25S CDS fragments derived from undamaged rRNA genes or that this fraction has already been repaired prior to taking the sample.

In accordance with the observations from psoralen crosslinking analysis, psoralen accessibility of the 18S CDS fragment decreased only moderately and a substantial amount of open rRNA genes was not degraded by the histone-MNase fusion proteins

(Figs. 3-16A and 3-16B, samples 30min, 18S, see graphs for profile analysis). Psoralen accessibility and concomitantly resistance to MNase cleavage of the 25S CDS fragment increased slightly 1h after irradiation (Figs. 3-16A and 3-16B, samples 1h, 25S CDS, see graphs for profile analysis). In the samples taken 2h and 4h after UV irradiation, the fraction persistent to cleavage by the histone-MNase fusion proteins of both rDNA fragments analysed, increased progressively (Figs. 3-16A and 3-16B, samples 2h and 4h, see also profile analysis). Again, when compared to opening of the 25S CDS fragment, a stronger opening of the 18S CDS fragment was evident, consistent with observations made in the psoralen crosslinking analysis performed in the corresponding wildtype strain (Fig. 3-15B).

The above results of ChEC/psoralen analysis suggest that the decrease of psoralen accessibility observed at the 3' end of 35S rRNA genes after UV irradiation of yeast cells is due to nucleosome assembly on open rRNA genes. This is in full accordance with the conclusions drawn in the earlier study (Conconi et al., 2005).

3.2.3 All 35S rRNA genes are associated with histones after UV irradiation in the absence of NER

To uncouple the dynamic processes of closing and opening after UV irradiation, histone association with 35S rRNA genes was analysed in UV irradiated yeast cells in the absence of NER.

To this end, ChEC/psoralen experiments were performed using *rad14Δ* yeast strains expressing histones H2A and H3 as MNase fusion proteins, respectively. Yeast cells were crosslinked with formaldehyde before (-UV), immediately after irradiation with UV light (0h) and during incubation in the dark (5min, 15min, 30min, 1h, 2h, 4h). In the samples taken before and immediately after UV irradiation closed 35S rRNA genes were preferentially degraded by the histone MNase fusion proteins whereas open, nucleosome depleted rDNA was resistant to cleavage by histone MNase fusion proteins (Figs. 3-17A and 3-17B, samples -UV and 0h, see profile analysis for quantitation). Psoralen accessibility of open rRNA genes started to decrease in the samples taken very early after UV irradiation (5min and 15min), but still the histone MNase fusion proteins degraded the faster migrating band, representing fully nucleosomal 35S rRNA genes with slight preference (Figs. 3-17A and 3-17B, samples 5min and 15min, see graphs for profile analysis). Interestingly, starting from 30min after induction of DNA damage by UV light, the whole 25S CDS fragment was uniformly degraded by the histone MNase fusion

proteins (Figs. 3-17A and 3-17B, samples 30min-4h, 25S, see graphs for profile analysis). This suggests that nucleosomes assembled on all 35S rRNA genes that were present in the open chromatin state before UV irradiation. At the 18S CDS fragment, however, a considerable difference in cleavage of the upper and lower part of the smear is noticeable, especially in the samples taken 1h, 2h and 4h during incubation in the dark (Figs. 3-17A and 3-17B, samples 1h-4h, 18S, see graphs for profile analysis). A possible explanation for the observed discrepancy between the 5'- and the 3' end of the 35S

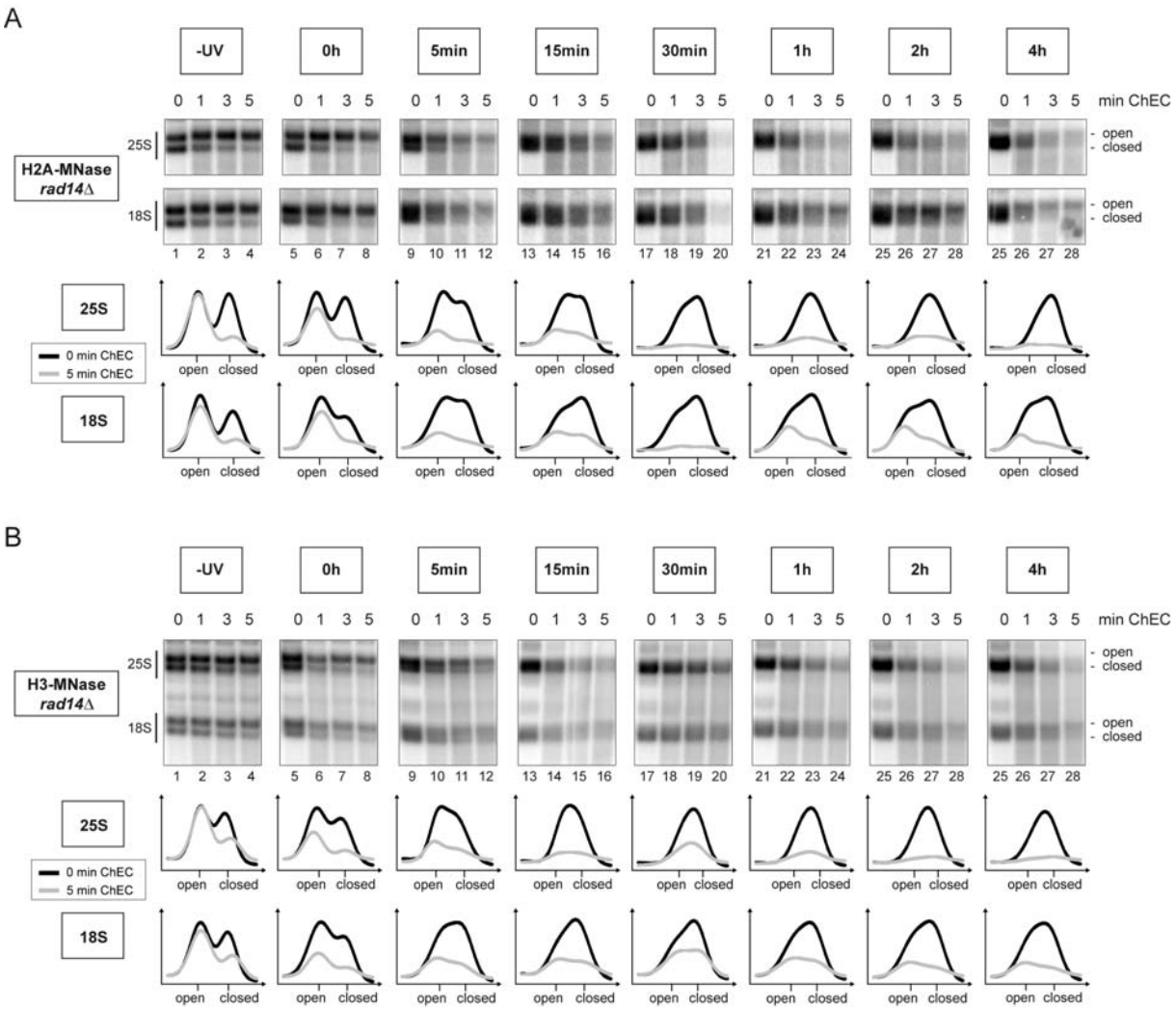

Figure 3-17. Histone molecules associate with all open rRNA genes after UV irradiation in a NER deficient strain.

(A and B) Yeast strains y2457 and y2458, carrying a complete deletion of *RAD14* (*rad14Δ*) and expressing histones H2A and H3 as MNase fusion proteins, respectively, were cultured at 30°C to exponential phase, irradiated and further cultured at 30°C. Samples were taken before (-UV) and at the indicated times after irradiation and were treated with formaldehyde. Crude nuclei were subjected to ChEC for the times indicated above each lane. After ChEC, nuclei were treated with psoralen and DNA was analysed in a Southern blot as described in the legend to Figure 3-2B. Profile analysis of individual Southern blot lanes was performed as described in the legend to Figure 3-2C, with the exception, that the values were normalised to background instead of using the peak value of fragments derived from closed rRNA genes.

rRNA gene could be that partial reopening, mediated by Pol I transcription, occurs at the 5' end. Thus, the extent of opening at the 5' end might depend on the position of the first DNA damage within the 35S rRNA gene sequence at which transcription will be terminated.

Taken together, these results indicate that nucleosomes assemble at all 35S rRNA genes after UV irradiation in the absence of NER. This suggests, that the subpopulation of histone MNase resistant fragments derived from open rRNA genes at all times after UV irradiation in a yeast wild type strain (see 3.2.1) are rather rRNA genes which have already undergone NER than rRNA genes which have not been damaged upon irradiation. In addition the data confirm that the extent of nucleosome assembly varies at the 5' and 3' end of the 35S rRNA gene.

3.2.4 RNA polymerase I and Hmo1 remain associated with 35S rRNA genes during UV induced nucleosome assembly

Previous analyses revealed that besides transcribing Pol I, the HMG box protein Hmo1 is a component of the open 35S rRNA gene chromatin state, which is largely depleted of histone molecules (Merz et al., 2008). In addition, it was shown as part of this work that Hmo1 prevents replication independent nucleosome assembly at the 35S rRNA genes (Wittner et al., 2011).

To investigate if Pol I and Hmo1 are constituents of 35S rRNA gene chromatin in the course of UV induced nucleosome assembly and NER, ChEC/psoralen analyses were performed with yeast strains expressing the largest Pol I subunit A190 and Hmo1 as MNase fusion proteins. Yeast cells were crosslinked with formaldehyde before (-UV), immediately after irradiation with UV light (0h) and during incubation in the dark (30min, 1h, 2h, 4h).

In the samples taken before and instantly after UV irradiation, Pol I- and Hmo1-MNase fusion proteins degraded selectively the open 35S rRNA genes (Figs. 3-18A and 3-18B, samples -UV and 0h, see graphs for profile analysis). As described before (subheading 3.2.1 and 3.2.2), the 25S CDS fragment derived from open rRNA genes was transformed into a smear migrating with slightly lower mobility than the band derived from the closed 35S rRNA genes 30min and 1h after UV irradiation. Interestingly, this smear was completely degraded by both, A190- and Hmo1 MNase fusion proteins (Figs. 3-18A and 3-18B, sample 30min, 25S, see graphs for profile analysis). Remarkably, the decrease in psoralen accessibility after UV irradiation was more pronounced in the samples derived

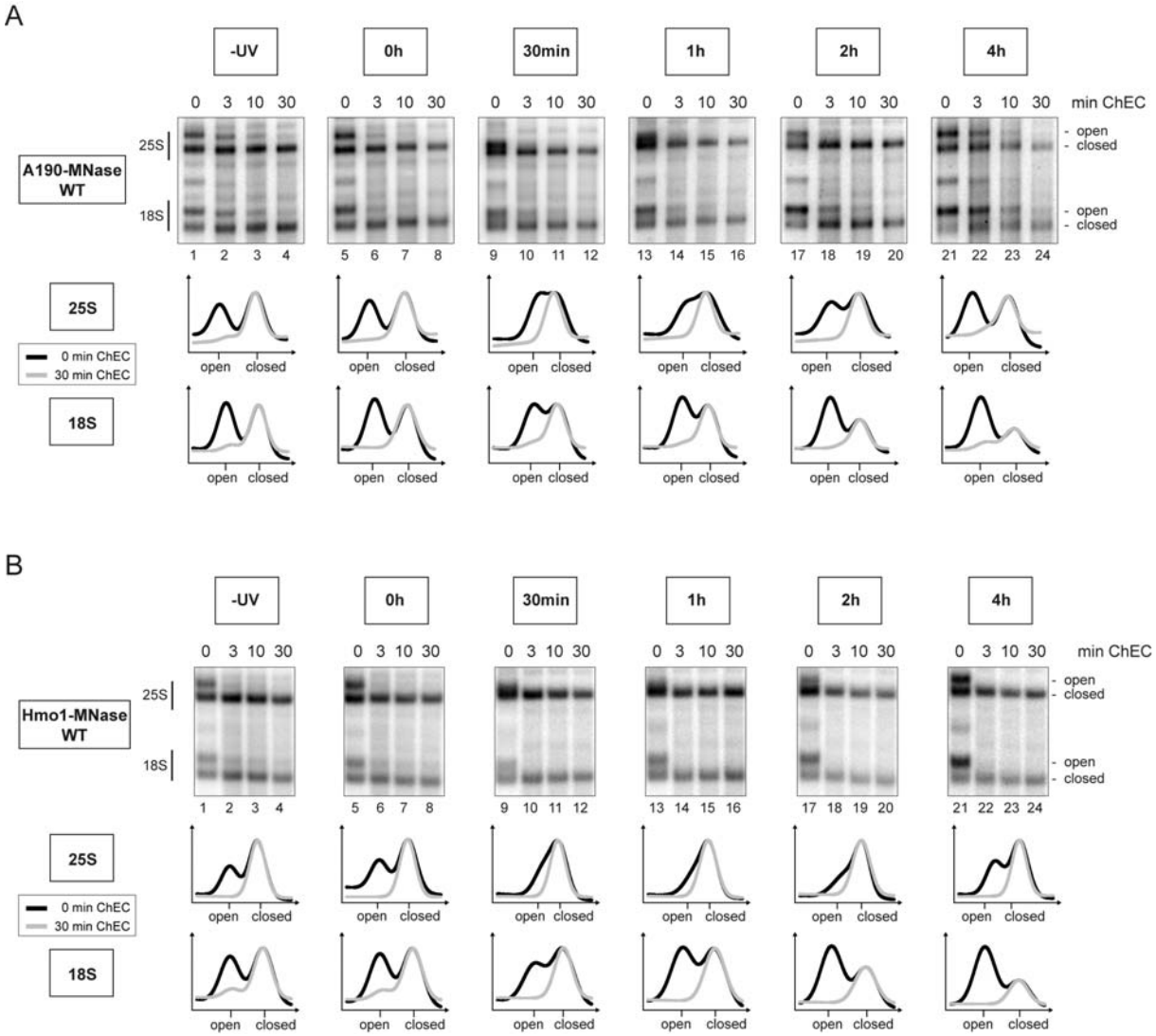

Figure 3-18. RNA polymerase I and Hmo1 are components of rRNA gene chromatin during NER.

(A and B) Yeast strains y2165 and y2166 histones A190 and Hmo1 as MNase fusion proteins, respectively, were cultured at 30°C to exponential phase, irradiated and further cultured at 30°C. Samples were taken before (-UV) and at the indicated times after irradiation and were treated with formaldehyde. Crude nuclei were subjected to ChEC for the times indicated above each lane. After ChEC, nuclei were treated with psoralen and DNA was analysed in a Southern blot as described in the legend to Figure 3-2B. Profile analysis of individual Southern blot lanes was performed as described in the legend to Figure 3-9.

from the strain expressing Hmo1-MNase in comparison to the Pol I-MNase-expressing strain (Figs. 3-18A and 3-18B, compare lanes 9 and 13, see graphs for profile analysis). Similar to the observations made during simultaneous G1 arrest and shutdown of Pol I transcription (subheading 3.1.6), this could indicate that Hmo1 stabilises the open 35S rRNA gene chromatin during UV induced nucleosome assembly and that the Hmo1-MNase fusion protein is partly impaired in this function. In the samples taken 2h and 4h after UV irradiation, open 35S rRNA gene chromatin was re-established and entirely degraded by A190- and Hmo1-MNase during ChEC, respectively (Figs. 3-18A and

3-18B, samples 2h and 4h, see graphs for profile analysis). Thus, Hmo1 and Rpa190 are components of the psoralen accessible fraction of rRNA genes at all time points after UV damage and during NER.

To test if the association of A190- and Hmo1-MNase at the 35S rRNA gene undergoes qualitative changes during UV induced nucleosome assembly, DNA was isolated from a fraction of crude nuclei derived from the experiment shown in Fig. 3-18, prior to treatment with psoralen. The DNA was digested with *Xcm*I and analysed in a Southern blot by indirect end labelling using probes detecting either a fragment containing the 35S rRNA gene promoter element and part of the open reading frame (Fig. 3-19A and 3-19B, top panel) or the terminator and intergenic spacer regions (Fig. 3-19A and 3-19B, bottom panel). The analysis revealed that the cleavage pattern derived by ChEC with A190-MNase remains unchanged at the entire ribosomal DNA after UV irradiation (Fig. 3-19A). Nevertheless, it is noticeable that cleavage events at the very 3' end of the 35S rRNA open reading frame decreased 30min, 1h and 2h after UV irradiation (Fig. 3-19A, bottom panel, region marked by black bar). Remarkably, signal intensities of induced cuts at the same region increased again 4h after incubation in the dark to the level observed before irradiation (Fig. 3-19A, compare lanes 26-28 with 46-48). Thus, A190-MNase induced cleavage events seem to be stronger at the 5' region than at the 3' region of the 35S rRNA gene during the transition of open to closed chromatin after UV irradiation. This is in good correlation with the observed differences in the psoralen accessibility of the 18S and 25S CDS fragments under these conditions (Fig. 3-18A and subheading 3.2.1).

ChEC analysis with Hmo1-MNase after UV irradiation showed slight qualitative changes of induced cuts. Whereas ChEC analysis of the sample taken immediately after UV irradiation yielded the identical cleavage pattern as the sample taken before UV treatment (Fig. 3-19B, compare lanes 2-4 with 6-8 and 26-28 with 30-32), some changes became noticeable starting 30min after incubation in the dark. Two prominent Hmo1-MNase cleavage sites situated in the 35S rRNA coding region got significantly weaker 30min after irradiation and did not reappear even 4h after incubation in the dark (Figs. 3-19B, top panel and Fig. 3-19C, left panel; positions of cleavage sites marked by asterisks). Besides, the appearance of a cleavage event, situated slightly more upstream, could be observed 30min after exposure to UV light (Figs. 3-19B, top panel and Fig. 3-19C, left panel; positions of cleavage sites marked by black square). Furthermore, one cut located at the 3' end of the rRNA precursor gene disappeared 30min after irradiation (Fig. 3-19B, bottom panel and Fig. 3-19C, right panel; lanes 26-28 and 30-32, cleavage sites marked by black dots). Instead, another cut appeared more upstream starting 30min after UV irradiation (Fig. 3-19B, bottom panel and Fig. 3-19C,

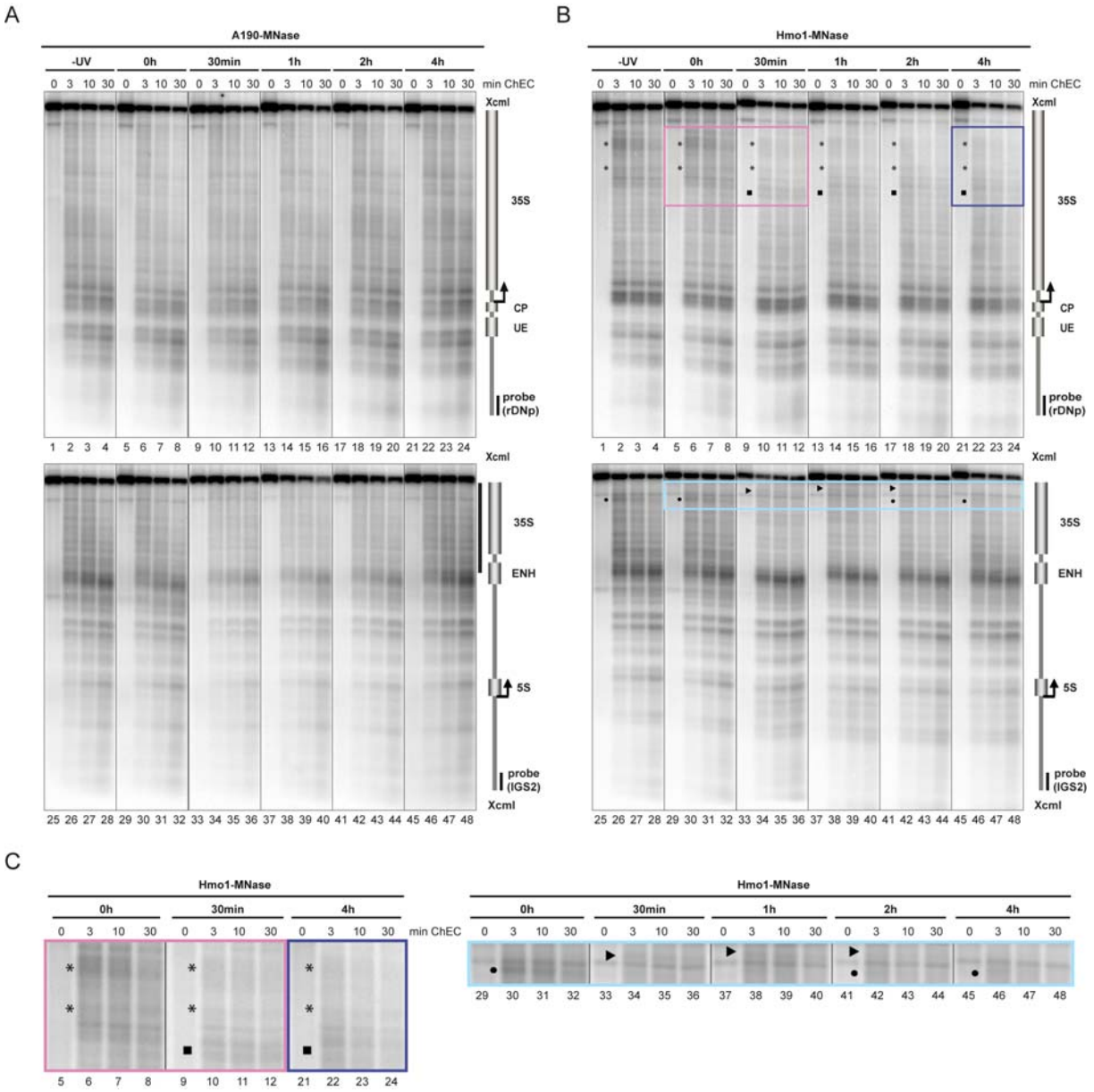

Figure 3-19. Qualitative analysis of A190 and Hmo1 association at the 35S rRNA gene after UV irradiation

(A-C) Yeast strains y2165 and y2166 histones A190 and Hmo1 as MNase fusion proteins, respectively, were cultured at 30°C to exponential phase, irradiated and further cultured at 30°C. Samples were taken before (-UV) and at the indicated times after irradiation and were treated with formaldehyde. Crude nuclei were subjected to ChEC for the times indicated above each lane. DNA was isolated from crude nuclei after ChEC without subsequent psoralen crosslinking, digested with *Xcm*I, and analysed in a Southern blot by indirect end labelling. The cartoons on the right show maps of the fragments analysed by indirect end labelling (see legend to Figure 3-1 for details). The positions of the radioactive probes used for the analysis are indicated (rDNp, IGS2). Symbols highlight changes in MNase accessibility and are referred to in the text. (C) Magnification of selected regions of the Southern blot shown in panel (B)

right panel; cleavage sites marked by black triangles). Interestingly, signal intensity of this cleavage event was reduced 2h and absent 4h after UV irradiation (Fig. 3-19B, bottom panel and Fig. 3-19C, right panel; cleavage sites marked by black triangles).

However, the cut observed before and immediately after UV irradiation reappeared at these late repair timepoints (Fig. 3-19B, bottom panel and Fig. 3-19C, right panel; lanes 41-48, cleavage sites marked by black dots).
Together with the ChEC/Psoralen analyses, these results demonstrate that Pol I and Hmo1 stay associated with the 35S rRNA genes during UV induced nucleosome assembly. Thus, UV irradiation leads to the transition of the open 35S rRNA gene chromatin to a state of heterogeneous psoralen accessibility sharing characteristic components of the open and closed chromatin state.

3.2.5 RNA polymerase I and Hmo1 stay part of 35S rRNA gene chromatin after UV induced nucleosome assembly in the absence of NER

The previous experiment showed that Pol I and Hmo1 are associated with open 35S rRNA genes upon transition to a less psoralen accessible state after UV irradiation in wild type cells. As described before (3.2.2), nucleosome assembly could not be detected in a small population of wild type cells, probably due to early removal of UV induced damage by NER and subsequent opening (3.2.3). Thus, it could be that Pol I and Hmo1 are components of rRNA gene chromatin which has been repaired and started to adopt the open state again.
To investigate if Pol I and Hmo1 remain associated with 35S rRNA gene chromatin even in the absence of repair, ChEC/psoralen experiments were performed with NER deficient *rad14Δ* yeast strains expressing A190 and Hmo1 as MNase fusion proteins, respectively. To this end, yeast cells were crosslinked with formaldehyde before (-UV), immediately after irradiation with UV light (0h) and during incubation in the dark (5min, 15min, 30min, 1h, 2h, 4h). In the samples taken prior to and instantly after UV irradiation Pol I- and Hmo1-MNase fusion proteins degraded selectively the entire open 35S rRNA genes (Figs. 3-20A and 3-20B, samples -UV and 0h, see graphs for profile analysis). A decrease of psoralen accessibility was evident in the Southern blot analysis of psoralen photocrosslinked rDNA derived from the 25S and 18S CDS 5min and 15min after UV irradiation (Figs. 3-20A and 3-20B, lanes 9 and 13, see profile analysis for quantitation). As observed before (subheading 3.2.4), the decrease in psoralen accessibility noticed 15min after UV irradiation was more pronounced in the samples derived from the strain expressing Hmo1-MNase in comparison to the Pol I-MNase-expressing strain (Figs. 3-20A and 3-20B, compare lanes 13, see graphs for profile analysis). Both, A190- and Hmo1-MNase selectively degraded the slower migrating fraction of both rDNA fragments analysed throughout the entire time course experiment, although degradation by A190-

MNase occurred with comparatively slower kinetics (Figs. 3-20A and 3-20B, samples 5min to 4h, see graphs for profile analysis). This leads to the conclusion that both proteins are still components of the psoralen accessible fraction of rRNA genes even in the absence of a functional NER pathway.

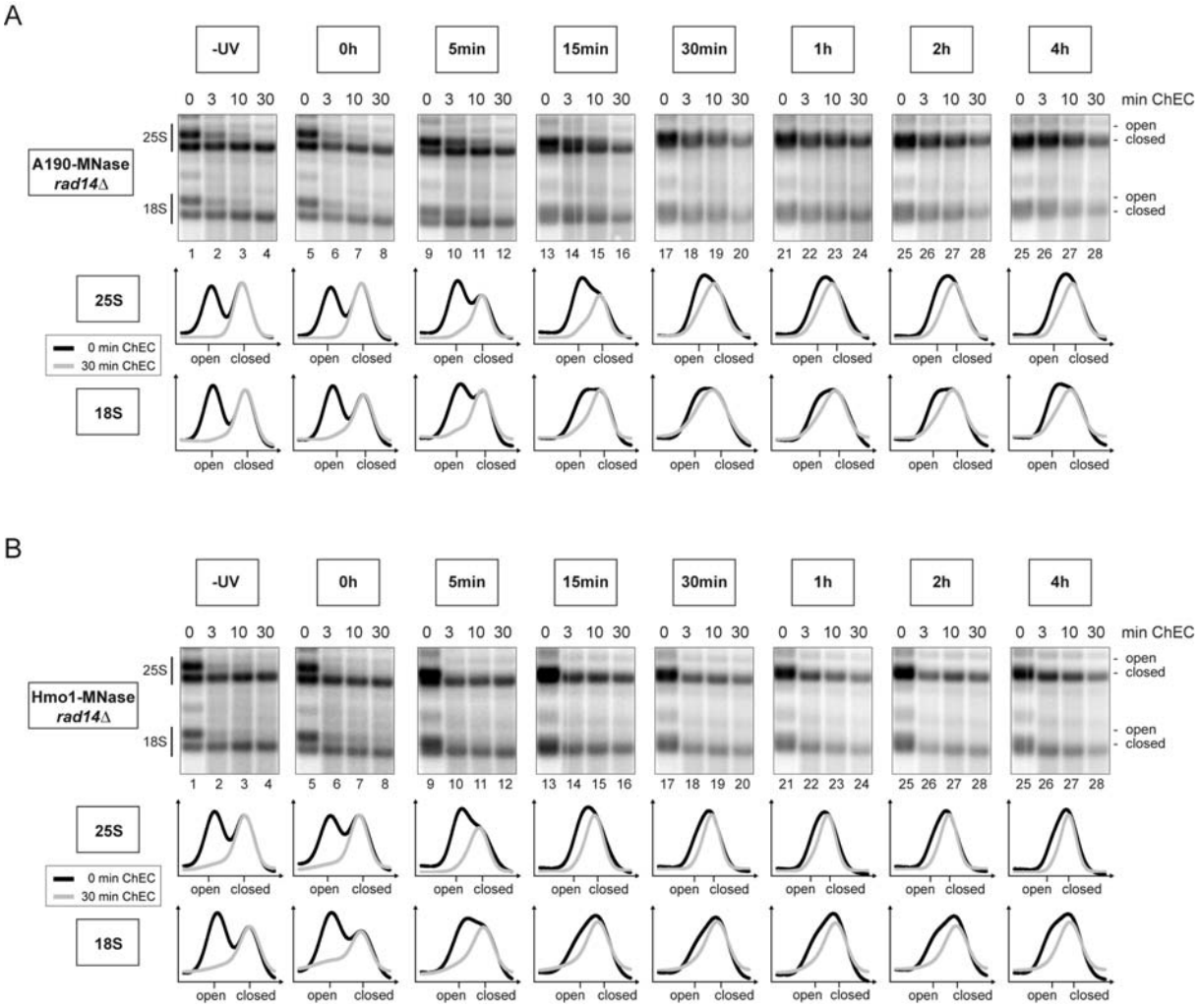

Figure 3-20. RNA polymerase I and Hmo1 remain associated with rRNA genes after UV irradiation in a NER deficient strain.

(A and B) Yeast strains y2459 and y2460, carrying a complete deletion of *RAD14* (*rad14Δ*) and expressing histones A190 and Hmo1 as MNase fusion proteins, respectively, were cultured at 30°C to exponential phase, irradiated and further cultured at 30°C. Samples were taken before (-UV) and at the indicated times after irradiation and were treated with formaldehyde. Crude nuclei were subjected to ChEC for the times indicated above each lane. After ChEC, nuclei were treated with psoralen and DNA was analysed in a Southern blot as described in the legend to Figure 3-2B. Profile analysis of individual Southern blot lanes was performed as described in the legend to Figure 3-9.

In addition, cleavage events mediated by either Pol I- or Hmo1-MNase fusion proteins within the 35S rRNA gene-coding sequence before and after UV irradiation were analysed. To this end, ChEC experiments without subsequent psoralen treatment were

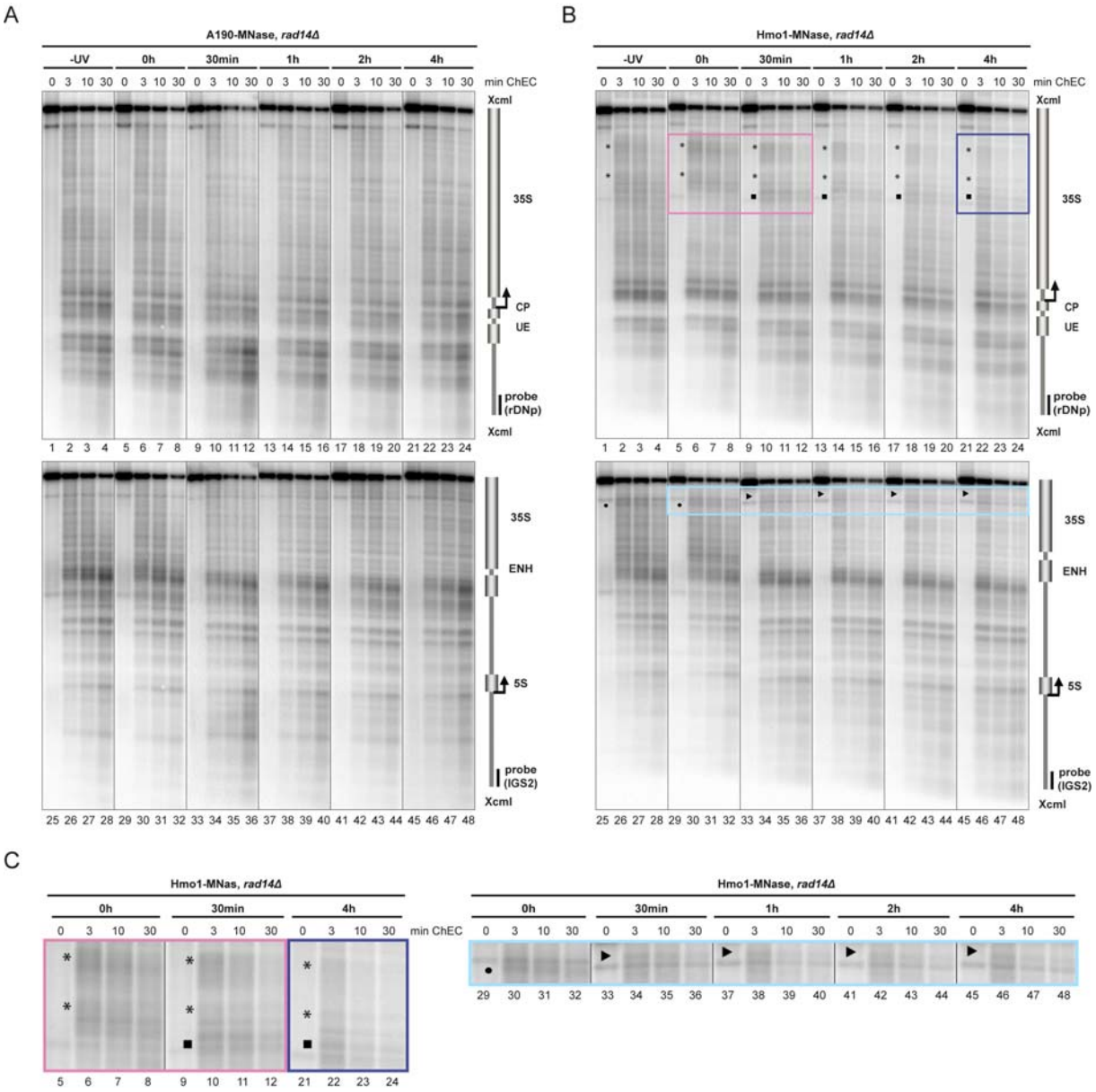

Figure 3-21. Pol I and Hmo1 are still bound to the 35S rRNA gene after UV irradiation in a NER deficient strain

(A and B) Yeast strains y2459 and y2460, carrying a complete deletion of *RAD14* (*rad14Δ*) and expressing histones A190 and Hmo1 as MNase fusion proteins, respectively, were cultured at 30°C to exponential phase, irradiated and further cultured at 30°C. Samples were taken before (-UV) and at the indicated times after irradiation and were treated with formaldehyde. Crude nuclei were subjected to ChEC for the times indicated above each lane. DNA was isolated from crude nuclei after ChEC without subsequent psoralen crosslinking, digested with *Xcm*I, and analysed in a Southern blot by indirect end labelling. The cartoons on the right show maps of the fragments analysed by indirect end labelling (see legend to Figure 3-1 for details). The positions of the radioactive probes used for the analysis are indicated (rDNp, IGS2). Symbols highlight changes in MNase accessibility and are referred to in the text. (C) Magnification of selected regions of the Southern blot shown in panel (B)

performed and the purified DNA was analysed by Southern blot and indirect end labelling. In agreement with the results obtained in the ChEC/psoralen analysis, A190- and Hmo1-MNase induced cuts can be observed in all samples taken during the experiment (Figs. 3-21A and 3-21B). Besides, the qualitative changes of Hmo1-MNase induced cleavage events also observed in the experiment with the corresponding wild type strain became also apparent in the *rad14Δ* strain (Fig. 3-21B, marked by asterisks, squares, dots and triangles). Interestingly, the additional cut introduced at the 3' end of the 35S coding sequence after UV irradiation stayed visible up to 4h after irradiation (Fig. 3-21B, bottom panel and Fig. 3-21C, right panel; cleavage sites marked by black triangles). In accordance with the interpretation of psoralen crosslinking experiments, resetting of chromatin structure to the state observed prior to UV irradiation is dependent on a functional NER pathway.

These results clearly demonstrate that Pol I and Hmo1 remain associated with 35S rRNA gene chromatin, even after UV induced nucleosome assembly in the absence of NER. This corroborates the interpretation that nucleosome assembly at open 35S rRNA genes after UV irradiation results in a mixed chromatin state containing nucleosomes, Pol I and Hmo1, exhibiting decreased psoralen accessibility.

4 Discussion

4.1 Establishment and maintenance of alternative chromatin states at the 35S rRNA genes

The results of the analyses performed in this work led to the conclusion that the interplay between Pol I transcription and replication is sufficient to explain the balance between open and closed chromatin states at the multicopy 35S rRNA genes in growing yeast cells. Accordingly, the 35S rRNA gene chromatin states exist in a dynamic equilibrium resulting from replication-dependent closing and Pol I transcription-dependent opening of genes (Fig. 4-1). In accordance with previous studies (Dammann et al., 1995; Lucchini and Sogo, 1995), the results do not support a model of stable, inheritable 35S rRNA gene chromatin in yeast.

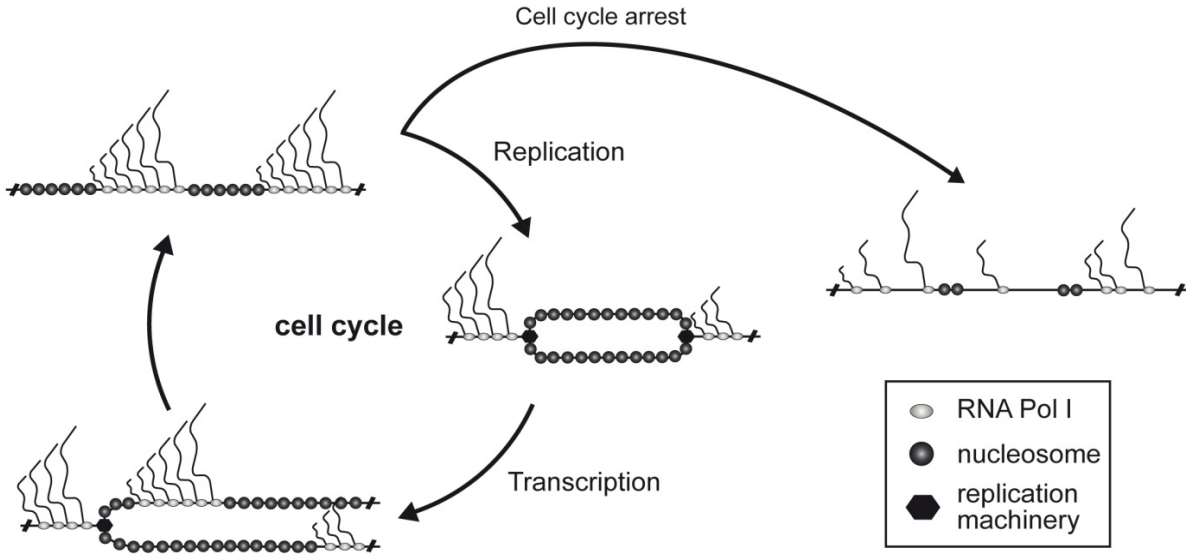

Figure 4-1. Model for the establishment of 35S rRNA gene chromatin states.
In dividing yeast cells, the ratio of open to closed rRNA gene chromatin states is the result of a dynamic equilibrium of replication-dependent nucleosome deposition and Pol I transcription-dependent nucleosome removal. Cell-cycle arrest and thus inhibition of replication, leads to virtually complete opening of rRNA genes, provided that Pol I transcription is ongoing. (modified from Wittner et al., 2011)

In higher eukaryotes, however, inactive rRNA genes may be propagated through DNA replication by a combination of various epigenetic marks, for instance, by DNA methylation (Grummt, 2007; McStay and Grummt, 2008). Besides, it has been suggested that in human cells, rRNA genes may be repressed allelically and that the mark for

inactivation of individual alleles is set very early in development by replication timing (Schlesinger et al., 2009). Nevertheless, a recent study revealed that transcriptionally inactive rRNA genes exist also in the absence of DNA methylation, proposing the existence of two different forms of closed rRNA genes in higher eukaryotes: one heritable over the next generations and dependent on DNA methylation and the other, comparable to the closed chromatin state in yeast, methylation-independent (Gagnon-Kugler et al., 2009). Accordingly, it is conceivable that also in higher eukaryotes, the balance between unmethylated open and closed rRNA genes results from the interplay between Pol I transcription and DNA replication.

4.1.1 DNA replication and Pol I transcription are required for the establishment of 35S rRNA chromatin states

To test if the characteristic chromatin structure of transcriptionally active 35S rRNA genes can be directly transmitted to the newly synthesised daughter strands during DNA replication, Lucchini and Sogo analysed the chromatin state of 35S rRNA genes derived from a yeast cell population enriched in S-phase (Lucchini and Sogo, 1995). In this study, using mainly the electron microscopic analysis of rRNA gene replication intermediates after psoralen crosslinking, they reported that 35S rRNA genes are assembled into nucleosomes within seconds after passage of the replication fork (Lucchini and Sogo, 1995). Besides, they found that (re)activation (opening) of genes may occur shortly after replication (Lucchini and Sogo, 1995).

In the present work, the dynamics of the ratio between open and closed 35S rRNA genes were investigated during the cell cycle by using the psoralen crosslinking technique. Fully consistent with the findings of the Sogo group, results obtained with cells released from different cell cycle arrest situations showed that the psoralen-accessible, open fraction of 35S rRNA genes decreases in the course of replication and increases immediately after completion of S phase (Figs. 3-2 to 3-6). Besides, the present study revealed that in proliferating yeast cells, replication is required to convert 35S rRNA genes into the closed chromatin state. Accordingly, cell cycle arrest and thus inhibition of replication leads to a conversion of almost the entire 35S rRNA gene population into the open chromatin state (Fig. 3-7). However, further experiments are needed to investigate whether the passage of the replication machinery alone or another S phase-specific event is responsible for this conversion. In yeast cells in which most of the 35S rRNA genes are actively transcribed, replication of chromosome XII, harbouring the rDNA locus, is impaired in the

presence of DNA-damaging agents (Ide et al., 2010). Thus, the replication-dependent re-establishment of the closed 35S rRNA gene chromatin structure seems to be required to ensure genome stability in yeast under certain conditions.

A recent study suggested that 35S rRNA genes switch their transcriptional state multiple times in the course of the cell cycle (Tan and van Oudenaarden, 2010). The latter conclusion is based on counting of transcripts from a chromosomally integrated Pol I reporter gene in single cells and mathematical modelling. However, the data obtained in this study do not support that rRNA genes are converted from the open into the closed chromatin state outside of S phase. On the other hand, the present study shows that open rRNA genes do not necessarily have to be transcriptionally active. Accordingly, open rRNA gene chromatin can be stably maintained when Pol I association with the open rRNA gene population is significantly reduced (Fig. 3-9C and 3-9D) or even in the complete absence of Pol I transcription (Fig. 3-12).

It is still an open question why only a fraction of rRNA genes is chosen for activation after passage of the replication fork. One likely explanation would be that the cellular amount of a transcription factor limits the number of rRNA genes suitable for Pol I transcription. A minimal set of factors required for promoter-dependent Pol I transcription initiation *in vitro* has been described in yeast (Keener et al., 1998). Thus, it is feasible to test this hypothesis in the future by over-expressing these factors individually or in combination.

Results from ChEC/psoralen analyses with strains expressing Pol I subunits fused to MNase suggest that during prolonged G1 arrest, either the Pol I density on open 35S rRNA genes decreases or that only a subpopulation of rRNA genes is actively transcribed under these conditions (Fig. 3-9C and 3-9D). Considering the rather decreasing coprecipitation of 35S rRNA gene fragments with the tagged Pol I subunit A190 during G1 arrest (Fig. 3-10), both scenarios are conceivable. Measuring the association of Pol I initiation factors with the 35S rRNA gene promoter could reveal if the complete set of open genes is suitable for Pol I transcription or if the number of initiation competent rRNA genes is unchanged during prolonged cell cycle arrest. A constant number of initiation competent 35S rRNA genes may suggest that the opening observed during cell cycle arrest results from stochastic assembly and disassembly events of initiation factors at rRNA gene promoters.

To shed more light on the molecular mechanisms involved in the establishment of 35S rRNA chromatin states it will be important to test the involvement of histone chaperones in both, Pol I transcription-dependent nucleosome eviction and replication-dependent nucleosome deposition at rRNA genes. One candidate factor is the facilitating chromatin

transcription (FACT) complex, which has been shown to play a role in Pol I transcription in higher eukaryotes (Birch et al., 2009). However, initial experiments using a strain carrying a temperature sensitive mutation in *SPT16* (Formosa et al., 2001), a gene encoding a FACT subunit, revealed that opening of 35S rRNA genes during G1 arrest is not inhibited after shift to the restrictive temperature (data not shown). Thus, FACT seems not to be required for Pol I transcription-dependent nucleosome eviction. Nevertheless, the combination of yeast genetics and biochemistry will allow answering the question if Pol I alone is capable to remove nucleosomes or if additional factors are involved in this process.

4.1.2 Maintenance of the open 35S rRNA gene chromatin state by Pol I and Hmo1

Experiments using a conditional mutant of the Pol I initiation factor Rrn3 revealed that inhibiting Pol I transcription initiation leads to a decrease in the number of open 35S rRNA genes (Fig. 4-2A), correlating with an overall increase of histone occupancy at 35S rRNA genes (Figs. 3-11A and 3-11B). Since replication occurs at least once after shut-down of Pol I transcription initiation (Figs. 3-11A and 3-11D), Pol I transcription appears to be crucial for the maintenance of open 35S rRNA genes in proliferating cells, presumably establishing the open chromatin state after replication. Despite being required for the establishment of the open 35S rRNA gene chromatin structure, Pol I transcription is dispensable for its maintenance in the absence of replication (Figs. 3-12 and 3-14B). In this situation, the presence of the HMG box protein Hmo1 stabilises the nucleosome-free state at 35S rRNA genes, preventing replication-independent nucleosome assembly (Figs. 3-12, 3-14 and 4-2B). Consistently, Hmo1 and histone association with genomic loci seem to be mutually exclusive in exponentially growing yeast cells (Merz et al., 2008; Bermejo et al., 2009) (Figs. 3-9A, 3-9B, 3-9E and 3-10).
Electron microscopy suggested the presence of nucleosome-depleted rRNA genes in many organisms (reviewed in Raska et al., 2004, 2006). Interestingly, the HMG box protein UBF, a potential functional homolog of Hmo1 in higher eukaryotes (Gadal et al., 2002), spreads over the entire rRNA-coding region (O'Sullivan et al., 2002). Furthermore, UBF associates with presumably nucleosome-free, noncondensed rDNA loops surrounding secondary constrictions of metaphase chromosomes (Gébrane-Younès et al., 1997). Although a coexistence of UBF-DNA complexes and histone molecules at mouse rRNA genes cannot be excluded at the moment (Sanij et al., 2008), a study in a

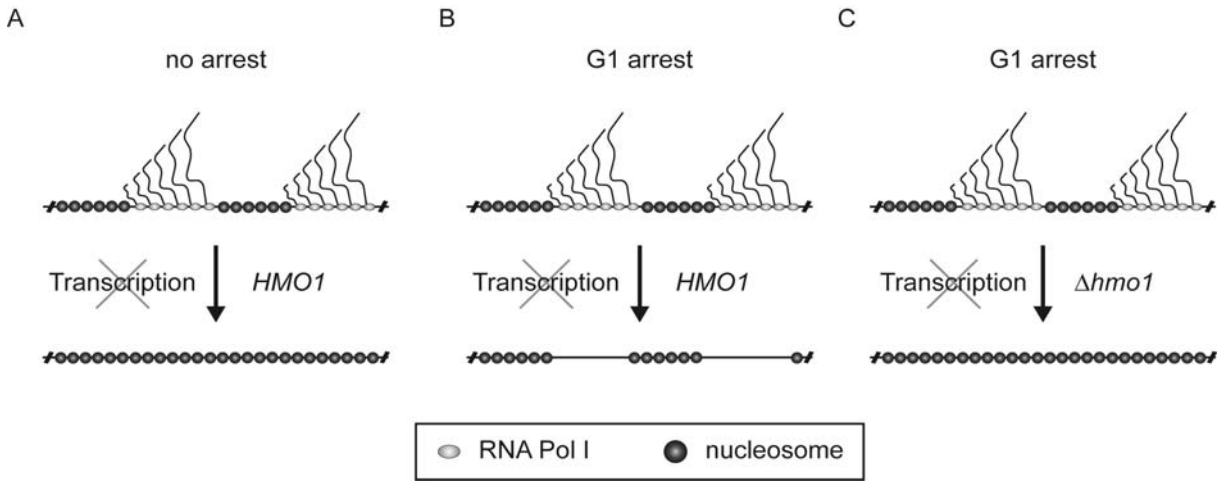

Figure 4-2. Model for the fate of the open 35S rRNA gene chromatin state after inhibition of Pol I transcription initiation.
(A) After inhibition of Pol I transcription initiation nucleosomes can assemble at open 35S rRNA genes, provided that replication is ongoing. (B) Hmo1 prevents replication-independent nucleosome deposition at open rRNA genes during G1 arrest in the absence of Pol I transcription. (C) Nucleosomes are deposited at open 35S rRNA genes during G1 arrest and shutdown of Pol I transcription in the absence of Hmo1.

human cell line demonstrated a striking anticorrelation between the interaction of histones and the interaction of UBF with rRNA genes (Gagnon-Kugler et al., 2009). In addition, UBF interaction with rRNA genes is reduced in S phase (Brown and Szyf, 2008), correlating with the passage of the replication fork and nucleosome deposition. This would be expected if UBF, as Hmo1, is binding preferentially to nucleosome-free rDNA. Furthermore, in the course of granulocyte differentiation, UBF protein levels decrease and its association with rRNA genes is strongly reduced, concomitant with the conversion of these loci into the closed chromatin state (Sanij et al., 2008). This resembles the situation in the *hmo1Δ* deletion strain inhibited in Pol I transcription upon cell-cycle arrest, wherein rRNA genes adopt the closed chromatin state (Fig. 3-14C and 4-2C). Thus, Hmo1 and UBF may help to maintain a nucleosome-depleted chromatin template outside of S phase in yeast and higher eukaryotes, respectively. This could allow the rapid resumption of rRNA gene transcription after downregulation by reduced Pol I loading (French et al., 2003; Claypool et al., 2004; Fahy et al., 2005; Philippi et al., 2010) or Pol I elongation (Stefanovsky et al., 2006) in response to extracellular stimuli without the necessity to overcome the nucleosomal barrier.

In the future, it will be interesting to obtain a more detailed view of the individual processes participating in the dynamic equilibrium of the chromatin states. This and earlier studies show that Pol I transcription is required to recruit Hmo1 to rRNA genes (Kasahara et al., 2007; Goetze et al., 2010), but it is still unclear how this occurs. As

described above (section 2.2.2.1), Hmo1 interacts genetically with Pol I (Gadal et al., 2002), but it is unknown whether the polymerase alone can recruit the HMG box protein to its target sites. Besides binding to 35S rRNA genes, Hmo1 associates with various genomic loci that are also bound by topoisomerase 2 (Bermejo et al., 2009); among them are many promoter regions of (highly transcribed) ribosomal protein genes. This could indicate that Hmo1 recognises specific topological features that are characteristic for DNA regions with high transcriptional activity. It has been shown that recombinant Hmo1 binds tightly to DNA minicircles that may have topological features resembling DNA structures occurring during recombination or during transcription initiation (Kamau et al., 2004). In the light of nuclear topoisomerase activities and the moderate dissociation constant of Hmo1-DNA complexes (Kamau et al., 2004), it is, however, a question how this interaction can be stably maintained *in vivo*. Additionally, the identification of activities that are responsible for replication-independent nucleosome assembly at rRNA genes in the absence of Hmo1 will be helpful to better understand its function in stabilising the open rRNA gene chromatin structure.

4.2 Changes in 35S rRNA gene chromatin after UV induced DNA damage

Very similar to the phenomena observed when cells enter and exit S phase, closing and re-opening of rRNA genes has also been observed after DNA damage by UV irradiation and subsequent NER (Conconi et al., 2005). In this previous study, psoralen crosslinking, restriction enzyme accessibility and MNase digestion revealed that open 35S rRNA genes are converted to the closed chromatin state after the occurrence of DNA lesions as a consequence of UV irradiation. Thus, psoralen accessibility of a fragment derived from the 3' end of the 35S rRNA coding region decreased rapidly after UV irradiation and the open chromatin structure was re-established during NER (Conconi et al., 2005). Interestingly, a decline in Pol I transcription was observed during UV induced closing of 35S rRNA genes and the NER dependent re-opening correlated well with the resumption of transcription (Conconi et al., 2005). Whereas a dynamic re-organisation of 35S rRNA gene chromatin structure after DNA damage and in course of repair has been described in this earlier study, a molecular characterisation of the observed alterations was still missing.

4.2.1 Nucleosome assembly at open 35S rRNA genes after UV irradiation leads to a chromatin structure with mixed protein composition

In the current work, the interaction of histone molecules with genomic DNA was directly monitored indicating that UV irradiation of yeast cells leads to a significant increase in the fraction of 35S rRNA genes being associated with histones (Fig. 3-16). In good accordance with earlier conclusions (Conconi et al., 2005), this suggests that nucleosomes are assembled at open 35S rRNA genes after induction of DNA lesions by UV light. However, a minor subpopulation of 35S rRNA genes still appeared to be histone depleted after UV irradiation of wild type yeast strains (Fig. 3-16A and 3-16B). In contrast, when the same experiments were carried out in NER deficient *rad14Δ* deletion strains, the entire 35S rRNA gene population did associate with histone molecules (Fig. 3-17A and 3-17B). Thus, we conclude that the histone-depleted 35S rRNA genes observed at all time points in UV irradiated yeast wild type cells belong to a subpopulation of rRNA genes which have been rapidly repaired. Pol I transcription can be resumed after NER of DNA lesions in the 35S rRNA genes, leading to the re-establishment of the open chromatin state (Conconi et al., 2005) (Fig. 3-15B).

Accordingly, it has been shown before that the removal of CPDs in the TS of formerly open rRNA genes by TCR initially occurs with fast kinetics whereas the remainder of rRNA genes is repaired with slower, GGR-like kinetics (Conconi et al., 2005). The molecular basis for this differential DNA repair behaviour is unknown.

Previous analyses indicated that Hmo1 and nucleosome association with genomic loci are mutually exclusive (Merz et al., 2008; Bermejo et al., 2009; Wittner et al., 2011). ChEC/psoralen analyses performed in this work revealed that after UV induced nucleosome deposition, the former open 35S rRNA genes exist in a mixed chromatin state, harbouring Pol I, Hmo1 and nucleosomes. It is conceivable that the mixed chromatin state consists of defined nucleosomal and non-nucleosomal stretches, the latter being still associated with Hmo1. Analyses performed in this work suggest that Hmo1 stabilises the open chromatin state in the absence of Pol I transcription and DNA replication, presumably by the inhibition of replication independent nucleosome assembly (subheading 3.1.7 and Wittner et al., 2011). Thus, it would be interesting to get more insight in the molecular mechanism leading to partial Hmo1 removal and the subsequent deposition of nucleosomes after UV irradiation. In growing yeast cells, the conversion of open to closed 35S rRNA gene chromatin is coupled to replication (subheading 3.1.1 and Wittner et al., 2011). Thus, it is tempting to speculate that the DNA synthesis step of NER is responsible for nucleosome assembly. Nevertheless, there is ample evidence speaking against the theory that replication is required for nucleosome deposition. Firstly, the transition from the open to the closed chromatin state occurs in the absence of the damage recognition protein Rad14 and the endonuclase Rad1 (Conconi, 2005). Both proteins, Rad1 and Rad14 are required for the incision step of the NER pathway that occurs prior to the DNA synthesis step (Prakash and Prakash, 2000). Furthermore, the inhibition of the DNA synthesis step does not prevent bidirectional nucleosome assembly initiated at a NER target site *in vitro* (Gaillard et al., 1997).

A mechanism leading to nucleosome deposition at DNA damage sites independent of the DNA synthesis step might involve the histone chaperone CAF-1 and the component of the replication machinery PCNA. Both protein complexes interact directly with each other (Shibahara and Stillman, 1999; Moggs et al., 2000) and interestingly, the CAF-1-PCNA complex is recruited to DNA damage sites in the absence of repair coupled DNA synthesis *in vitro* (Moggs et al., 2000). Besides, PCNA is required for chromatin assembly at single strand DNA breaks *in vitro* (Moggs et al., 2000) and *in vivo* CAF-1 and PCNA are recruited to UV induced damage sites (Green and Almouzni, 2003). However, the dual incision step of NER appears to be indispensable for CAF-1 and

PCNA recruitment (Green and Almouzni, 2003). As mentioned above, the incision step and thus the presence of nicked DNA seem not to be required for nucleosome assembly at damaged yeast 35S rRNA genes. Accordingly, further experiments are required to answer, whether PCNA and CAF-1 are involved in the DNA damage dependent assembly of nucleosomes at the open yeast 35S rRNA genes.

By using a conditional mutant of PCNA (Ayyagari et al., 1995; Amin and Holm, 1996) it could be tested if the conversion of the open to the closed 35S rRNA chromatin state can still occur under restrictive conditions. Furthermore, there is already evidence that the CAF-1 histone chaperone plays a role in the repair of UV damage in DNA, since yeast mutants in which all three genes encoding the CAF-1 subunits have been deleted exhibit increased sensitivity towards UV light (Kaufman et al., 1997; Game and Kaufman, 1999). Thus, experiments with this triple deletion mutant could reveal if CAF-1 is directly involved in the conversion of 35S rRNA gene chromatin structure.

Since NER of DNA lesions is impeded by the presence of nucleosomes, it is still an open question why damaged 35S rRNA genes become nucleosomal after DNA damage by UV irradiation. It could be that packaging of 35S rRNA genes into nucleosomes is important to prevent genomic instability after DNA damage. A recent study showed that yeast cells harbouring an artificially decreased number of rDNA copies, with all 35S rRNA genes present in the open chromatin state, exhibit increased sensitivity towards DNA damage induced by UV light (Ide et al., 2010). Thus, the closed 35S rRNA genes appear to be crucial to ensure genome integrity after DNA damage. In this regard, it will be interesting to test if the occurrence of DNA lesions following UV irradiation in a low copy strain leads to the transition of open to closed 35S rRNA genes comparable to the situation in wild type cells. Besides, measuring the NER rates in such a strain may help to improve the understanding how chromatin structure influences DNA repair. In consideration of the knowledge about NER in 35S rRNA genes so far, one would expect that due to the nucleosome depleted chromatin state of 35S rRNA genes in a low copy strain, CPDs should be removed faster than in a wild type strain.

The discovery of a mutant or a condition preventing UV induced nucleosome assembly will allow addressing the question if closure of 35S rRNA genes is a prerequisite for NER *in vivo*. Preliminary data obtained in experiments with yeast strains being irradiated during G1 arrest suggest that nucleosome assembly is inhibited or at least diminished under this condition (data not shown). Furthermore, the kinetics of re-opening of 35S rRNA genes appear to be accelerated during G1 arrest (data not shown), suggesting that the rate of NER is also enhanced. Since open 35S rRNA genes are repaired more

efficient than closed rRNA genes (Conconi et al., 2002, 2005) and 35S rRNA genes are continuously opening during cell cycle arrest (Fig. 3-7), faster CPD removal might be caused by the increase of the fraction of open 35S rRNA genes. By measuring the rate of NER dependent CPD removal during G1 arrest, additional insight about the impact of chromatin on DNA repair will be gained. In addition, the analysis of repair kinetics during G1 arrest in combination with the inhibition of Pol I transcription and UV irradiation might reveal the contribution of Pol I transcription to NER in 35S rRNA genes.

4.2.2 Nucleosome deposition after UV irradiation and nucleosome removal during NER occurs in a 5'-3'-gradient at the 35S rRNA genes

After UV irradiation of yeast cells, psoralen accessibility of DNA fragments situated either at the 5' end or at the 3' end of the 35S rRNA gene changes differentially with regard to the degree of crosslinking and the kinetics of closing and opening (Fig. 3-15). Thus, the results indicate that UV induced chromatin transitions at the 35S rRNA gene occur in a 5'-3' gradient.

In general, changes in both, psoralen accessibility and association with histone molecules were less pronounced at the 5' end than at the 3' end of 35S rRNA genes in wild type and *rad14Δ* cells (Figs. 3-15B, 3-15C, 3-16 and 3-17). In addition, NER dependent (re-)opening occurred with much faster kinetics at the 5' end than at the 3' end (Fig 3-15B). One explanation for this phenomenon might be the different size of the rRNA gene fragments analysed. The fragment bearing the 3' end is approximately 1kb larger than the fragment bearing the 5' end and thus is likely to carry more CPDs in average, which in turn may lead to increased nucleosome assembly and prolonged repair times.

Interestingly, during NER the fraction of open rRNA genes steadily increases (Fig. 3-15B). Very similar to the situation after cell cycle arrest (Fig. 3-7), 35S rRNA genes are continuously opening under this condition and 4h after UV irradiation a majority of the 35S rRNA genes are open at the 5' end (Fig. 3-15B). Interestingly, flow cytometric data suggest that cell cycle progression is impeded in G1 or at the G1/S transition after UV irradiation and thus that DNA replication is inhibited (Fig. 3-15B).

The (re-)establishment of the open chromatin structure after UV irradiation at the 35S rRNA genes is dependent on functional NER (Conconi et al., 2005) (Fig. 3-15) and the establishment of the open 35S rRNA gene chromatin state has been correlated with Pol I transcription (Fig. 3-12). Thus, the differences in the degree of opening at the 5' and 3'

end of the 35S rRNA genes during NER of DNA lesions might be explained by gradual 5'-3' removal of CPDs and the successive re-opening by Pol I transcription until the next CPD is reached. Thus, continuous Pol I initiation and elongation up to the first DNA lesion will stabilise the open chromatin state at the 5' end of the rRNA gene explaining why it remains largely psoralen accessible in contrast to the 3' end of the gene (Figs. 3-15B, 3-15C, 3-16 and 3-17).

Accordingly, additional data correlating Pol I association with the (re-)establishment of the open 35S rRNA gene chromatin state during NER showed that shortly after UV irradiation Pol I association decreases significantly at a certain 35S rRNA gene region situated approximately 3kb downstream of the transcription start site (Tremblay et al., submitted). Interestingly, under the conditions used for UV irradiation almost all 35S rRNA genes contain a CPD within the sequence spanning the first 3kb of the 35S rRNA CDS (Tremblay et al., submitted). Accordingly, Tremblay et. al. concluded that transcription initiation is still ongoing after induction of UV damage and that Pol I elongates until it is stopped at the first CPD in the sequence, where it finally dissociates, leading to nucleosome assembly downstream of the DNA lesion. It is known that Pol II is stalled at CPDs in the TS (Selby et al., 1997) and that the arrested polymerase recruits factors involved in TCR (Lainé and Egly, 2006). A similar mechanism might also apply to Pol I and due to the high density of polymerases at the transcribed 35S rRNA genes (French et al., 2003), the observed dissociation of Pol I might result from the collision between elongating and stalled polymerases.

Along these lines, ChEC and ChEC/Psoralen analyses performed in the current study indicate that Pol I stays associated with the entire 35S rRNA gene sequence of former actively transcribed genes, even after nucleosome assembly (Figs. 3-18, 3-19, 3-20 and 3-21). However, if polymerases are stalled at all DNA lesions in the 35S rRNA gene and stalled polymerases would serve as the trigger for TCR, it is still elusive why CPDs should be repaired in a 5'-3' gradient. This may indicate that it is in fact the continuous dissociation of Pol I, induced by the collision between elongating and stalled polymerases occurring only at the CPD located next to the transcription start site that serves as the signal for the recruitment of the NER machinery.

5 Material and Methods

5.1 Material

5.1.1 Chemicals

Chemicals were purchased at the highest available purity from Sigma-Aldrich, Merck, Fluka, Roth or J.T.Baker, except agarose electrophoresis grade (Invitrogen), bromine phenol blue (Serva), G418/Geneticin (Gibco), milk powder (Sukofin), Nonidet P-40 substitute (NP40) (USB Corporation), Tris ultrapure (USB Corporation) and Tween 20 (Serva). Ingredients for growth media were purchased from BD Biosciences (Bacto Agar, Bacto Peptone, Bacto Tryptone and Bacto Yeast Extract), Q-Biogene, Bio101, Inc. or Sunrise Science Products (Complete supplement mixtures (CSM), Yeast nitrogen base (YNB), amino acids and adenine) and Sigma-Aldrich (D(+)-glucose, amino acids and uracil). Water was always purified with an Elga Purelab Ultra device prior to use.

5.1.2 Media and buffers

Unless stated otherwise, all solutions have been prepared in water that has a resistivity of 18.2 MΩ-cm and total organic content of less than five parts per billion. The pH values were measured at room temperature. Percentage is mass per volume (m/v) and pH was adjusted with HCl or NaOH if not indicated otherwise.

media & buffer	ingredients	concentration
LB medium	Tryptone	10g/l
	Yeast extract	5g/l
	NaCl	5g/l
	1M NaOH	1ml/l
	Agar (plates)	20g/l
	Autoclave	
LB/Amp	Ampicillin in LB medium,	50µg/ml
YPD	Yeast extract	10g/l
	Peptone	20g/l
	Glucose	20g/l
	Agar (plates)	20g/l
	Autoclave	

YPD with Geneticin	YPD + Geneticin (Gibco) in YPD	400mg/l
YPAD	YPD + adenine hemisulfate salt	100mg/l
Synthetic medium (SDC)	YNB CSM Glucose/Galactose Agar (plates) Autoclave	6.7g/l see product sheet 20g/l 20g/l
IR buffer	Tris-HCl pH 8 EDTA	50mM 20mM
IRN buffer	Tris-HCl pH 8 EDTA NaCl	50mM 20mM 0.5M
TBE buffer	Tris Boric acid EDTA	90mM 90mM 1mM
10 x DNA loading buffer	Bromphenol blue Xylen cyanol Glycerine	0.25% 0.25% 40%
TE buffer	Tris-HCl pH 8 EDTA	10mM 1mM
20 x SSC	NaCl Tri-sodium citrate dehydrate pH7 with HCl	3M 0.3M
Buffer A	Tris-HCl pH 7.4 Spermine Spermidine KCl EDTA	15mM 0.2mM 0.5mM 80mM 2-4mM
Buffer Ag	Buffer A without EDTA EGTA	 0.1mM
Protease Inhibitors 100x	Benzamidine PMSF	33mg/ml 17mg/ml
4 x Upper Tris	Tris SDS Bromphenol blue pH 6.8 with HCl	0.5M 0.40%
4 x Lower Tris	Tris SDS pH 8.8 with HCl	1.5M 0.40%

Transfer buffer (Western Blot)	Tris	25mM
	Glycine	192mM
	Methanol	20%
10 x Electrophoresis buffer (SDS-PAGE)	Tris	250mM
	Glycin	1.9 M
	SDS	1.00%
10 x PBS	NaCl	1.37M
	KCl	27mM
	Na2HPO4·2H2O	10mM
	KH2PO4	20mM
	pH 7.4 with HCl or NaOH	
PBST	PBS	1x
	Tween 20	0.05%
ChIP Lysis buffer	Hepes pH 7.5	50mM
	NaCl	140mM
	EDTA	5mM
	EGTA	5mM
	Triton X100	1%
	DOC	0.10%
ChIP Wash buffer I	Hepes pH 7.5	50mM
	NaCl	500mM
	EDTA	2mM
	Triton X100	1%
	DOC	0.10%
ChIP Wash buffer II	Tris-HCl pH 8	10mM
	LiCl	250mM
	EDTA	2mM
	Nonidet P40	0.50%
	DOC	0.50%
HU buffer SDS	Tris-HCl pH 6.8	5%
	EDTA	200mM
	β-mercapto-ethanol	1mM
	Urea	1.50%
	Bromophenolblue; store at -20°C	8M
TELit LiOAc	Tris-HCl pH 8	100mM
	EDTA pH 8	10mM
	pH 8 with HOAc	1mM
LitSorb Sorbitol	dissolved in TELit	1M
	autoclave, store at room temperature	40%
LitPEG	Polyethylene glycol (PEG3350 (Sigma))	
	dissolved in TELit, autoclave, store at RT	

5.1.3 Nucleic acids

A) Nucleotides

For synthesis of DNA molecules the “desoxynucleotide solution mix” by New England Biolabs was used which contains each of the four desoxynucleotides in 10mM concentration.

B) Oligonucleotides

oligo-nucleotides	sequence	purpose	gene/locus
941	GATGGTACCGGTACGGGTTCATTTGATGTGTTAGCAAAGGTTCCAAATGCGGCTTCGTACGCTGCAGGTCGAC	Primer to obtain amplicon of K643 for genomic integration of MNase-3xHA KanMX6	*RPA190*
942	CTACCGCGGAAACTAATATTAAATCGTAATAATTATGGGACCTTTTGCCTGCTTATCGATGAATTCGAGCTCG	Primer to obtain amplicon of K643 for genomic integration of MNase-3xHA KanMX6	*RPA190*
937	GATGGTACCGAAAACACCAGTGAAAGCAATGATGGTGAATCGAGTGATAGTGATTCGTACGCTGCAGGTCGAC	Primer to obtain amplicon of K643 for genomic integration of MNase-3xHA KanMX6	*RPA43*
938	CTACCGCGGAACGTATATCTTTATTTGTTTTGATTTTTTCTCATTTTTCCCGTCATCGATGAATTCGAGCTCG	Primer to obtain amplicon of K643 for genomic integration of MNase-3xHA KanMX6	*RPA43*
935	GATGGTACCAAGAAGAAGAAGGATAAGAAGAAGGACAAATCCAACTCTTCTATTTCGTACGCTGCAGGTCGAC	Primer to obtain amplicon of K643 for genomic integration of MNase-3xHA KanMX6	*HMO1*
936	CTACCGCGGATTTTAGAAAGACAGTAGAGTAATAGTAACGAGTTTGTCCGTCCAATCGATGAATTCGAGCTCG	Primer to obtain amplicon of K643 for genomic integration of MNase-3xHA KanMX6	*HMO1*
797	TCAAGTTGGCTAGAAGATTAAGAGGTGAAAGATCACGGATCCCCGGGTTAATTAA	Primer to obtain amplicon of K643 for genomic integration of MNase-3xHA KanMX6	*HHT1*

847	CTACCGCGGTGTGTTTTTGTTC GTTTTTTACTAAAACTGATGACA ATCAACAAAATCGATGAATTCG AGCTCG	Primer to obtain amplicon of K643 for genomic integration of MNase-3xHA KanMX6	*HHT1*
1356	GATGGTACCCTTGTTGCCAAAG AAGTCTGCCAAGGCTACCAAG GCTTCTCAAGAATTATCGTACG CTGCAGGTCGAC	Primer to obtain amplicon of K643 for genomic integration of MNase-3xHA KanMX6	*HTA1*
1357	CTACCGCGGGGAGAAGCAGTT TAGTTCCTTCCGCCTTCTTTAAA ATACCAGAACCGATCATCGATG AATTCGAGCTCG	Primer to obtain amplicon of K643 for genomic integration of MNase-3xHA KanMX6	*HTA1*
1354	GATGGTACCCTTATACTCTAGG ATGTACATCCTACCACACACAA CAAGCCTGTCACACCTACGACT CACTATAGGG	Primer to obtain amplicon of K643 for genomic integration of MNase-3xHA KanMX6	*HMO1*
1355	CTACCGCGGTATTTATTTTAGAA AGACAGTAGAGTAATAGTAACG AGTTTGTCCGTCCATCCATGGA AAAGAGAAG	Primer to obtain amplicon of K643 for genomic integration of MNase-3xHA KanMX6	*HMO1*
817	GAGGGACGGTTGAAAGTG	Primer to obtain template for Southern probe preparation from genomic DNA	*35S rRNA gene*
818	ATACGCTTCAGAGACCCTAA	Primer to obtain template for Southern probe preparation from genomic DNA	*35S rRNA gene*
1163	TGTTGCTAGATCGCCTGGTA	Primer to obtain template for Southern probe preparation from genomic DNA	*GAL1*
1164	TTTCCGGTGCAAGTTTCTTT	Primer to obtain template for Southern probe preparation from genomic DNA	*GAL1*
626	CCATTCCGTGAAACACC	Primer to obtain template for Southern probe preparation from genomic DNA	*35S rRNA gene*
627	AAGAAAGAAACCGAAATCTC	Primer to obtain template for Southern probe preparation from genomic DNA	*35S rRNA gene*
2208	GCGGCGAGCGCTATCGATGAA TTCGAGCTCG	Primer to obtain amplicon of K936 for genomic integration of *kl TRP1*	*kl TRP1*

2209	GATGATGCGCGCCGTACGCTG CAGGTCGAC	Primer to obtain amplicon of K936 for genomic integration of *kl TRP1*	*kl TRP1*
1502	AACAACGAAACGCCTTCATC	Primer to obtain amplicon of pBS1479 for genomic integration of *kl TRP1*	*kl TRP1*
1504	AGGGAGCTCTCCATGGAAAAG AGAAG	Primer to obtain amplicon of pBS1479 for genomic integration of *kl TRP1*	*kl TRP1*
920	GCCATATCTACCAGAAAGCACC	Primer used for qPCR amplifying a region in 5S rDNA together with primer 921	*5S*
921	GATTGCAGCACCTGAGTTTCG	Primer used for qPCR amplifying a region in 5S rDNA together with primer 920	*5S*
969	TCATGGAGTACAAGTGTGAGGA	Primer used for qPCR amplifying rDNA promoter region together with primer 970	*Prom*
970	TAACGAACGACAAGCCTACTC	Primer used for qPCR amplifying rDNA promoter region together with primer 969	*Prom*
2481	GGTGGTAAATTCCATCTAAAGC TAAATATT	Primer used for qPCR amplifying a region in 25S rDNA together with primer rDNA8 Th rev	*25S_1*
2482	TTTGAAAAGAGAGTGAAAAAGT ACGTG	Primer used for qPCR amplifying a region in 25S rDNA together with primer rDNA8 Th fo	*25S_1*
710	TGGAGCAAAGAAATCACCGC	Primer used for qPCR amplifying a region in 25S rDNA together with primer 711	*25S_2*
711	CCGCTGGATTATGGCTGAAC	Primer used for qPCR amplifying a region in 25S rDNA together with primer 710	*25S_2*
712	GAGTCCTTGTGGCTCTTGGC	Primer used for qPCR amplifying a region in 18S rDNA together with primer 713	*18S_2*
713	AATACTGATGCCCCCGACC	Primer used for qPCR amplifying a region in 18S rDNA together with primer 712	*18S_2*

2688	TCCCTTGGGTTGAAGTTCTG	Primer used for qPCR amplifying a region at the 3`-end of *NUP57* together with primer 2689	*NUP57*
2689	ACGAATCAACAACGCGGTA	Primer used for qPCR amplifying a region at the 3`-end of *NUP57* together with primer 2688	*NUP57*
611	AGGCGAAGAAAACCCACAAA	Primer used for qPCR amplifying a region within the ORF of *NOC1* together with primer 2689	*NOC1*
612	GTCGTCAGCATCCTCGTCAG	Primer used for qPCR amplifying a region within the ORF of *NOC1* together with primer 2688	*NOC1*
3040	ACTAGAAAAAGAGTTTGGATCTTCGTAGTGAAGGTATCGAACGTAACGCTTAGTGGGCCATCGCCCTGA	Primer obtain *RAD14* KO amplicon of K355 for genomic integration of *LEU2*	*LEU2*
3041	AACACCTTATTATGACTTTCTTGTTATATTCTTATATACATAACCAACATAAAATCCTCCAATATCAAAT	Primer obtain *RAD14* KO amplicon of K355 for genomic integration of *LEU2*	*LEU2*

C) DNA probes for Southern Blot detection

name	**synthesis**	**locus**	**restriction enzyme**	**fragment size (kb)**
3.5kb rDNA	digest of pNOY373 with *Nco*I and purification of 3.5kb fragment	rDNA	*Eco*RI	2.6, 1.9, 0.7
rDNp	PCR from genomic DNA using primers 817 and 818	rDNA	*Eco*RI	2.4
rDNp	PCR from genomic DNA using primers 817 and 818	rDNA	*Xcm*I	4.9
GAL1	PCR from genomic DNA using primers 1163, 1164	GAL1-10	*Eco*RI	1.9
ETS1	PCR from genomic DNA using primers 626, 627	rDNA	*Eco*RI	1.9
IGS2	PCR from genomic DNA using primers 1161, 1162	rDNA	*Xcm*I	4.3kb

D) Plasmids

plasmid	Nr.	Cloning	Function	Reference
pBluescript KS (+/-)	1		LacZ T3 and T7 promoter M13 - 20 T7 and SK primer Col E 1 - Origin f1ori (+or -)	Stratagene
pKM9	643	PCR with primers 839, 840 from pYM1 (V36; 3xHA-Tag) via *Bbs*I, *Bss*HII in *Bbs*I, *Bss*HII from pFA6a-MN-KanMX6 (K456)	(PCR-) template, cloning	Katharina Merz
pKM14	648	PCR with primers 941, 942 from pKM9 via *Kpn*I and *Sac*II in pBluescript KS	genomic C-terminal MNase tagging by recombination, linearisation with *Kpn*I, *Sac*II	Katharina Merz
pKM15	649	PCR with primers 935, 936 from pKM9 via *Kpn*I and *Sac*II in pBluescript KS	genomic C-terminal MNase tagging by recombination, linearisation with *Kpn*I, *Sac*II	Katharina Merz
pKM18	652	PCR with primers 941, 942 from pKM9 via *Kpn*I and *Sac*II in pBluescript KS	genomic C-terminal MNase tagging by recombination, linearisation with *Kpn*I, *Sac*II	Katharina Merz
pKM20	654	PCR with primers 1018, 846 from pKM9 via *Kpn*I and *Sac*II in pBluescript KS	genomic C-terminal MNase tagging by recombination, linearisation with *Kpn*I, *Sac*II	Katharina Merz
pW217	1184	see in Methods	exchange of genomic *BAR1* with *HIS3*, digest with *Xba*I	Wolfgang Seufert
pMW_BAR1-KO-TRP	1229	see in Methods	exchange of genomic *BAR1* with k.l.*TRP1*, digest with *Xba*I	this study
pB3.1	355	Leu2 marker framed with RS-sites, lexA SOS-box eliminated by *Bae*I-digest of pB2 and religation after blunting with Klenow	Shuttle vector for RecR-expression in yeast under the control of the *GAL1* promoter.	Achim Griesenbeck

5.1.4 Enzymes and Polypeptides

All enzymes were used with the provided buffers.

enzyme/polypeptide	manufacturer
Go Taq Polymerase	Promega
Herculase	Stratagene
Restriction endonucleases	New England Biolabs
T4-DNA-ligase	New England Biolabs
Zymolyase T100	Seikagaku Corporation
Prestained protein-marker broad range	New England Biolabs
α-Mating Factor acetate salt	Sigma

5.1.5 Antibodies

antibody	origin	dilution	manufacturer
3F10 anti-HA	monoclonal rat	1:5000	Roche
Goat anti-rat (peroxidase-conjugated)	goat	1:2500	Jackson ImmunoResearch

5.1.6 Organisms

A) Host bacteria

For cloning, the electro-competent *E. coli* strain “XL1BlueMRF” (Stratagene) was used. Genotype: Δ(mcrA)183, Δ(mcrCB-hsdSMR-mrr)173, endA1, supE44, thi-1, recA1, gyrA96, relA1, lac, λ-, *F´, proAB, lacIqZΔM15, tn10(tetr)+.

B) Yeast strains

Establishment of strains expressing MNase fusion proteins

All yeast strains expressing fusion proteins with a C-terminal micrococcal nuclease (MNase) marked by a triple hemagglutinin (HA) epitope were generated as described previously (Merz et al., 2008). Proper expression of the MNase fusion proteins was tested by Western blot analysis (data not shown). None of the MNase tags led to an obvious growth phenotype, except for y2116 which grew slightly slower than the other strains (data not shown).

Establishment of knock-out strains

HMO1 deletion was performed as described before (Merz et al., 2008).

To establish *BAR1* deletion strains, a 3.5kb *Hind*III/*Xho*I genomic fragment containing *BAR1* was subcloned into *Hind*III, *Sal*I digested pUC13. A 0.4kb *Bgl*II/*Sal*I fragment within the *BAR1* coding sequence was replaced by a *Bam*HI/*Xho*I fragment of pJJ215 (Jones and Prakash, 1990) containing the *HIS3* gene. The resulting plasmid, pW217, was digested with *Xba*I, precipitated with ethanol and transformed into yeast cells to replace the endogenous *BAR1* locus by homologous recombination. K936 was generated by inserting the *TRP1* gene of *Kluyveromyces lactis* (*kl TRP1*), amplified with primers 1502/1503 from pBS1479 (Puig et al., 2001) and digested with *Sma*I/*Sac*I into *Sma*I/*Sac*I digested K643 (Merz et al., 2008). The *kl TRP1* gene amplified with primers 2208/2209 from K936 was digested with *Afe*I/*Bss*HI and cloned into *Afe*I/*Bss*HI digested pW217. The resulting plasmid, K1229, was digested with *Blp*I/*Eco*RV, precipitated with ethanol and transformed into NOY1071 cells to replace the endogenous *BAR1* locus by homologous recombination.

To establish *RAD14* deletion strains the *LEU2* gene was amplified with primers 3040 and 3041 from plasmid K355. Primers 3040 and 3041 contain 50bp of DNA sequence homologous to the 5' sequence upstream of the ATG, and 50bp of sequence homologous to the DNA downstream of the stop codon of the *RAD14* open reading frame, respectively. The amplicon was directly used for transformation.

name	genotype	reference or source
NOY505	*MATa ade2-1 ura3-1 trp1-1 leu2-3,112 his3-11 can1-100*	(Nogi et al., 1991)
NOY1075	*MATa ade2-1 ura3-1 trp1-1 leu2-3,112 his3-11,15 can1-100 rrn3 (S213P)*	(Claypool et al., 2004)
y1704	*MATa ade2-1 ura3-1 trp1-1 leu2-3,112 his3-11 can1-100 bar1::HIS3 RPA43-MNase-3xHA:kanMX6*	this study
y1717	*MATa ade2-1 ura3-1 trp1-1 leu2-3,112 his3-11 can1-100 bar1::HIS3 RPA190-MNase-3xHA:kanMX6*	this study
y1757	*MATa ade2-1 ura3-1 trp1-1 leu2-3,112 his3-11 can1-100 bar1::HIS3*	this study
y1759	*MATa ade2-1 ura3-1 trp1-1 leu2-3,112 his3-11 can1-100 bar1::kl TRP1 fob1::HIS3 RDN: ~25 copies*	this study
y1761	*MATa ade2-1 ura3-1 trp1-1 leu2-3,112 his3-11 can1-100 bar1::HIS3 HMO1-MNase-3xHA:kanMX6*	this study

y1867 (K2032)	*MATa ade2-1 ura3-1 trp1-1 leu2-3,112 his3-11,15 can1-100 cdc7-1*	(Moll et al., 1991)
y1925 (W9313)	*MATa ade2-1 ura3-1 trp1-1 leu2-3,112 his3-11 can1-100 cdc15-2*	(Schwab et al., 1997)
y1995	*MATa ade2-1 ura3-1 trp1-1 leu2-3,112 his3-11 can1-100 bar1::HIS3 HHT1-MNase-3xHA:kanMX6*	this study
y2116	*MATa ade2-1 ura3-1 trp1-1 leu2-3,112 his3-11 can1-100 bar1::HIS3 HTA1-MNase-3xHA:kanMX6*	this study
y2022	*MATa ade2-1 ura3-1 trp1-1 leu2-3,112 his3-11,15 can1-100 rrn3 (S213P) bar1::HIS3*	this study
y2119	*MATa ade2-1 ura3-1 trp1-1 leu2-3,112 his3-11,15 can1-100 rrn3 (S213P) bar1::HIS3 HMO1-MNase-3xHA:kanMX6*	this study
y2120	*MATa ade2-1 ura3-1 trp1-1 leu2-3,112 his3-11,15 can1-100 rrn3 (S213P) bar1::HIS3 HHF2-MNase-3xHA:kanMX6*	this study
y2121	*MATa ade2-1 ura3-1 trp1-1 leu2-3,112 his3-11,15 can1-100 rrn3 (S213P) bar1::HIS3 HTB2-MNase-3xHA:kanMX6*	this study
y2122	*MATa ade2-1 ura3-1 trp1-1 leu2-3,112 his3-11 can1-100 bar1::HIS3 HHF2-MNase-3xHA:kanMX6*	this study
y2123	*MATa ade2-1 ura3-1 trp1-1 leu2-3,112 his3-11,15 can1-100 rrn3 (S213P) bar1::HIS3 A190-MNase-3xHA:kanMX6*	this study
y2138	*MATa ade2-1 ura3-1 trp1-1 leu2-3,112 his3-11 can1-100 bar1::HIS3 hmo1::URA3*	this study
y2139	*MATa ade2-1 ura3-1 trp1-1 leu2-3,112 his3-11,15 can1-100 rrn3 (S213P) bar1::HIS3 hmo1::URA3*	this study
y1862	*MATα his3-200 leu2-1 met15-0 trp1-63 ura3-167 RDN1::Ty1-MET15 RDN1::mURA3-HIS3*	(Smith et al., 1999)
y2456	*MATα his3-200 leu2-1 met15-0 trp1-63 ura3-167 RDN1::Ty1-MET15 RDN1::mURA3-HIS3 rad14::LEU2*	this study
y2163	*MATα his3-200 leu2-1 met15-0 trp1-63 ura3-167 RDN1::Ty1-MET15 RDN1::mURA3-HIS3 rad14::LEU2 HTA1_MNase_3xHA_KAN_MX6*	this study
y2164	*MATα his3-200 leu2-1 met15-0 trp1-63 ura3-167 RDN1::Ty1-MET15 RDN1::mURA3-HIS3 rad14::LEU2 HHT1_MNase_3xHA_KAN_MX6*	this study
y2165	*MATα his3-200 leu2-1 met15-0 trp1-63 ura3-167 RDN1::Ty1-MET15 RDN1::mURA3-HIS3 rad14::LEU2 HMO1_MNase_3xHA_KAN_MX6*	this study
y2166	*MATα his3-200 leu2-1 met15-0 trp1-63 ura3-167 RDN1::Ty1-MET15 RDN1::mURA3-HIS3 rad14::LEU2 RPA190_MNase_3xHA_KAN_MX6*	this study
y2457	*MATα his3-200 leu2-1 met15-0 trp1-63 ura3-167 RDN1::Ty1-MET15 RDN1::mURA3-HIS3 HTA1_MNase_3xHA_KAN_MX6*	this study

y2458	*MATα his3-200 leu2-1 met15-0 trp1-63 ura3-167 RDN1::Ty1-MET15 RDN1::mURA3-HIS3 HHT1_MNase_3xHA_KAN_MX6*	this study
y2459	*MATα his3-200 leu2-1 met15-0 trp1-63 ura3-167 RDN1::Ty1-MET15 RDN1::mURA3-HIS3 HMO1_MNase_3xHA_KAN_MX6*	this study
y2460	*MATα his3-200 leu2-1 met15-0 trp1-63 ura3-167 RDN1::Ty1-MET15 RDN1::mURA3-HIS3 RPA190_MNase_3xHA_KAN_MX6*	this study

5.1.7 Equipment

device	manufacturer
Eraser	Raytest
BAS cassette 2040	Fuji
BAS-III imaging plate	Fuji
Biofuge Fresco refrigerated tabletop centrifuge	Hereaus
Biofuge Pico tabletop centrifuge	Hereaus
Blacklight blue lamps 15 W	Sankyo-Denki
Branson Sonifier 250	Branson
C412 centrifuge	Jouan
CT422 refrigerated centrifuge	Jouan
DNA cross-linking system Fluo-Link tFL20.M	Vilber Loumat
Electrophoresis system model 45-2010-i	Peqlab Biotechnologie GmBH
Electroporation device Micropulser	Biorad
Gel Max UV transilluminator	INTAS
Hybridisation tubes	Bachofer, Rettberg
Hybradisation oven	Peqlab Biotechnologie GmBH
IKA-Vibrax VXR	IKA
Incubators	Memmert
LAS-3000 chemiluminescence imager	Fuji
NanoDrop ND-1000 spectrophotometer	Peqlab Biotechnologie GmBH
PCR Sprint thermocycler	Hybaid
peqSTAR 96 Universal Gradient	Peqlab Biotechnologie GmBH
Power Pac 3000 power supplies	Biorad
Rotor Gene RG-3000	Corbett Research
Shake incubators Multitron / Minitron	Infors
Stratalinker 1800	Stratagene
Sub-cell Gt Agarose Gel Electrophoresis System	Biorad
Thermomixer® Dry Block Heating Shaker	Eppendorf
Trans-Blot SD Semi-dry transfer cell	Biorad
Ultrospec 3100pro spectrophotometer	Amersham

5.1.8 Consumables

consumable	manufacturer
2-log-ladder	New England Biolabs
BM Chemiluminescence Blotting Substrate (POD)	Roche
ColorPlus Prestained Protein Marker, Broad Range (7-175 kDa)	New England Biolabs
Filter paper 3MM	Whatman
Gene pulser cuvettes	BioRad
Glass beads (0.75-1 mm)	Roth
Immobilon-P transfer membrane	Millipore
Multiwell plates (24 wells)	Sarstedt
Positive TM membrane	MP Biomedicals
ProbeQuant™ G-50 Micro Columns	GE Healthcare
Protein G SepharoseTM 4 Fast Flow	GE Healthcare
Protein Marker, Broad Range (2-212 kDa)	New England Biolabs
Salmon Sperm DNA (10 mg/ml)	Invitrogen
SYBR Green	Roche
SYBR Safe DNA Gel Stain	Invitrogen

5.2 Methods

5.2.1 Enzymatic manipulation of DNA

A) Polymerase chain reaction (PCR)

PCR was performed in 30-50µl reactions in 0.2 or 0.5ml reaction tubes. Each reaction contained the DNA to be amplified, 0.25mM desoxynucleotides, 20pmol of the forward and the reverse primer, PCR buffer to a final concentration 1x with 1.5 mM $MgCl_2$ and 2.5U GoTaq polymerase. Semi-hotstart was performed to eliminate primer-dimers, mispriming and secondary structure of the primer molecules. The reaction tubes were placed into the PCR machine block when the temperature had reached 80°C. DNA was initially denatured by heating the samples 3 minutes to 95°C. Amplification was performed in 30 cycles. Each cycle consisted of denaturation of double-stranded DNA (15 seconds at 95°C), annealing of primers to matching DNA sequences (30 seconds at 3°C below melting temperature of the primers) and amplification (1 min per 1kb at 72°C). When all cycles were complete, amplification was continued for 10 minutes at 72°C. Temperature adjusted to 4°C for storage.

B) Sequence specific restriction endonucleases

Restriction enzyme digestion was performed in buffer and temperature conditions as indicated by NEB. ChEC samples were digested in 20µl reactions over night. Control digestions for cloning were performed in 50µl reactions with 1µl of restriction enzyme per 1µg of DNA. Total glycerol concentration (present in restriction enzyme storage buffer) should not exceed 5%.

C) DNA ligation

To clone DNA sequences into vectors, the quantity of purified DNA fragments digested with restriction endonuclease(s) was measured by UV spectrometry (see 5.2.3). A three-time excess of insert DNA compared to the vector DNA fragment was incubated in a 10µl ligase reaction (400U) T4 DNA ligase NEB, 50mM Tris-HCl, 10mM $MgCl_2$, 1mM ATP, 10mM dithiothreitol, 25µg/ml BSA) 1h at room temperature or over night at 16°C. One µl of ligation reaction was used for *E.coli* transformation (see 5.2.16).

5.2.2 Purification of nucleic acids

A) Plasmid Isolation

Plasmid DNA was isolated from *E. coli* cultures with the use of kits (Invitrogen). In brief, pelleted cells were lysed with a buffer containing NaOH and SDS. Genomic DNA and proteins were precipitated when the alkaline lysate was neutralised with KOAc. The supernatant which still contained the plasmids was transferred to an anion exchange column which bound the DNA under low salt conditions. Remaining RNA and proteins were removed by washing steps. Then, plasmid DNA was eluted with high salt buffers, desalted by isopropanol precipitation and resuspended in TE or water. Minipreps (up to 5ml of *E. coli* culture) were prepared with the Invitrogen PureLink Quick Plasmid miniprep kit. Midipreps (50ml of *E. coli* culture, yield up to 100µg of DNA) were prepared with the Invitrogen PureLink Quick Plasmid midiprep kit. Preparations were performed as indicated in the manual.

B) Isolation of genomic DNA from yeast

A culture of yeast cells was grown overnight in 5ml YPD or YPAD. Cells were spun down and resuspended in 500µl H_2O. Cells were spun down again and resuspended in 500µl 1M sorbitol, 0.1M EDTA. 3µl of 2% zymolyase (10mM TrisCl pH8, 5% glucose, 2% zymolyase) were added and incubated for 60 minutes at 37°C. Spheroblasts were spun down at 5000rpm for 5 minutes (table-top centrifuge). After addition of 500µl IR buffer and 50µl 10% SDS, the samples were vortexed until lysis was complete (about 1 minute at full speed). Samples were incubated for 30 minutes at 65°C. For precipitation of nucleic acids, 200µl of 5M KOAc was added and samples were kept on ice for 20 minutes. Samples were spun down at 13000rpm for 20 minutes at 4°C and the supernatant was transferred to a new microtube. 1.5µl of RNAseA (100mg/ml) were added and samples were incubated at room temperature over night. After addition of 750µl ispropanol, DNA was precipitated at room temperature for 5 minutes and pelleted (13000rpm, 5 minutes in table-top centrifuge). The pellet was washed once with ice-cold 70% EtOH and spun again (13000rpm, 5 minutes in table-top centrifuge). The supernatant was discarded and the DNA pellet air-dried to eliminate remnants of ethanol. The dry pellet was resuspended in 50µl TE buffer.

C) Phenol Extraction

DNA was extracted with phenol-chloroform from aqueous samples. About one volume of phenol-chloroform-isoamyl alcohol (25:24:1, Roth) was added to the sample. Samples were vortexed until the solution was milky. Samples were centrifuged full speed for at least 3 minutes at room temperature. An aliquot of the upper aqueous phase was transferred to a new reaction tube. The white layer of denatured protein in between the upper aqueous and the lower phenol phase should not be disturbed.

D) Ethanol precipitation

If samples did not yet contain at least 0.25M salt, an equal volume of IRN was added to the sample. DNA was precipitated by addition of 2.5 volumes of 100% ethanol; to precipitate small amounts of DNA, glycogen (5µl of 20mg/ml stock solution) was supplemented. Samples were kept at -20°C for at least 1 hour. DNA was pelleted at full speed for 20 minutes at 4°C. To remove excess salt, the pellet was washed with ice-cold

70% ethanol. The supernatant was discarded, the pellet air-dried and resuspended in TE or water.

E) Purification of PCR products

DNA samples from restricition digests and PCR products were purified with the "QIAquick PCR purification Kit" (Qiagen). DNA above an exclusion size (depending on experimental conditions) was bound to a silicate gel column while smaller DNA molecules, salts, nucleotides, enzymes and glycerol were removed. DNA was eluted with 2mM or 10mM Tris-Cl, pH 8.

5.2.3 Quantitative and qualitative analysis of nucleic acids

A) UV spectrometry

Concentration of pure DNA samples was measured by nanodrop UV spectroscopy at 260nm wavelength ($1OD_{260}$ = 50µg/ml). To determine contamination with proteins and RNA, absorbance was concomitantly measured at 280nm. The ratio of OD_{260}/OD_{280} of pure DNA is between 1.8 and 2.0.

B) Native agarose gel electrophoresis

Agarose gel electrophoresis was used to separate DNA fragments of different lengths. In this work, electrophoresis was performed routinely with 1.0% (w/v) agarose, 1xTBE gels containing SYBR SAFE (except for psoralen crosslinked DNA samples), and 1xTBE as electrophoresis buffer. To determine the lengths of the fragments, 1µg of DNA standard (2log ladder) was used in a concentration of 500µg/ml in 1xDNA loading buffer. Electrophoresis was performed at 3 to 5 volts per cm.

C) Southern blot

DNA was transferred from an agarose gel to a positively charged nylon membrane (Positive$_{TM}$ Membrane, MP Biomedicals) by Southern blot. For denaturation of double-stranded DNA, the gel was incubated twice for 15 minutes in 0.5M NaOH, 1.5M NaCl on a shaker. Subsequently, the gel was incubated twice for 15 minutes in transfer buffer (1M

NH_4OAc). The DNA was transferred upwards with capillary flow of transfer buffer through a blotting pile. The pile consisted of from bottom to top: a bridge of 2 thin Whatman papers placed over a reservoir of 1M NH4OAc (Whatman 3MM, Whatman, 17x34cm) framed with parafilm to prevent bypass of capillary flow, the gel (upside down), the membrane, three thin Whatman papers (15x20cm) and recycling paper towels (about 10cm). All layers apart from the recycling paper towels were soaked in 1M NH_4OAc. The pile was covered with a glass or plastic plate. A weight (about 0.5kg) assured that the capillary transfer was not interrupted. It is important that no air bubbles remain between the membrane and the gel. Blotting was performed overnight or for at least 6h (1% gel). Afterwards, the DNA was crosslinked to the membrane ($0.3J/cm_2$). In this step, thymine bases are covalently bound to the amino groups of the membrane. The membrane can be dried and stored at room temperature.

D) Hybridisation with radioactively labelled DNA probes

Up to three blots can be stacked into one hybridisation tube, separated by meshes. Membranes were pre-hybridised for 1h at hybridisation temperature (65°C) with hybridisation buffer (0.5M sodium phosphate buffer pH 7.2, 7% SDS). The buffer used for pre-hybridisation was discarded and new prewarmed hybridisation buffer (15ml) was poured into the tube. The probe was mixed with 150µl salmon sperm DNA (end concentration 100µg/ml), boiled at 95°C for five to ten minutes and pipetted into the tube. Hybridisation was done overnight at hybridisation temperature with the tubes rotating in a hybridisation oven. After hybridisation, the hybridisation buffer containing the probe can be stored at -20°C and reused. First, blots were rinsed once with 50ml 3x SSC, 0.1% SDS. Blots were washed at hybridisation temperature while rotating the tube in the hybridisation oven. Three washing buffers with decreasing salt and rising SDS-concentration were used in the following order:

Wash 1: 0.3x SSC, 0.1% SDS
Wash 2: 0.1x SSC, 0.1% SDS
Wash 3: 0.1x SSC, 1.5% SDS

Each wash step was performed twice for 15min. Afterwards the blots were dried and stored at room temperature.

E) Detection of radioactive probes

A BAS-III imaging plate (IP) was erased with the Eraser (Raytest). The blot was put into a BAS cassette 2040 and the IP was taken out of the eraser in the dark and put onto the blot. The time of exposure depends on the radioactive signal. IPs were scanned with 100µM resolution in a phosphor imager (FLA3000 by Fujifilm).

F) Quantification of Southern Blots with MultiGauge

For quantitative analysis of Southern blot signals the profile quantitation module of the *MultiGauge 3.0* (Fujifilm) software was used. Data was transferred to *Excel* (Microsoft) for data refinement and graphical representation. To obtain profiles of open and closed ribosomal rRNA genes in psoralen crosslinking and ChEC/psoralen analyses, signal intensities in each lane were normalised (or not if indicated) to the respective peak values and plotted against the distance of migration in the gel. Raw data were processed with the PeakFit software (Systat Software Inc.) using a Gaussian basis function (r^2 values fit >0.98).

G) Quantitative real-time PCR (qPCR)

qPCR was used to measure the amount of a specific DNA fragment with high accuracy. The amount of DNA present at the end of each single PCR cycle was detected by measuring the fluorescence of SYBR-Green (Roche). SYBR-Green is a dye that shows fluorescence when bound to DNA double helices, but not in solution (excitation at 509nm, emission at 526nm). Therefore, the intensity of the fluorescence signal allows direct measurement of the amount of DNA present in a sample. qPCR reactions were performed in 0.1ml, the reaction volume was 20µl. The reaction contained 4µl of DNA sample and 16µl of master mix. The master mix contained 4pmol of the forward and the reverse primer, 0.25µl of a 1:400000 SYBR-Green stock solution in DMSO, 0.4U HotStarTaq-polymerase (Qiagen) and premix. Premix consisted of $MgCl_2$ (to adjust a final concentration of 2.5mM in the qPCR reaction), dNTPs (final concentration 0.2mM in the qPCR reaction) and 10 x PCR buffer (Qiagen; 1 x final concentration in the qPCR reaction). SYBR-Green was thawed in the dark. qPCR was performed in a Rotor-Gene RG3000 system (Corbett Research). SYBR-Green was excited at 480nm; fluorescence was recorded at 510nm. Data was evaluated by analysing the data with the comparative quantitation module of the RotorGene analysis software.

5.2.4 Yeast cultures and formaldehyde crosslinking (FA-X)

Yeast cultures were cultivated overnight and then crosslinked in exponential phase (final OD_{600} = 0.4-0.6). Yeast Peptone Dextrose (YPD) medium was used as growth medium and supplemented with adenine if the strain is auxotrophic for adenine. Growth temperature was 30°C, except for experiments involving yeast strains carrying the temperature-sensitive alleles of *rrn3-ts*, *cdc15-2* or *cdc7-1*. In these cases, cells were cultured at 24°C or 30°C (permissive condition) before temperature shift to 37°C (restrictive condition). (The temperature plays a very important role during formaldehyde crosslinking and, thus, on the outcome of ChEC and ChIP assays. At high temperature, crosslinking of proteins to proteins and proteins to DNA is more efficient than at lower temperatures. Therefore, variation in the kinetics of DNA degradation by MNase tagged proteins may be a consequence of the temperature at which formaldehyde crosslinking was performed. The most likely explanations for this phenomenon are as follows. (1) At low temperatures the crosslink is weak, increasing the occurrence of nonspecific degradation. (2) MNase activity could be compromised by excessive crosslinking at higher temperatures.) Formaldehyde was added to a final concentration of 1% and cells were fixed for 15 minutes at growth temperature while shaking. Excess formaldehyde was quenched with glycine (final concentration 125mM) for at least five minutes at room temperature Cells were harvested in 50ml tubes (4,200 × g, 5min at 4°C in a microcentrifuge), suspended in 1ml of water, and transferred into 1.5ml microtubes. Yeast cells were collected by centrifugation (16,000 × g, 1min at 4°C in a microcentrifuge; supernatant was discarded), and the pellets were frozen in liquid nitrogen and stored at −20°C. Alternatively, cells were used immediately without freezing.

5.2.5 Ethanol fixation of yeast cells

Yeast cells were fixed with 70% ethanol prior to flow cytometric analysis. Ethanol fixed yeast cells can be stored for long periods at 4°C, but also at -20°C. In detail, 5ml yeast culture were collected by centrifugation, washed with 700µl cold water, resuspended in 300µl water and fixed by addition of 700µl of cold 100% ethanol.

5.2.6 Cell cycle analysis

In general block and release experiments were performed like described in the literature with minor modifications (Futcher, 1999; Day et al., 2004). For G1 arrest *bar1*Δ strains were cultured in the presence of 50ng/ml alpha factor for up to 5h. For block and release experiments cells were arrested for 2h in G1 and released by 2 wash steps and transfer into fresh YPAD medium. For late anaphase arrest *cdc15-2* mutant cells were cultured at 37°C for up to 5h. For block and release experiments cells were arrested for 3h in late anaphase before temperature was reduced to 24°C. For arrest at the G1/S transition, a *cdc7-1* mutant strain was incubated at 37°C up to 3h. For G2/M arrest a wild type strain was cultured in the presence of 10µg/ml nocodazole for 1.5h. Cells were released from the block by 2 wash steps and transfer into fresh medium.

5.2.7 UV irradiation

UV irradiation was performed as described previously (Conconi et al., 2005; Tremblay et al., 2008). Yeast strains were grown in YP(A)D medium to early log phase (OD600 of 0.4). A 50ml aliquot of yeast culture was fixed with formaldehyde as a control (-UV). Cultures were harvested by centrifugation, washed in ice-cold phosphate-buffered saline (PBS), and resuspended in the same buffer (1/3 of initial volume of yeast culture). Cell suspensions were poured into trays to ~2-mm depth and irradiated with 180 J/m^2 of UV light with the wavelength of 254nm (Stratalinker 1800). An aliquot of 15ml of yeast culture was collected by centrifugation, resuspended in fresh YP(A)D and fixed with formaldehyde (0h). Then, cells were harvested, resuspended in YP(A)D medium, and incubated in the dark at 30°C with continuous shaking. At the indicated repair times (see Results), samples were fixed with formaldehyde for psoralen crosslinking or ChEC/psoralen analyses. When flow cytometric analysis was performed, cells were fixed with ethanol as described in 5.2.5 at all time points.

5.2.8 Flow cytometry

To measure the DNA content of yeast cells, flow cytometry was performed (Haase and Lew, 1997). Ethanol fixed cells (2x10^6) were washed and resuspended in sodium citrate (50mM, pH 7.0). After sonication to separate cell aggregates, cellular RNA was digested

by incubation with RNase A (final concentration 0.57 mg/ml) at 50°C for 1h. Then proteinase K (final concentration 0.57 mg/ml) was added, and cells were incubated for another hour at 50°C. Cells were stained with 1mM Sytox Green (Molecular Probes) at 4°C overnight and analysed with the CA-III flow cytometer (Partec). Data was evaluated with WinMDI 2.8 software. In the DNA histograms, relative fluorescence intensities are given on the horizontal axes, and cell numbers are given on the vertical axes.

5.2.9 Preparation of nuclei

All steps were performed on ice. Cells were washed in 0.6ml of buffer A and 1× Protease inhibitors and then collected by centrifugation (16,000 × g, 2min at 4°C in a microcentrifuge; supernatant was discarded). The washing step was repeated three times in total. Finally, cells were suspended in 350µl of buffer A, 1× Protease inhibitors and ~500µl of glass beads were added. Note: There must be enough buffer solution to cover the beads by a thin layer. Cell disruption was done for 10min at maximum speed on the Vibrax shaker at 4°C. To collect the cell lysates, the bottom and cap of microtubes were pierced with a hot needle and placed in a 15ml tube. After centrifugation (130 × g, 1 min at 4°C in a microcentrifuge) the glass beads remained in the microtubes and were discarded. The crude cell lysates, which were collected in the 15ml tubes, were transferred into new 1.5ml microtubes and centrifuged at 16,000 × g for 2min at 4°C (microcentrifuge). The supernatants were discarded and the pellets (containing crude nuclei) were suspended in 0.6ml of buffer A and 1× Protease inhibitors. After another centrifugation step (16,000 × g for 2min at 4°C) supernatants were removed. Buffer A contains 2mM EDTA, which inhibits premature MNase activation if Ca^{2+} is released from the endoplasmic reticulum. The EDTA concentration can be increased up to 4mM without affecting the quality of the experiment. The nuclei pellets can be frozen in liquid nitrogen and stored at -80°C or were used immediately in a ChEC assay.

5.2.10 Chromatin Endogenous Cleavage (ChEC)

Nuclei isolated from formaldehyde-crosslinked cells were suspended in buffer Ag and 1×Protease inhibitors in a total volume of 550–600µl (The volume to suspend crude nuclei is calculated such that it exceeds the summed volume of all samples of the ChEC time course by at least 50µl), and pre-incubated at 30°C, thermomixer set at 750rpm, for

3min. After vigorous vortexing, two 80µl aliquots of the nuclei suspensions were transferred to new tubes and used as controls (0min ChEC): no calcium was added. For the rest of the nuclei suspensions, MNase-fusion proteins were activated by the addition of $CaCl_2$ (2µl of 0.1M stock solution per 100µl reaction volume; the final concentration is 2mM) and incubated at 30°C with constant shaking (thermomixer set at 750rpm). As the digestion of an exogenous plasmid added after nuclei preparation was quite high in the experiment shown in Fig. 3-16 (data not shown), the temperature during ChEC was decreased to 16°C for the experiment shown in Fig. 3-18. At different time intervals, 80µl aliquots were taken, transferred to 1.5ml microtubes containing 100µl of IRN buffer and mixed to stop the MNase activity (The incubation time in $CaCl_2$ containing buffer is carefully chosen and depends on the protein that is tagged with MNase. Namely, for very abundant proteins it is advisable to add naked, linear plasmid DNA to the nuclei to have an exogenous control for unspecific digestion. It is conceivable that MNase fusion proteins cut DNA surrounding their binding site and, thus, releasing themselves in the solvent and cutting more DNA non-specifically, like free MNases. After Southern blotting the membrane can be hybridised with the plasmid-specific probe to monitor the amount of nonspecific degradation. It is important to mix the suspension before taking aliquots because nuclei sediment.). Samples mixed with IRN can be kept at room temperature. At the end of the time course, 100µl of IRN were added to the “0 min ChEC” aliquots. For ChEC/psoralen analyses, continue to subheading 5.2.12. For ChEC analyses, follow the steps described in subheading 5.2.13.

5.2.11 Psoralen crosslinking

For psoralen crosslinking yeast culture, formaldehyde crosslinking and preparation of nuclei was performed as described in 5.2.4 and 5.2.9. Crude nuclei were resuspended in 500µl IRN buffer and 50µl were pipetted into non-coated 24 well plates (The remaining nuclei suspension can be frozen at -80°C and reused). 150µl IRN were added (final volume 200µl) and the suspension was mixed gently. 10µl of 4,5’,8-trimethylpsoralen (psoralen) (0.2mg/ml) were added and samples were incubated for 5min on ice and in the dark. Subsequently, the suspensions were irradiated with UVA light (315–400nm) at a distance of 2–3cm for 5min on ice (Remove the lid of the 24-well plate prior to UV irradiation since plastic filters UV light). As a mock control, ethanol was added instead of psoralen. The psoralen crosslinking step was repeated three times (total addition of

psoralen: 40µl; total UV irradiation time: 20min). The samples were transferred into 1.5ml microtubes.

5.2.12 Chromatin Endogenous Cleavage Psoralen Photocrosslinking Assay (ChEC/psoralen)

ChEC samples were split into 1/3 (60µl) for the ChEC–psoralen and 2/3 (120µl) for the ChEC assay. For the ChEC–psoralen assay, 60µl of the nuclei suspension were mixed with 140µl of IRN buffer and transferred to a 24-well plate. Psoralen photocrosslinking was performed as described in 5.2.11.

5.2.13 DNA workup of ChEC and ChEC/psoralen samples

Nuclei were treated with 2µl RNase A (20 mg/ml), mixed and incubated at 37°C for 1h. 10µl of 10% SDS and 2µl of Proteinase K (20mg/ml) were added, mixed, and samples were incubated for 1h at 56°C. Formaldehyde crosslink was reversed by incubation at 65°C overnight. DNA was extracted with phenol–chloroform–isoamyl alcohol. 1x volume of IRN and 2.5x volume of ethanol were added and DNA was precipitated at −20°C for at least 20min. DNA was collected by centrifugation at 16,000 x g for 20min at 4°C. DNA was dried for 5–10min at room temperature and resuspended in 25µl of TE buffer.

5.2.14 Restriction digest and agarose gel electrophoresis of ChEC and ChEC/psoralen samples

12µl of each sample were digested with the appropriate restriction enzyme in a final volume of 20µl as recommended by the manufacturer overnight (For the mock ethanol control (no psoralen) it is sufficient to digest 1µl of DNA solution). 10× DNA loading buffer was added to the samples prior to loading on a 1% agarose gel (250-300ml, 15 × 20 cm) (For ChEC, gels containing SYBR® Safe were prepared. However, SYBR® Safe cannot be used for gels that are employed to analyse DNA from ChEC–psoralen assay, since these DNA intercalating molecules mitigate the shift in migration promoted by psoralen crosslinking). DNA prepared from the ChEC assay was separated at 6V/cm during 6h in TBE running buffer. DNA prepared from the ChEC–psoralen assay was separated at 6V/cm for 8h in the same running buffer. After electrophoresis, the agarose gels used to

separate psoralen crosslinked DNA were irradiated 2min with 254nm UV light (UV-Transilluminator, INTAS) on both sides (This is a crucial step. Irradiation with short wave UV (254 nm) reverses the covalent bonds between psoralen and pyrimidines on the opposite DNA strands. This allows DNA denaturation prior to Southern blotting and, thus, the hybridisation with the radioactively labelled single-stranded probe).

5.2.15 Chromatin Immunoprecipitation (ChIP)

ChIP was performed mainly as described (Hecht and Grunstein, 1999) in three to six independent experiments for each protein. Formaldehyde fixed cells from 50ml of an exponentially growing yeast culture were washed (1min, 13000 rpm, 4°C) with 1ml of cold ChIP lysis buffer and suspended in 400µl of ChIP lysis buffer. EGTA and EDTA in the buffer suppress MNase activity. Glass beads (Ø 0.75-1.0 mm, Roth) were added and cells were disrupted on a VXR basic IKA Vibrax orbital shaker for 3x15min with full speed at 4°C (keep 2min on ice after first and second 15min step). DNA was sonicated in a volume of 1ml ChIP lysis buffer using a Branson Sonifier 250 to obtain an average DNA fragment size of 500-1000bp. Cell debris was removed by centrifugation (20min, 13000rpm, 4°C). The chromatin extracts were split into three aliquots. 40µl of each aliquot served as an input control. 250µl of each aliquot were incubated for 90min at 4°C with 1µg of a monoclonal α-HA antibody (3F10, Roche) and 125µl of Protein G sepharose (Amersham) to enrich the MNase-HA_3-tagged proteins bound by the antibody. After immunoprecipitation, the beads were washed three times with ChIP lysis buffer, twice with ChIP washing buffer I and twice with ChIP washing buffer II followed by a final washing step with TE buffer. 250µl of buffer IRN were added to the beads (IPs) and to the input samples. DNA was isolated as described for ChEC experiments (see 5.2.13). Both, DNA derived from input and IP were resuspended in 50µl of TE buffer. Relative DNA amounts present in input and IP DNA were determined by quantitative PCR using a RotorGene 3000 system (Corbett Life Science) and the comparative analysis software module. Primer pairs used for amplification are listed in 5.1.3B. Input DNA was diluted 1:1000, and IP DNA was diluted 1:100 prior to analysis. Retention of specific DNA-fragments was calculated as the fraction of total input DNA. The mean values and error bars were derived from three to six independent ChIP experiments analysed in triplicate quantitative PCR reactions.

5.2.16 Manipulation of *Escherichia coli*

A) Preparation of electrocompetent bacteria

An overnight culture of *E. coli* XL1-Blue in SOB medium (OD_{600} ~ 3) was diluted 1:100 in SOB prewarmed to 37°C; this culture was grown with vigorous aeration at 300rpm and 37°C for about 3h, until the OD_{600} reached a value between 0.4 and 0.6. Then, the culture was chilled on ice for 15min before being centrifuged for 10min at 1000rpm and 4°C in a GS3 rotor. Centrifugation was repeated after resuspension of the pellet in 400ml ice-cold, sterile water and, after that, in 200ml ice-cold, sterile water. The washed pellet was resuspended in 10ml cold, sterile 10% (v/v) glycerol, transferred to a Falcon tube and centrifuged at 2000rpm and 4°C for 10min. After resuspension of the pellet in 1.5ml cold, sterile 10% (v/v) glycerol (about $1–3 \cdot 10^{10}$ cells/ml) 50–100µl aliquots were stored at –80°C.

B) Transformation by electroporation

The required number of aliquots plus a background control aliquot was thawed on ice and pipetted into a chilled 0.2cm electroporation cuvette. About 1ng of plasmid or up to 3µl of a ligation sample were pipetted into the cell drop. Pulsing was performed with programme EC2 in a micropulser. Immediately after the pulse, 1ml 37°C LB medium was added and the sample was transferred in a microreaction tube following an incubation step for 30-60min at 37°C. 100µl of the supernatant was plated on LB-Amp. The residual cells were spun down for one minute at 5000rpm in a microcentrifuge. About 800µl were discarded and the pellet was resuspended in the remaining supernatant, plated onto LB-Amp and incubated overnight at 37°C.

C) Liquid culture

A single colony was picked from a plate and transferred into a sterile tube containing 5-50ml of LB-Amp (50µg/ml ampicillin). The culture was incubated at 37°C overnight.

5.2.17 Manipulation of *Saccharomyces cerevisiae*

A) Preparation of competent yeast cells

50ml of an exponentially growing yeast culture was pelleted (2000rpm, 5min at room temperature). The pellet was washed at room temperature with 25ml autoclaved H_2O, then with 5ml SORB. The pellet was resuspended in 500µl SORB, transferred to a reaction tube and pelleted again. The supernatant was completely removed, the pellet then resuspended in 360µl SORB. 40µl of salmon sperm DNA (Invitrogen) was boiled at 95°C for 5 minutes and added to the cell suspension. After mixing, 50µl aliquots were transferred to fresh reaction tubes and placed at -80°C for storage.

B) Transformation of competent yeast cells

Treatment of yeast cells with alkali cations (e.g. Li^+, Cs^+, K^+) is effective to induce competence of yeast cells to take up linear and circular DNA molecules. The cell aliquot was thawed on ice, DNA (~10µg) was added to the cells and the sample was mixed. 6 volumes of LitPEG were added; samples were mixed thoroughly and incubated at room temperature for about 30 minutes. 1/9 of total volume (cells plus DNA plus LitPEG) of pure, sterile DMSO was added, samples were mixed and heat-shocked at 42°C for about 15 minutes. Cells were pelleted (2000rpm, 3 minutes at room temperature in a table-top centrifuge), the supernatant was completely removed and the cells were resuspended in sterile water and plated on the selective medium. When cells were selected for antibiotic resistance (e.g. geniticin) they were resuspended after the heat-shock in 1ml appropriate rich medium (without antibiotics). Cells were grown at appropriate temperature (30°C for wild-type cells, 24°C for temperature sensitive strains) for about 1-2 generation times. After that, cells were pelleted, 9/10 of the supernatant were discarded. The cell pellet was resuspended in the remaining supernatant and plated on selective medium. When cells were selected for resistance to geneticin, they should be replica-plated to identify positive clones. Note, that temperature-sensitive strains in this study were also exposed to the heat-shock at 42°C, since these cells were still viable after this treatment and the transformation rate was increased in comparison to a heat-shock at 30°C.

C) Liquid culture

Yeast cultures were inoculated with a single colony from plates. Cultures were grown in the respective medium at optimal growth temperature. Precultures were grown in sterile plastic tubes (10ml tube volume, 5ml maximal culture volume). Other cultures were grown in glass flasks; usually the culture volume did not exceed 1/3 of the flask volume.

D) Permanent culture in glycerol

2ml of a stationary yeast culture grown overnight were mixed with 1ml of sterile 50% glycerol and separated to two aliquots. Cells were frozen on dry ice and stored at -80°C.

E) Establishment of MNase fusion strains

For each target gene, a PCR was performed with overhang primers. The primers are composed of a 5' sequence complementary to the target gene (50bp immediately before or after the stop codon) and 3' sequence complementary to pKM9 (S3 and S2 adapter, priming before and after the MNase-HA_3-KanMX cassette). The PCR was performed with a proofreading enzyme (Herculase); the PCR product was cloned into pBluescript and sequenced. After verification of sequence correctness, the plasmid was prepared with a Midi-prep kit. The insert was excised with restriction enzyme digestion and transformed into competent yeast cells. The KanMX marker was used for selection on Geneticin plates; initial plates were replica-plated. To screen for positive clones, colonies were stroked out, protein was isolated (denaturing protein isolation) and checked for HA signals of correct size (molecular weight of the protein factor plus 22kDa for the tag) by Western blot.

5.2.18 Protein biochemical methods

A) Denaturing protein extraction of yeast cells

About 1ml (or less, depends on abundance of the desired protein) of an overnight yeast liquid culture was spun down. Cells were resuspended in 1ml ice-cold water. Samples were chilled on ice and supplemented with 150µl of pre-treatment solution (1.85M NaOH, 1M β-mercapto-ethanol) for 15 minutes on ice. Proteins were precipitated with 150µl

55% trichloroacetic acid for 10 minutes on ice and pelleted (13000rpm, 10minutes at 4°C in table-top centrifuge). The supernatant was discarded and the pellet resuspended in 30-50µl HU-buffer (5% SDS, 200mM Tris pH6.8, 1mM EDTA, 2.13mM β-mercapto-ethanol, 8M urea, bromophenolblue; store at -20°C). If colour turns yellow, the pH of the suspension is too acidic and must be neutralised with ammonia gas until the colour turns (dark) blue again. Proteins were denatured for 10 minutes at 65°C while shaking. Insoluble cell particles were pelleted (13000 rpm, 1min at room temperature). An adequate volume of the supernatant was analysed by Western blot.

B) SDS-Polyacrylamide gel electrophoresis

Proteins were separated according to molecular weight by vertical, discontinuous SDS-PAGE according to Laemmli (1970). The discontinuous system consisted of a lower separating gel and an upper stacking gel:

separating gel	**6%**	**8%**	**10%**	**12.5%**	**14.5%**
H2O	5.5ml	4.82ml	4.2ml	3.3ml	2.68ml
4x Lower Tris	2.5ml	2.5ml	2.5ml	2.5ml	2.5ml
30% Acrylamide (AA) + 0.8% Bis-AA	2.0ml	2.68ml	3.3ml	4.2ml	4.82ml
10% SDS	100µl				
TEMED	5µl				
25% APS	50µl				

stacking gel	**6%**	**4%**
H2O	2.75ml	3.05ml
4x Upper Tris	1.25ml	1.25ml
30% AA + 0.8% bAA	1.00ml	0.65ml
10% SDS	100µl	
TEMED	5µl	
25% APS	50µl	

Pre-stained marker (NEB) was used as a molecular weight marker. The bands were stained blue so they were visible in the gel and on the membrane. Gels were run at 140V for 1.5h or until the bromophenolblue band reached the lower border of the gel.

C) Western blot

After SDS-PAGE, proteins are associated with SDS and therefore negatively charged. Consequently, proteins can be blotted by semi-dry transfer to a PVDF-membrane by the electric current (BIORAD semi-dry transfer apparatus). Three layers of thin Whatman paper were soaked in blotting buffer (25mM Tris, 190mM glycine, 20% methanol, pH8.3)

and piled on the lower electrode (anode) of the semi-transfer device. The membrane (Immobilon PSQ 0.2µm, Millipore) was first soaked in methanol, then in blotting buffer and subsequently put onto the pile of Whatman papers. Air bubbles were carefully removed as they prevent the flow of the electric current. The membrane must be kept wet (with blotting buffer) all the time. The gel apparatus was disassembled, the gel was transferred onto the membrane. Air bubbles were removed and the gel was covered with three more layers of soaked Whatman paper. The blot was run at 24V for 1.5h. After blotting, the marker bands and lanes should be marked with a pen.

D) Ponceau staining

Western blots can be stained with Ponceau (0.5% Ponceau in 1% acetic acid) to control if proteins transfer worked properly. Staining was performed for one to three minutes at room temperature in a tray. Afterwards, the membrane was washed with water.

E) Detection of proteins by chemiluminescence

The membrane was blocked with blocking solution (5% milk powder in 1x PBST) to prevent unspecific binding of the antibody. Blocking was performed in a tray for 1h at room temperature or overnight at 4°C while shaking. The membrane was wrapped into a 50ml falcon tube containing the first antibody dilution (appropriate dilution in 1x PBST with 5% milk powder, 3ml for large membrane) and rotated at room temperature for 1h. After three five-minute washes with 1x PBST in a tray, the membrane was wrapped into a 50ml falcon tube with the second antibody (appropriate dilution in 1x PBST with 5% milk powder, 3ml for large membrane) and rotated at room temperature for half an hour. The membrane was washed three times for five minutes with 1x PBST. The secondary antibody was coupled to horseradish peroxidase (POD) which catalyses the oxidation of diacylhydrazides via an activated intermediate that decays to the ground state by emission of light in the visible range. The membrane was put between two sheets of a thin plastic bag (Roth) and covered with a liquid film of reaction substrates (BM chemiluminescence blotting substrate (POD), Roche). The position of the PSM bands and lanes were marked with a fluorescent pen. Detection followed immediately after addition of the substrate in a LAS-3000 fluorescence reader (Fuji).

6 References

Adkins, M. W., and Tyler, J. K. (2006). Transcriptional activators are dispensable for transcription in the absence of Spt6-mediated chromatin reassembly of promoter regions. Mol. Cell *21*, 405–416.

Adkins, M. W., Howar, S. R., and Tyler, J. K. (2004). Chromatin disassembly mediated by the histone chaperone Asf1 is essential for transcriptional activation of the yeast PHO5 and PHO8 genes. Mol. Cell *14*, 657–666.

Amin, A. D., Vishnoi, N., and Prochasson, P. (2011). A global requirement for the HIR complex in the assembly of chromatin. Biochimica Et Biophysica Acta. Available at: http://www.ncbi.nlm.nih.gov/pubmed/21820090 [Accessed November 23, 2011].

Amin, N. S., and Holm, C. (1996). In vivo analysis reveals that the interdomain region of the yeast proliferating cell nuclear antigen is important for DNA replication and DNA repair. Genetics *144*, 479–493.

Annunziato, A. T. (2005). Split decision: what happens to nucleosomes during DNA replication? J. Biol. Chem. *280*, 12065–12068.

Aprikian, P., Moorefield, B., and Reeder, R. H. (2001). New model for the yeast RNA polymerase I transcription cycle. Mol. Cell. Biol. *21*, 4847–4855.

Ayyagari, R., Impellizzeri, K. J., Yoder, B. L., Gary, S. L., and Burgers, P. M. (1995). A mutational analysis of the yeast proliferating cell nuclear antigen indicates distinct roles in DNA replication and DNA repair. Mol. Cell. Biol. *15*, 4420–4429.

Balajee, A. S., Dianova, I., and Bohr, V. A. (1999). Oxidative damage-induced PCNA complex formation is efficient in xeroderma pigmentosum group A but reduced in Cockayne syndrome group B cells. Nucleic Acids Res. *27*, 4476–4482.

Barbet, N. C., Schneider, U., Helliwell, S. B., Stansfield, I., Tuite, M. F., and Hall, M. N. (1996). TOR controls translation initiation and early G1 progression in yeast. Mol. Biol. Cell *7*, 25–42.

Baxevanis, A. D., and Landsman, D. (1998). Histone Sequence Database: new histone fold family members. Nucleic Acids Res. *26*, 372–375.

Bell, S. P., and Dutta, A. (2002). DNA replication in eukaryotic cells. Annu. Rev. Biochem. *71*, 333–374.

Belotserkovskaya, R., Oh, S., Bondarenko, V. A., Orphanides, G., Studitsky, V. M., and Reinberg, D. (2003). FACT facilitates transcription-dependent nucleosome alteration. Science *301*, 1090–1093.

Berger, A. B., Decourty, L., Badis, G., Nehrbass, U., Jacquier, A., and Gadal, O. (2007). Hmo1 is required for TOR-dependent regulation of ribosomal protein gene transcription. Mol. Cell. Biol. *27*, 8015–8026.

Bermejo, R., Capra, T., Gonzalez-Huici, V., Fachinetti, D., Cocito, A., Natoli, G., Katou, Y., Mori, H., Kurokawa, K., Shirahige, K., et al. (2009). Genome-organizing factors Top2 and Hmo1 prevent chromosome fragility at sites of S phase transcription. Cell *138*, 870–884.

Bernstein, B. E., Liu, C. L., Humphrey, E. L., Perlstein, E. O., and Schreiber, S. L. (2004). Global nucleosome occupancy in yeast. Genome Biol. *5*, R62.

Birch, J. L., and Zomerdijk, J. C. B. M. (2008). Structure and function of ribosomal RNA gene chromatin. Biochem. Soc. Trans. *36*, 619–624.

Birch, J. L., Tan, B. C.-M., Panov, K. I., Panova, T. B., Andersen, J. S., Owen-Hughes, T. A., Russell, J., Lee, S.-C., and Zomerdijk, J. C. B. M. (2009). FACT facilitates chromatin transcription by RNA polymerases I and III. EMBO J. *28*, 854–865.

Boeger, H., Griesenbeck, J., Strattan, J. S., and Kornberg, R. D. (2003). Nucleosomes unfold completely at a transcriptionally active promoter. Mol. Cell *11*, 1587–1598.

Bohr, V. A., Smith, C. A., Okumoto, D. S., and Hanawalt, P. C. (1985). DNA repair in an active gene: removal of pyrimidine dimers from the DHFR gene of CHO cells is much more efficient than in the genome overall. Cell *40*, 359–369.

Boye, E., Skjølberg, H. C., and Grallert, B. (2009). Checkpoint regulation of DNA replication. Methods Mol. Biol. *521*, 55–70.

Brewer, B. J., and Fangman, W. L. (1988). A replication fork barrier at the 3' end of yeast ribosomal RNA genes. Cell *55*, 637–643.

Brewer, B. J., Lockshon, D., and Fangman, W. L. (1992). The arrest of replication forks in the rDNA of yeast occurs independently of transcription. Cell *71*, 267–276.

Brown, S. E., and Szyf, M. (2008). Dynamic epigenetic states of ribosomal RNA promoters during the cell cycle. Cell Cycle *7*, 382–390.

Bryk, M., Banerjee, M., Murphy, M., Knudsen, K. E., Garfinkel, D. J., and Curcio, M. J. (1997). Transcriptional silencing of Ty1 elements in the RDN1 locus of yeast. Genes Dev *11*, 255–269.

Bucceri, A., Kapitza, K., and Thoma, F. (2006). Rapid accessibility of nucleosomal DNA in yeast on a second time scale. EMBO J. *25*, 3123–3132.

Burkhalter, M. D., and Sogo, J. M. (2004). rDNA enhancer affects replication initiation and mitotic recombination: Fob1 mediates nucleolytic processing independently of replication. Mol Cell *15*, 409–421.

Buttinelli, M., Di Mauro, E., and Negri, R. (1993). Multiple nucleosome positioning with unique rotational setting for the Saccharomyces cerevisiae 5S rRNA gene in vitro and in vivo. Proc. Natl. Acad. Sci. U.S.A. *90*, 9315–9319.

Cech, T., and Pardue, M. L. (1977). Cross-linking of DNA with trimethylpsoralen is a probe for chromatin structure. Cell *11*, 631–640.

Christians, F. C., and Hanawalt, P. C. (1993). Lack of transcription-coupled repair in mammalian ribosomal RNA genes. Biochemistry *32*, 10512–10518.

Christians, F. C., and Hanawalt, P. C. (1994). Repair in ribosomal RNA genes is deficient in xeroderma pigmentosum group C and in Cockayne's syndrome cells. Mutat. Res. *323*, 179–187.

Ciejek, E., and Thorner, J. (1979). Recovery of S. cerevisiae a cells from G1 arrest by alpha factor pheromone requires endopeptidase action. Cell *18*, 623–635.

Cioci, F., Vu, L., Eliason, K., Oakes, M., Siddiqi, I. N., and Nomura, M. (2003). Silencing in yeast rDNA chromatin: reciprocal relationship in gene expression between RNA polymerase I and II. Mol Cell *12*, 135–145.

Citterio, E., Vermeulen, W., and Hoeijmakers, J. H. (2000). Transcriptional healing. Cell *101*, 447–450.

Clapier, C. R., and Cairns, B. R. (2009). The biology of chromatin remodeling complexes. Annu. Rev. Biochem. *78*, 273–304.

Claypool, J. A., French, S. L., Johzuka, K., Eliason, K., Vu, L., Dodd, J. A., Beyer, A. L., and Nomura, M. (2004). Tor pathway regulates Rrn3p-dependent recruitment of yeast RNA polymerase I to the promoter but does not participate in alteration of the number of active genes. Mol. Biol. Cell *15*, 946–956.

Cohn, S. M., and Lieberman, M. W. (1984). The distribution of DNA excision-repair sites in human diploid fibroblasts following ultraviolet irradiation. J. Biol. Chem. *259*, 12463–12469.

Conconi, A. (1987). Correlation between gene activity and chromatin structure in mouse erythroleukemia cells ([S.l.]: [s.n.]).

Conconi, A. (2005). The yeast rDNA locus: a model system to study DNA repair in chromatin. DNA Repair (Amst.) *4*, 897–908.

Conconi, A., Bespalov, V. A., and Smerdon, M. J. (2002). Transcription-coupled repair in RNA polymerase I-transcribed genes of yeast. Proc. Natl. Acad. Sci. U.S.A *99*, 649–654.

Conconi, A., Jager-Vottero, P., Zhang, X., Beard, B. C., and Smerdon, M. J. (2000). Mitotic viability and metabolic competence in UV-irradiated yeast cells. Mutat. Res. *459*, 55–64.

Conconi, A., Losa, R., Koller, T., and Sogo, J. M. (1984). Psoralen-crosslinking of soluble and of H1-depleted soluble rat liver chromatin. J. Mol. Biol. *178*, 920–928.

Conconi, A., Paquette, M., Fahy, D., Bespalov, V. A., and Smerdon, M. J. (2005). Repair-independent chromatin assembly onto active ribosomal genes in yeast after UV irradiation. Mol. Cell. Biol *25*, 9773–9783.

Conconi, A., Widmer, R. M., Koller, T., and Sogo, J. M. (1989). Two different chromatin structures coexist in ribosomal RNA genes throughout the cell cycle. Cell *57*, 753–761.

Corpet, A., and Almouzni, G. (2009). Making copies of chromatin: the challenge of nucleosomal organization and epigenetic information. Trends Cell Biol. *19*, 29–41.

Dammann, R., Lucchini, R., Koller, T., and Sogo, J. M. (1993). Chromatin structures and transcription of rDNA in yeast Saccharomyces cerevisiae. Nucleic Acids Res *21*, 2331–2338.

Dammann, R., Lucchini, R., Koller, T., and Sogo, J. M. (1995). Transcription in the yeast rRNA gene locus: distribution of the active gene copies and chromatin structure of their flanking regulatory sequences. Mol. Cell. Biol *15*, 5294–5303.

Davis, A. H., Reudelhuber, T. L., and Garrard, W. T. (1983). Varigated chromatin structures of mouse ribosomal RNA genes. J. Mol. Biol. *167*, 133–155.

Day, A., Schneider, C., and Schneider, B. L. (2004). Yeast cell synchronization. Methods Mol Biol *241*, 55–76.

Downs, J. A., Kosmidou, E., Morgan, A., and Jackson, S. P. (2003). Suppression of homologous recombination by the Saccharomyces cerevisiae linker histone. Mol. Cell *11*, 1685–1692.

den Dulk, B., Brandsma, J. A., and Brouwer, J. (2005). The Rad4 homologue YDR314C is essential for strand-specific repair of RNA polymerase I-transcribed rDNA in Saccharomyces cerevisiae. Mol. Microbiol. *56*, 1518–1526.

Elion, E. A., and Warner, J. R. (1986). An RNA polymerase I enhancer in Saccharomyces cerevisiae. Mol. Cell. Biol. *6*, 2089–2097.

Elion, E. A., and Warner, J. R. (1984). The major promoter element of rRNA transcription in yeast lies 2 kb upstream. Cell *39*, 663–673.

English, C. M., Adkins, M. W., Carson, J. J., Churchill, M. E. A., and Tyler, J. K. (2006). Structural basis for the histone chaperone activity of Asf1. Cell *127*, 495–508.

Fahy, D., Conconi, A., and Smerdon, M. J. (2005). Rapid changes in transcription and chromatin structure of ribosomal genes in yeast during growth phase transitions. Exp Cell Res *305*, 365–373.

Fan, Y., Nikitina, T., Morin-Kensicki, E. M., Zhao, J., Magnuson, T. R., Woodcock, C. L., and Skoultchi, A. I. (2003). H1 linker histones are essential for mouse development and affect nucleosome spacing in vivo. Mol. Cell. Biol. *23*, 4559–4572.

Fatica, A., and Tollervey, D. (2002). Making ribosomes. Curr. Opin. Cell Biol. *14*, 313–318.

Ferreiro, J. A., Powell, N. G., Karabetsou, N., Kent, N. A., Mellor, J., and Waters, R. (2004). Cbf1p modulates chromatin structure, transcription and repair at the Saccharomyces cerevisiae MET16 locus. Nucleic Acids Res. *32*, 1617–1626.

Foe, V. E., Wilkinson, L. E., and Laird, C. D. (1976). Comparative organization of active transcription units in Oncopeltus fasciatus. Cell *9*, 131–146.

Formosa, T., Eriksson, P., Wittmeyer, J., Ginn, J., Yu, Y., and Stillman, D. J. (2001). Spt16-Pob3 and the HMG protein Nhp6 combine to form the nucleosome-binding factor SPN. EMBO J *20*, 3506–3517.

Franke, W. W., Scheer, U., Spring, H., Trendelenburg, M. F., and Krohne, G. (1976). Morphology of transcriptional units of rDNA. Evidence for transcription in apparent spacer intercepts and cleavages in the elongating nascent RNA. Exp. Cell Res. *100*, 233–244.

Freidkin, I., and Katcoff, D. J. (2001). Specific distribution of the Saccharomyces cerevisiae linker histone homolog HHO1p in the chromatin. Nucleic Acids Res. *29*, 4043–4051.

French, S. L., Osheim, Y. N., Cioci, F., Nomura, M., and Beyer, A. L. (2003). In exponentially growing Saccharomyces cerevisiae cells, rRNA synthesis is determined by the summed RNA polymerase I loading rate rather than by the number of active genes. Mol. Cell. Biol *23*, 1558–1568.

French, S. L., Osheim, Y. N., Schneider, D. A., Sikes, M. L., Fernandez, C. F., Copela, L. A., Misra, V. A., Nomura, M., Wolin, S. L., and Beyer, A. L. (2008). Visual analysis of the yeast 5S rRNA gene transcriptome: regulation and role of La protein. Mol. Cell. Biol. *28*, 4576–4587.

Friedberg, E. C., Walker, G. C., and Siede, W. (2005). DNA Repair and Mutagenesis 2nd ed. (Asm Pr).

Fritz, L. K., and Smerdon, M. J. (1995). Repair of UV damage in actively transcribed ribosomal genes. Biochemistry *34*, 13117–13124.

Fritz, L. K., Suquet, C., and Smerdon, M. J. (1996). Strand breaks are repaired efficiently in human ribosomal genes. J. Biol. Chem. *271*, 12972–12976.

Fry, C. J., and Peterson, C. L. (2001). Chromatin remodeling enzymes: who's on first? Curr. Biol. *11*, R185–R197.

Futcher, B. (1999). Cell cycle synchronization. Methods Cell Sci *21*, 79–86.

Gadal, O., Labarre, S., Boschiero, C., and Thuriaux, P. (2002). Hmo1, an HMG-box protein, belongs to the yeast ribosomal DNA transcription system. EMBO J *21*, 5498–5507.

Gagnon-Kugler, T., Langlois, F., Stefanovsky, V., Lessard, F., and Moss, T. (2009). Loss of human ribosomal gene CpG methylation enhances cryptic RNA polymerase II transcription and disrupts ribosomal RNA processing. Mol. Cell *35*, 414–425.

Gaillard, P. H., Moggs, J. G., Roche, D. M., Quivy, J. P., Becker, P. B., Wood, R. D., and Almouzni, G. (1997). Initiation and bidirectional propagation of chromatin assembly from a target site for nucleotide excision repair. EMBO J. *16*, 6281–6289.

Gale, J. M., and Smerdon, M. J. (1988). UV-induced pyrimidine dimers and trimethylpsoralen cross-links do not alter chromatin folding in vitro. Biochemistry *27*, 7197–7205.

Gambus, A., Jones, R. C., Sanchez-Diaz, A., Kanemaki, M., van Deursen, F., Edmondson, R. D., and Labib, K. (2006). GINS maintains association of Cdc45 with MCM in replisome progression complexes at eukaryotic DNA replication forks. Nat. Cell Biol. *8*, 358–366.

Game, J. C., and Kaufman, P. D. (1999). Role of Saccharomyces cerevisiae chromatin assembly factor-I in repair of ultraviolet radiation damage in vivo. Genetics *151*, 485–497.

Gasser, R., Koller, T., and Sogo, J. M. (1996). The stability of nucleosomes at the replication fork. J. Mol. Biol. *258*, 224–239.

Gébrane-Younès, J., Fomproix, N., and Hernandez-Verdun, D. (1997). When rDNA transcription is arrested during mitosis, UBF is still associated with non-condensed rDNA. J. Cell. Sci *110 (Pt 19)*, 2429–2440.

Goetze, H., Wittner, M., Hamperl, S., Hondele, M., Merz, K., Stoeckl, U., and Griesenbeck, J. (2010). Alternative Chromatin Structures of the 35S rRNA Genes in Saccharomyces cerevisiae Provide a Molecular Basis for the Selective Recruitment of RNA Polymerases I and II. Mol. Cell. Biol *30*, 2028–2045.

van Gool, A. J., Verhage, R., Swagemakers, S. M., van de Putte, P., Brouwer, J., Troelstra, C., Bootsma, D., and Hoeijmakers, J. H. (1994). RAD26, the functional S. cerevisiae homolog of the Cockayne syndrome B gene ERCC6. EMBO J. *13*, 5361–5369.

Gottesfeld, J. M., Bagi, G., Berg, B., and Bonner, J. (1976). Sequence composition of the template-active fraction of rat liver chromatin. Biochemistry *15*, 2472–2483.

Gottschling, D. E., Aparicio, O. M., Billington, B. L., and Zakian, V. A. (1990). Position effect at S. cerevisiae telomeres: reversible repression of Pol II transcription. Cell *63*, 751–762.

Götze, H. (2010). Function of the upstream activating factor in chromatin structure organization and transcriptional regulation at the yeast ribosomal DNA. Available at: http://epub.uni-regensburg.de/12558/ [Accessed December 28, 2011].

Green, C. M., and Almouzni, G. (2003). Local action of the chromatin assembly factor CAF-1 at sites of nucleotide excision repair in vivo. EMBO J. *22*, 5163–5174.

Green, C. M., and Almouzni, G. (2002). When repair meets chromatin. First in series on chromatin dynamics. EMBO Rep. *3*, 28–33.

Green, E. M., Antczak, A. J., Bailey, A. O., Franco, A. A., Wu, K. J., Yates, J. R., 3rd, and Kaufman, P. D. (2005). Replication-independent histone deposition by the HIR complex and Asf1. Curr. Biol. *15*, 2044–2049.

Groth, A., Rocha, W., Verreault, A., and Almouzni, G. (2007). Chromatin Challenges during DNA Replication and Repair. Cell *128*, 721–733.

Grummt, I. (2007). Different epigenetic layers engage in complex crosstalk to define the epigenetic state of mammalian rRNA genes. Hum. Mol. Genet. *16 Spec No 1*, R21–R27.

Guzder, S. N., Habraken, Y., Sung, P., Prakash, L., and Prakash, S. (1995). Reconstitution of yeast nucleotide excision repair with purified Rad proteins, replication protein A, and transcription factor TFIIH. J. Biol. Chem. *270*, 12973–12976.

Guzder, S. N., Sommers, C. H., Prakash, L., and Prakash, S. (2006). Complex Formation with Damage Recognition Protein Rad14 Is Essential for Saccharomyces cerevisiae Rad1-Rad10 Nuclease To Perform Its Function in Nucleotide Excision Repair In Vivo. Molecular and Cellular Biology *26*, 1135–1141.

Haaf, T., Hayman, D. L., and Schmid, M. (1991). Quantitative determination of rDNA transcription units in vertebrate cells. Exp. Cell Res. *193*, 78–86.

Haase, S. B., and Lew, D. J. (1997). Flow cytometric analysis of DNA content in budding yeast. Meth. Enzymol. *283*, 322–332.

Haeusler, R. A., and Engelke, D. R. (2006). Spatial organization of transcription by RNA polymerase III. Nucleic Acids Res. *34*, 4826–4836.

Hall, D. B., Wade, J. T., and Struhl, K. (2006). An HMG protein, Hmo1, associates with promoters of many ribosomal protein genes and throughout the rRNA gene locus in Saccharomyces cerevisiae. Mol. Cell. Biol. *26*, 3672–3679.

Han, M., and Grunstein, M. (1988). Nucleosome loss activates yeast downstream promoters in vivo. Cell *55*, 1137–1145.

Hanawalt, P. C. (2000). DNA repair. The bases for Cockayne syndrome. Nature *405*, 415–416.

Hansen, J. C., Tse, C., and Wolffe, A. P. (1998). Structure and function of the core histone N-termini: more than meets the eye. Biochemistry *37*, 17637–17641.

Hanson, C. V., Shen, C. K., and Hearst, J. E. (1976). Cross-linking of DNA in situ as a probe for chromatin structure. Science *193*, 62–64.

Happel, N., and Doenecke, D. (2009). Histone H1 and its isoforms: contribution to chromatin structure and function. Gene *431*, 1–12.

Hartwell, L. H., and Weinert, T. A. (1989). Checkpoints: controls that ensure the order of cell cycle events. Science *246*, 629–634.

Hecht, A., and Grunstein, M. (1999). Mapping DNA interaction sites of chromosomal proteins using immunoprecipitation and polymerase chain reaction. Meth. Enzymol. *304*, 399–414.

Heitman, J., Movva, N. R., and Hall, M. N. (1991). Targets for cell cycle arrest by the immunosuppressant rapamycin in yeast. Science *253*, 905–909.

Higashinakagawa, T., Wahn, H., and Reeder, R. H. (1977). Isolation of ribosomal gene chromatin. Dev. Biol. *55*, 375–386.

Hoeijmakers, J. H. (2001). Genome maintenance mechanisms for preventing cancer. Nature *411*, 366–374.

Hontz, R. D., French, S. L., Oakes, M. L., Tongaonkar, P., Nomura, M., Beyer, A. L., and Smith, J. S. (2008). Transcription of multiple yeast ribosomal DNA genes requires targeting of UAF to the promoter by Uaf30. Mol Cell Biol *28*, 6709–6719.

Horn, P. J., and Peterson, C. L. (2002). Molecular biology. Chromatin higher order folding--wrapping up transcription. Science *297*, 1824–1827.

Hörz, W., and Zachau, H. G. (1980). Deoxyribonuclease II as a probe for chromatin structure. I. Location of cleavage sites. J. Mol. Biol. *144*, 305–327.

Hunting, D. J., Dresler, S. L., and Lieberman, M. W. (1985). Multiple conformational states of repair patches in chromatin during DNA excision repair. Biochemistry *24*, 3219–3226.

Iben, S., Tschochner, H., Bier, M., Hoogstraten, D., Hozák, P., Egly, J. M., and Grummt, I. (2002). TFIIH plays an essential role in RNA polymerase I transcription. Cell *109*, 297–306.

Ide, S., Miyazaki, T., Maki, H., and Kobayashi, T. (2010). Abundance of ribosomal RNA gene copies maintains genome integrity. Science *327*, 693–696.

Imai, S., Armstrong, C. M., Kaeberlein, M., and Guarente, L. (2000). Transcriptional silencing and longevity protein Sir2 is an NAD-dependent histone deacetylase. Nature *403*, 795–800.

Jenuwein, T., and Allis, C. D. (2001). Translating the histone code. Science *293*, 1074–1080.

Jones, H. S., Kawauchi, J., Braglia, P., Alen, C. M., Kent, N. A., and Proudfoot, N. J. (2007). RNA polymerase I in yeast transcribes dynamic nucleosomal rDNA. Nat. Struct. Mol. Biol *14*, 123–130.

Jones, J. S., and Prakash, L. (1990). Yeast Saccharomyces cerevisiae selectable markers in pUC18 polylinkers. Yeast *6*, 363–366.

Kamau, E., Bauerle, K. T., and Grove, A. (2004). The Saccharomyces cerevisiae high mobility group box protein HMO1 contains two functional DNA binding domains. J. Biol. Chem. *279*, 55234–55240.

Kasahara, K., Ohtsuki, K., Ki, S., Aoyama, K., Takahashi, H., Kobayashi, T., Shirahige, K., and Kokubo, T. (2007). Assembly of regulatory factors on rRNA and ribosomal protein genes in Saccharomyces cerevisiae. Mol. Cell. Biol. *27*, 6686–6705.

Kaufman, P. D., Kobayashi, R., and Stillman, B. (1997). Ultraviolet radiation sensitivity and reduction of telomeric silencing in Saccharomyces cerevisiae cells lacking chromatin assembly factor-I. Genes Dev. *11*, 345–357.

Keener, J., Dodd, J. A., Lalo, D., and Nomura, M. (1997). Histones H3 and H4 are components of upstream activation factor required for the high-level transcription of yeast rDNA by RNA polymerase I. Proc. Natl. Acad. Sci. U.S.A. *94*, 13458–13462.

Keener, J., Josaitis, C. A., Dodd, J. A., and Nomura, M. (1998). Reconstitution of yeast RNA polymerase I transcription in vitro from purified components. TATA-binding protein is not required for basal transcription. J. Biol. Chem. *273*, 33795–33802.

Keys, D. A., Lee, B. S., Dodd, J. A., Nguyen, T. T., Vu, L., Fantino, E., Burson, L. M., Nogi, Y., and Nomura, M. (1996). Multiprotein transcription factor UAF interacts

with the upstream element of the yeast RNA polymerase I promoter and forms a stable preinitiation complex. Genes Dev. *10*, 887–903.

Kim, U. J., Han, M., Kayne, P., and Grunstein, M. (1988). Effects of histone H4 depletion on the cell cycle and transcription of Saccharomyces cerevisiae. EMBO J. *7*, 2211–2219.

Kimura, H., and Cook, P. R. (2001). Kinetics of core histones in living human cells: little exchange of H3 and H4 and some rapid exchange of H2B. J. Cell Biol. *153*, 1341–1353.

Knezetic, J. A., and Luse, D. S. (1986). The presence of nucleosomes on a DNA template prevents initiation by RNA polymerase II in vitro. Cell *45*, 95–104.

Kobayashi, T. (2006). Strategies to maintain the stability of the ribosomal RNA gene repeats--collaboration of recombination, cohesion, and condensation. Genes Genet. Syst. *81*, 155–161.

Kobayashi, T., and Ganley, A. R. D. (2005). Recombination regulation by transcription-induced cohesin dissociation in rDNA repeats. Science *309*, 1581–1584.

Kobayashi, T., and Horiuchi, T. (1996). A yeast gene product, Fob1 protein, required for both replication fork blocking and recombinational hotspot activities. Genes Cells *1*, 465–474.

Kobayashi, T., Heck, D. J., Nomura, M., and Horiuchi, T. (1998). Expansion and contraction of ribosomal DNA repeats in Saccharomyces cerevisiae: requirement of replication fork blocking (Fob1) protein and the role of RNA polymerase I. Genes Dev. *12*, 3821–3830.

Kobayashi, T., Hidaka, M., Nishizawa, M., and Horiuchi, T. (1992). Identification of a site required for DNA replication fork blocking activity in the rRNA gene cluster in Saccharomyces cerevisiae. Mol. Gen. Genet. *233*, 355–362.

Kobayashi, T., Horiuchi, T., Tongaonkar, P., Vu, L., and Nomura, M. (2004). SIR2 regulates recombination between different rDNA repeats, but not recombination within individual rRNA genes in yeast. Cell *117*, 441–453.

Kobayashi, T., Nomura, M., and Horiuchi, T. (2001). Identification of DNA cis elements essential for expansion of ribosomal DNA repeats in Saccharomyces cerevisiae. Mol. Cell. Biol. *21*, 136–147.

Koberna, K., Malínský, J., Pliss, A., Masata, M., Vecerova, J., Fialová, M., Bednár, J., and Raska, I. (2002). Ribosomal genes in focus: new transcripts label the dense fibrillar components and form clusters indicative of “Christmas trees” in situ. J. Cell Biol. *157*, 743–748.

Kornberg, R. D., and Lorch, Y. (1995). Interplay between chromatin structure and transcription. Curr. Opin. Cell Biol. *7*, 371–375.

Kressler, D., Linder, P., and de La Cruz, J. (1999). Protein trans-acting factors involved in ribosome biogenesis in Saccharomyces cerevisiae. Mol. Cell. Biol. *19*, 7897–7912.

Kristjuhan, A., and Svejstrup, J. Q. (2004). Evidence for distinct mechanisms facilitating transcript elongation through chromatin in vivo. EMBO J. *23*, 4243–4252.

Kulaeva, O. I., Gaykalova, D. A., and Studitsky, V. M. (2007). Transcription through chromatin by RNA polymerase II: histone displacement and exchange. Mutat. Res. *618*, 116–129.

Kulkens, T., van der Sande, C. A., Dekker, A. F., van Heerikhuizen, H., and Planta, R. J. (1992). A system to study transcription by yeast RNA polymerase I within the chromosomal context: functional analysis of the ribosomal DNA enhancer and the RBP1/REB1 binding sites. EMBO J *11*, 4665–4674.

Lainé, J.-P., and Egly, J.-M. (2006). When transcription and repair meet: a complex system. Trends Genet. *22*, 430–436.

Laird, C. D., Wilkinson, L. E., Foe, V. E., and Chooi, W. Y. (1976). Analysis of chromatin-associated fiber arrays. Chromosoma *58*, 169–190.

Lalo, D., Steffan, J. S., Dodd, J. A., and Nomura, M. (1996). RRN11 encodes the third subunit of the complex containing Rrn6p and Rrn7p that is essential for the initiation of rDNA transcription by yeast RNA polymerase I. J. Biol. Chem. *271*, 21062–21067.

Landry, J., Sutton, A., Tafrov, S. T., Heller, R. C., Stebbins, J., Pillus, L., and Sternglanz, R. (2000). The silencing protein SIR2 and its homologs are NAD-dependent protein deacetylases. Proc. Natl. Acad. Sci. U.S.A. *97*, 5807–5811.

Landsman, D. (1996). Histone H1 in Saccharomyces cerevisiae: a double mystery solved? Trends Biochem. Sci. *21*, 287–288.

Längst, G., and Becker, P. B. (2004). Nucleosome remodeling: one mechanism, many phenomena? Biochim. Biophys. Acta *1677*, 58–63.

Lavelle, C. (2007). Transcription elongation through a chromatin template. Biochimie *89*, 516–527.

Leadon, S. A., and Lawrence, D. A. (1992). Strand-selective repair of DNA damage in the yeast GAL7 gene requires RNA polymerase II. J. Biol. Chem. *267*, 23175–23182.

Lee, C.-K., Shibata, Y., Rao, B., Strahl, B. D., and Lieb, J. D. (2004). Evidence for nucleosome depletion at active regulatory regions genome-wide. Nat. Genet. *36*, 900–905.

Lee, K. P., Baxter, H. J., Guillemette, J. G., Lawford, H. G., and Lewis, P. N. (1982). Structural studies on yeast nucleosomes. Can. J. Biochem. *60*, 379–388.

Léger-Silvestre, I., Trumtel, S., Noaillac-Depeyre, J., and Gas, N. (1999). Functional compartmentalization of the nucleus in the budding yeast Saccharomyces cerevisiae. Chromosoma *108*, 103–113.

Li, B., Carey, M., and Workman, J. L. (2007). The role of chromatin during transcription. Cell *128*, 707–719.

Lin, C. W., Moorefield, B., Payne, J., Aprikian, P., Mitomo, K., and Reeder, R. H. (1996). A novel 66-kilodalton protein complexes with Rrn6, Rrn7, and TATA-binding protein to promote polymerase I transcription initiation in Saccharomyces cerevisiae. Mol. Cell. Biol. *16*, 6436–6443.

Lindahl, T., and Wood, R. D. (1999). Quality control by DNA repair. Science *286*, 1897–1905.

Linskens, M. H., and Huberman, J. A. (1988). Organization of replication of ribosomal DNA in Saccharomyces cerevisiae. Mol. Cell. Biol. *8*, 4927–4935.

Liu, X., and Smerdon, M. J. (2000). Nucleotide excision repair of the 5 S ribosomal RNA gene assembled into a nucleosome. J. Biol. Chem. *275*, 23729–23735.

Livingstone-Zatchej, M., Marcionelli, R., Möller, K., de Pril, R., and Thoma, F. (2003). Repair of UV lesions in silenced chromatin provides in vivo evidence for a compact chromatin structure. J. Biol. Chem. *278*, 37471–37479.

Long, E. O., and Dawid, I. B. (1980). Repeated genes in eukaryotes. Annu. Rev. Biochem. *49*, 727–764.

Lorch, Y., LaPointe, J. W., and Kornberg, R. D. (1987). Nucleosomes inhibit the initiation of transcription but allow chain elongation with the displacement of histones. Cell *49*, 203–210.

Lu, J., Kobayashi, R., and Brill, S. J. (1996). Characterization of a high mobility group 1/2 homolog in yeast. J. Biol. Chem *271*, 33678–33685.

Lu, X., Wontakal, S. N., Emelyanov, A. V., Morcillo, P., Konev, A. Y., Fyodorov, D. V., and Skoultchi, A. I. (2009). Linker histone H1 is essential for Drosophila development, the establishment of pericentric heterochromatin, and a normal polytene chromosome structure. Genes Dev. *23*, 452–465.

Lucchini, R., and Sogo, J. M. (1992). Different chromatin structures along the spacers flanking active and inactive Xenopus rRNA genes. Mol. Cell. Biol. *12*, 4288–4296.

Lucchini, R., and Sogo, J. M. (1995). Replication of transcriptionally active chromatin. Nature *374*, 276–280.

Lucchini, R., Pauli, U., Braun, R., Koller, T., and Sogo, J. M. (1987). Structure of the extrachromosomal ribosomal RNA chromatin of Physarum polycephalum. J. Mol. Biol. *196*, 829–843.

Luger, K. (2003). Structure and dynamic behavior of nucleosomes. Curr. Opin. Genet. Dev. *13*, 127–135.

Luger, K., and Richmond, T. J. (1998). The histone tails of the nucleosome. Curr. Opin. Genet. Dev. *8*, 140–146.

Maresca, T. J., and Heald, R. (2006). The long and the short of it: linker histone H1 is required for metaphase chromosome compaction. Cell Cycle *5*, 589–591.

Marzluff, W. F., and Duronio, R. J. (2002). Histone mRNA expression: multiple levels of cell cycle regulation and important developmental consequences. Curr. Opin. Cell Biol. *14*, 692–699.

Marzluff, W. F., Wagner, E. J., and Duronio, R. J. (2008). Metabolism and regulation of canonical histone mRNAs: life without a poly(A) tail. Nat. Rev. Genet. *9*, 843–854.

Mason, P. B., and Struhl, K. (2005). Distinction and relationship between elongation rate and processivity of RNA polymerase II in vivo. Mol. Cell *17*, 831–840.

Mason, P. B., and Struhl, K. (2003). The FACT complex travels with elongating RNA polymerase II and is important for the fidelity of transcriptional initiation in vivo. Mol. Cell. Biol. *23*, 8323–8333.

Mathis, D. J., and Gorovsky, M. A. (1976). Subunit structure of rDNA-containing chromatin. Biochemistry *15*, 750–755.

Matsui, S., and Busch, H. (1977). Isolation and characterization of rDNA-containing chromatin from nucleoli. Exp. Cell Res. *109*, 151–161.

McStay, B., and Grummt, I. (2008). The epigenetics of rRNA genes: from molecular to chromosome biology. Annu. Rev. Cell Dev. Biol. *24*, 131–157.

Meeks-Wagner, D., and Hartwell, L. H. (1986). Normal stoichiometry of histone dimer sets is necessary for high fidelity of mitotic chromosome transmission. Cell *44*, 43–52.

Meier, A., Livingstone-Zatchej, M., and Thoma, F. (2002). Repair of active and silenced rDNA in yeast: the contributions of photolyase and transcription-couples nucleotide excision repair. J. Biol. Chem. *277*, 11845–11852.

Mello, J. A., and Almouzni, G. (2001). The ins and outs of nucleosome assembly. Curr. Opin. Genet. Dev. *11*, 136–141.

Mello, J. A., Silljé, H. H. W., Roche, D. M. J., Kirschner, D. B., Nigg, E. A., and Almouzni, G. (2002). Human Asf1 and CAF-1 interact and synergize in a repair-coupled nucleosome assembly pathway. EMBO Rep. *3*, 329–334.

Mellon, I. (2005). Transcription-coupled repair: a complex affair. Mutat. Res. *577*, 155–161.

Mellon, I., Bohr, V. A., Smith, C. A., and Hanawalt, P. C. (1986). Preferential DNA repair of an active gene in human cells. Proc. Natl. Acad. Sci. U.S.A. *83*, 8878–8882.

Merz, K. (2008). In vivo Analyse der Chromatinstruktur ribosomaler DNA in S. cerevisiae. Available at: http://epub.uni-regensburg.de/10683/ [Accessed December 28, 2011].

Merz, K., Hondele, M., Goetze, H., Gmelch, K., Stoeckl, U., and Griesenbeck, J. (2008). Actively transcribed rRNA genes in S. cerevisiae are organized in a specialized chromatin associated with the high-mobility group protein Hmo1 and are largely devoid of histone molecules. Genes Dev *22*, 1190–1204.

Milkereit, P., and Tschochner, H. (1998). A specialized form of RNA polymerase I, essential for initiation and growth-dependent regulation of rRNA synthesis, is disrupted during transcription. EMBO J. *17*, 3692–3703.

Miller, O. L., Jr, and Beatty, B. R. (1969). Visualization of nucleolar genes. Science *164*, 955–957.

Moggs, J. G., Grandi, P., Quivy, J. P., Jónsson, Z. O., Hübscher, U., Becker, P. B., and Almouzni, G. (2000). A CAF-1-PCNA-mediated chromatin assembly pathway triggered by sensing DNA damage. Mol. Cell. Biol. *20*, 1206–1218.

Moll, T., Tebb, G., Surana, U., Robitsch, H., and Nasmyth, K. (1991). The role of phosphorylation and the CDC28 protein kinase in cell cycle-regulated nuclear import of the S. cerevisiae transcription factor SWI5. Cell *66*, 743–758.

Mougey, E. B., O'Reilly, M., Osheim, Y., Miller, O. L., Jr, Beyer, A., and Sollner-Webb, B. (1993). The terminal balls characteristic of eukaryotic rRNA transcription units in chromatin spreads are rRNA processing complexes. Genes Dev. *7*, 1609–1619.

Mueller, J. P., and Smerdon, M. J. (1995). Repair of plasmid and genomic DNA in a rad7 delta mutant of yeast. Nucleic Acids Res. *23*, 3457–3464.

Muller, M., Lucchini, R., and Sogo, J. M. (2000). Replication of yeast rDNA initiates downstream of transcriptionally active genes. Mol. Cell *5*, 767–777.

Muscarella, D. E., Vogt, V. M., and Bloom, S. E. (1987). Characterization of ribosomal RNA synthesis in a gene dosage mutant: the relationship of topoisomerase I and chromatin structure to transcriptional activity. J. Cell Biol. *105*, 1501–1513.

Musters, W., Knol, J., Maas, P., Dekker, A. F., van Heerikhuizen, H., and Planta, R. J. (1989). Linker scanning of the yeast RNA polymerase I promoter. Nucleic Acids Res. *17*, 9661–9678.

Natsume, R., Eitoku, M., Akai, Y., Sano, N., Horikoshi, M., and Senda, T. (2007). Structure and function of the histone chaperone CIA/ASF1 complexed with histones H3 and H4. Nature *446*, 338–341.

Németh, A., and Längst, G. (2008). Chromatin organization of active ribosomal RNA genes. Epigenetics *3*, 243–245.

Ness, P. J., Labhart, P., Banz, E., Koller, T., and Parish, R. W. (1983). Chromatin structure along the ribosomal DNA of Dictyostelium. Regional differences and changes accompanying cell differentiation. J. Mol. Biol. *166*, 361–381.

Nogi, Y., Yano, R., and Nomura, M. (1991). Synthesis of large rRNAs by RNA polymerase II in mutants of Saccharomyces cerevisiae defective in RNA polymerase I. Proc. Natl. Acad. Sci. U.S.A *88*, 3962–3966.

O'Sullivan, A. C., Sullivan, G. J., and McStay, B. (2002). UBF binding in vivo is not restricted to regulatory sequences within the vertebrate ribosomal DNA repeat. Mol. Cell. Biol *22*, 657–668.

Oakes, M., Aris, J. P., Brockenbrough, J. S., Wai, H., Vu, L., and Nomura, M. (1998). Mutational analysis of the structure and localization of the nucleolus in the yeast Saccharomyces cerevisiae. J. Cell Biol. *143*, 23–34.

Orphanides, G., LeRoy, G., Chang, C. H., Luse, D. S., and Reinberg, D. (1998). FACT, a factor that facilitates transcript elongation through nucleosomes. Cell *92*, 105–116.

Orphanides, G., Wu, W. H., Lane, W. S., Hampsey, M., and Reinberg, D. (1999). The chromatin-specific transcription elongation factor FACT comprises human SPT16 and SSRP1 proteins. Nature *400*, 284–288.

Le Page, F., Klungland, A., Barnes, D. E., Sarasin, A., and Boiteux, S. (2000). Transcription coupled repair of 8-oxoguanine in murine cells: the ogg1 protein is required for repair in nontranscribed sequences but not in transcribed sequences. Proc. Natl. Acad. Sci. U.S.A. *97*, 8397–8402.

Palomera-Sanchez, Z., and Zurita, M. (2011). Open, repair and close again: chromatin dynamics and the response to UV-induced DNA damage. DNA Repair (Amst.) *10*, 119–125.

Parsons, B. J. (1980). Psoralen photochemistry. Photochem. Photobiol. *32*, 813–821.

Patterton, H. G., Landel, C. C., Landsman, D., Peterson, C. L., and Simpson, R. T. (1998). The biochemical and phenotypic characterization of Hho1p, the putative linker histone H1 of Saccharomyces cerevisiae. J. Biol. Chem. *273*, 7268–7276.

Paule, M. R. (1999). Transcription of Ribosomal RNA Genes by Eukaryotic RNA Polymerase I (Springer, Berlin).

Peterson, C. L., and Laniel, M.-A. (2004). Histones and histone modifications. Curr. Biol. *14*, R546–R551.

Petes, T. D. (1979). Yeast ribosomal DNA genes are located on chromosome XII. Proc. Natl. Acad. Sci. U.S.A. *76*, 410–414.

Peyroche, G., Milkereit, P., Bischler, N., Tschochner, H., Schultz, P., Sentenac, A., Carles, C., and Riva, M. (2000). The recruitment of RNA polymerase I on rDNA is mediated by the interaction of the A43 subunit with Rrn3. EMBO J *19*, 5473–5482.

Philippi, A., Steinbauer, R., Reiter, A., Fath, S., Leger-Silvestre, I., Milkereit, P., Griesenbeck, J., and Tschochner, H. (2010). TOR-dependent reduction in the expression level of Rrn3p lowers the activity of the yeast RNA Pol I machinery, but does not account for the strong inhibition of rRNA production. Nucleic Acids Res *38*, 5315–5326.

Philippsen, P., Thomas, M., Kramer, R. A., and Davis, R. W. (1978). Unique arrangement of coding sequences for 5 S, 5.8 S, 18 S and 25 S ribosomal RNA in Saccharomyces cerevisiae as determined by R-loop and hybridization analysis. J. Mol. Biol. *123*, 387–404.

Philpott, A., Krude, T., and Laskey, R. A. (2000). Nuclear chaperones. Semin. Cell Dev. Biol. *11*, 7–14.

Piñeiro, M., Puerta, C., and Palacián, E. (1991). Yeast nucleosomal particles: structural and transcriptional properties. Biochemistry *30*, 5805–5810.

Piper, P. W., Celis, J., Kaltoft, K., Leer, J. C., Nielsen, O. F., and Westergaard, O. (1976). Tetrahymena ribosomal RNA gene chromatin is digested by micrococcal nuclease at sites which have the same regular spacing on the DNA as corresponding sites in the bulk nuclear chromatin. Nucleic Acids Res. *3*, 493–505.

Powers, T., and Walter, P. (1999). Regulation of ribosome biogenesis by the rapamycin-sensitive TOR-signaling pathway in Saccharomyces cerevisiae. Mol. Biol. Cell *10*, 987–1000.

Prakash, S., and Prakash, L. (2000). Nucleotide excision repair in yeast. Mutation Research/Fundamental and Molecular Mechanisms of Mutagenesis *451*, 13–24.

Puig, O., Caspary, F., Rigaut, G., Rutz, B., Bouveret, E., Bragado-Nilsson, E., Wilm, M., and Séraphin, B. (2001). The tandem affinity purification (TAP) method: a general procedure of protein complex purification. Methods *24*, 218–229.

Raska, I. (2003). Oldies but goldies: searching for Christmas trees within the nucleolar architecture. Trends Cell Biol. *13*, 517–525.

Raska, I., Koberna, K., Malínský, J., Fidlerová, H., and Masata, M. (2004). The nucleolus and transcription of ribosomal genes. Biol Cell *96*, 579–594.

Raska, I., Shaw, P. J., and Cmarko, D. (2006). Structure and function of the nucleolus in the spotlight. Curr. Opin. Cell Biol. *18*, 325–334.

Ravanat, J. L., Douki, T., and Cadet, J. (2001). Direct and indirect effects of UV radiation on DNA and its components. J. Photochem. Photobiol. B, Biol. *63*, 88–102.

Reeder, R. H. (1989). Regulatory elements of the generic ribosomal gene. Curr. Opin. Cell Biol. *1*, 466–474.

Reeder, R. H., Guevara, P., and Roan, J. G. (1999). Saccharomyces cerevisiae RNA polymerase I terminates transcription at the Reb1 terminator in vivo. Mol. Cell. Biol. *19*, 7369–7376.

Reeves, R. (1977). Analysis and reconstruction of Xenopus ribosomal chromatin nucleosomes. Eur. J. Biochem. *75*, 545–560.

Reeves, R. (1976). Ribosomal genes of Xenopus laevis: evidence of nucleosomes in transcriptionally active chromatin. Science *194*, 529–532.

Reeves, R., and Jones, A. (1976). Genomic transcriptional activity and the structure of chromatin. Nature *260*, 495–500.

Reinke, H., and Hörz, W. (2003). Histones are first hyperacetylated and then lose contact with the activated PHO5 promoter. Mol. Cell *11*, 1599–1607.

Rice, J. C., and Allis, C. D. (2001). Histone methylation versus histone acetylation: new insights into epigenetic regulation. Curr. Opin. Cell Biol. *13*, 263–273.

Roth, S. Y., Denu, J. M., and Allis, C. D. (2001). Histone acetyltransferases. Annu. Rev. Biochem. *70*, 81–120.

Russell, P. (1998). Checkpoints on the road to mitosis. Trends Biochem. Sci. *23*, 399–402.

Sancho, M., Diani, E., Beato, M., and Jordan, A. (2008). Depletion of human histone H1 variants uncovers specific roles in gene expression and cell growth. PLoS Genet. *4*, e1000227.

Sandmeier, J. J., French, S., Osheim, Y., Cheung, W. L., Gallo, C. M., Beyer, A. L., and Smith, J. S. (2002). RPD3 is required for the inactivation of yeast ribosomal DNA genes in stationary phase. EMBO J *21*, 4959–4968.

Sanij, E., Poortinga, G., Sharkey, K., Hung, S., Holloway, T. P., Quin, J., Robb, E., Wong, L. H., Thomas, W. G., Stefanovsky, V., et al. (2008). UBF levels determine the number of active ribosomal RNA genes in mammals. J. Cell Biol *183*, 1259–1274.

Sarker, A. H., Tsutakawa, S. E., Kostek, S., Ng, C., Shin, D. S., Peris, M., Campeau, E., Tainer, J. A., Nogales, E., and Cooper, P. K. (2005). Recognition of RNA polymerase II and transcription bubbles by XPG, CSB, and TFIIH: insights for transcription-coupled repair and Cockayne Syndrome. Mol. Cell *20*, 187–198.

Scheer, U., and Hock, R. (1999). Structure and function of the nucleolus. Curr. Opin. Cell Biol. *11*, 385–390.

Scheer, U., Hügle, B., Hazan, R., and Rose, K. M. (1984). Drug-induced dispersal of transcribed rRNA genes and transcriptional products: immunolocalization and silver staining of different nucleolar components in rat cells treated with 5,6-dichloro-beta-D-ribofuranosylbenzimidazole. J. Cell Biol. *99*, 672–679.

Schermer, U. J., Korber, P., and Hörz, W. (2005). Histones are incorporated in trans during reassembly of the yeast PHO5 promoter. Mol. Cell *19*, 279–285.

Schlesinger, S., Selig, S., Bergman, Y., and Cedar, H. (2009). Allelic inactivation of rDNA loci. Genes Dev. *23*, 2437–2447.

Schmid, M., Arib, G., Laemmli, C., Nishikawa, J., Durussel, T., and Laemmli, U. K. (2006). Nup-PI: the nucleopore-promoter interaction of genes in yeast. Mol. Cell *21*, 379–391.

Schmid, M., Durussel, T., and Laemmli, U. K. (2004). ChIC and ChEC; genomic mapping of chromatin proteins. Mol Cell *16*, 147–157.

Schultz, M. C., Brill, S. J., Ju, Q., Sternglanz, R., and Reeder, R. H. (1992). Topoisomerases and yeast rRNA transcription: negative supercoiling stimulates initiation and topoisomerase activity is required for elongation. Genes Dev. *6*, 1332–1341.

Schwab, M., Lutum, A. S., and Seufert, W. (1997). Yeast Hct1 is a regulator of Clb2 cyclin proteolysis. Cell *90*, 683–693.

Schwabish, M. A., and Struhl, K. (2004). Evidence for eviction and rapid deposition of histones upon transcriptional elongation by RNA polymerase II. Mol. Cell. Biol. *24*, 10111–10117.

Selby, C. P., Drapkin, R., Reinberg, D., and Sancar, A. (1997). RNA polymerase II stalled at a thymine dimer: footprint and effect on excision repair. Nucleic Acids Res. *25*, 787–793.

Shibahara, K., and Stillman, B. (1999). Replication-dependent marking of DNA by PCNA facilitates CAF-1-coupled inheritance of chromatin. Cell *96*, 575–585.

Siddiqi, I. N., Dodd, J. A., Vu, L., Eliason, K., Oakes, M. L., Keener, J., Moore, R., Young, M. K., and Nomura, M. (2001). Transcription of chromosomal rRNA genes by both RNA polymerase I and II in yeast uaf30 mutants lacking the 30 kDa subunit of transcription factor UAF. EMBO J *20*, 4512–4521.

Sinden, R. R., Bat, O., and Kramer, P. R. (1999). Psoralen cross-linking as probe of torsional tension and topological domain size in vivo. Methods *17*, 112–124.

Smerdon, M. J. (1986). Completion of excision repair in human cells. Relationship between ligation and nucleosome formation. J. Biol. Chem. *261*, 244–252.

Smerdon, M. J., and Conconi, A. (1999). Modulation of DNA damage and DNA repair in chromatin. Prog. Nucleic Acid Res. Mol. Biol. *62*, 227–255.

Smerdon, M. J., and Lieberman, M. W. (1980). Distribution within chromatin of deoxyribonucleic acid repair synthesis occurring at different times after ultraviolet radiation. Biochemistry *19*, 2992–3000.

Smerdon, M. J., and Lieberman, M. W. (1978). Nucleosome rearrangement in human chromatin during UV-induced DNA- reapir synthesis. Proc. Natl. Acad. Sci. U.S.A. *75*, 4238–4241.

Smerdon, M. J., Kastan, M. B., and Lieberman, M. W. (1979). Distribution of repair-incorporated nucleotides and nucleosome rearrangement in the chromatin of normal and xeroderma pigmentosum human fibroblasts. Biochemistry *18*, 3732–3739.

Smith, J. S., and Boeke, J. D. (1997). An unusual form of transcriptional silencing in yeast ribosomal DNA. Genes Dev *11*, 241–254.

Smith, J. S., Brachmann, C. B., Celic, I., Kenna, M. A., Muhammad, S., Starai, V. J., Avalos, J. L., Escalante-Semerena, J. C., Grubmeyer, C., Wolberger, C., et al. (2000). A phylogenetically conserved NAD+-dependent protein deacetylase activity in the Sir2 protein family. Proc. Natl. Acad. Sci. U.S.A. *97*, 6658–6663.

Smith, J. S., Caputo, E., and Boeke, J. D. (1999). A genetic screen for ribosomal DNA silencing defects identifies multiple DNA replication and chromatin-modulating factors. Mol. Cell. Biol *19*, 3184–3197.

Smith, S., and Stillman, B. (1989). Purification and characterization of CAF-I, a human cell factor required for chromatin assembly during DNA replication in vitro. Cell *58*, 15–25.

Sogo, J. M., Ness, P. J., Widmer, R. M., Parish, R. W., and Koller, T. (1984). Psoralen-crosslinking of DNA as a probe for the structure of active nucleolar chromatin. J. Mol. Biol *178*, 897–919.

Sogo, J. M., Stahl, H., Koller, T., and Knippers, R. (1986). Structure of replicating simian virus 40 minichromosomes. The replication fork, core histone segregation and terminal structures. J. Mol. Biol. *189*, 189–204.

Stancheva, I., Lucchini, R., Koller, T., and Sogo, J. M. (1997). Chromatin structure and methylation of rat rRNA genes studied by formaldehyde fixation and psoralen cross-linking. Nucleic Acids Res. *25*, 1727–1735.

Stefanovsky, V., Langlois, F., Gagnon-Kugler, T., Rothblum, L. I., and Moss, T. (2006). Growth factor signaling regulates elongation of RNA polymerase I transcription in mammals via UBF phosphorylation and r-chromatin remodeling. Mol. Cell *21*, 629–639.

Steffan, J. S., Keys, D. A., Dodd, J. A., and Nomura, M. (1996). The role of TBP in rDNA transcription by RNA polymerase I in Saccharomyces cerevisiae: TBP is required for upstream activation factor-dependent recruitment of core factor. Genes Dev. *10*, 2551–2563.

Sterner, D. E., and Berger, S. L. (2000). Acetylation of histones and transcription-related factors. Microbiol. Mol. Biol. Rev. *64*, 435–459.

Stevnsner, T., May, A., Petersen, L. N., Larminat, F., Pirsel, M., and Bohr, V. A. (1993). Repair of ribosomal RNA genes in hamster cells after UV irradiation, or treatment with cisplatin or alkylating agents. Carcinogenesis *14*, 1591–1596.

Stillman, B. (1986). Chromatin assembly during SV40 DNA replication in vitro. Cell *45*, 555–565.

Strahl, B. D., and Allis, C. D. (2000). The language of covalent histone modifications. Nature *403*, 41–45.

Sweder, K. S., and Hanawalt, P. C. (1992). Preferential repair of cyclobutane pyrimidine dimers in the transcribed strand of a gene in yeast chromosomes and plasmids is dependent on transcription. Proc. Natl. Acad. Sci. U.S.A. *89*, 10696–10700.

Tan, B. C.-M., Chien, C.-T., Hirose, S., and Lee, S.-C. (2006). Functional cooperation between FACT and MCM helicase facilitates initiation of chromatin DNA replication. EMBO J. *25*, 3975–3985.

Tan, R. Z., and van Oudenaarden, A. (2010). Transcript counting in single cells reveals dynamics of rDNA transcription. Mol. Syst. Biol. *6*, 358.

Telford, D. J., and Stewart, B. W. (1989). Micrococcal nuclease: its specificity and use for chromatin analysis. Int. J. Biochem *21*, 127–137.

Teng, Y., Yu, Y., Ferreiro, J. A., and Waters, R. (2005). Histone acetylation, chromatin remodelling, transcription and nucleotide excision repair in S. cerevisiae: studies with two model genes. DNA Repair (Amst.) *4*, 870–883.

Thoma, F. (1999). Light and dark in chromatin repair: repair of UV-induced DNA lesions by photolyase and nucleotide excision repair. EMBO J. *18*, 6585–6598.

Thoma, F. (2005). Repair of UV lesions in nucleosomes--intrinsic properties and remodeling. DNA Repair (Amst.) *4*, 855–869.

Tijsterman, M., de Pril, R., Tasseron-de Jong, J. G., and Brouwer, J. (1999). RNA polymerase II transcription suppresses nucleosomal modulation of UV-induced (6-4) photoproduct and cyclobutane pyrimidine dimer repair in yeast. Mol. Cell. Biol. *19*, 934–940.

Tornaletti, S., and Hanawalt, P. C. (1999). Effect of DNA lesions on transcription elongation. Biochimie *81*, 139–146.

Toussaint, M., Levasseur, G., Tremblay, M., Paquette, M., and Conconi, A. (2005). Psoralen photocrosslinking, a tool to study the chromatin structure of RNA polymerase I--transcribed ribosomal genes. Biochem Cell Biol *83*, 449–459.

Tremblay, M., Levasseur, G., and Conconi, A. UV light induced DNA lesions cause dissociation of RNA polymerase-I and inactivation of rRNA genes. (submitted)

Tremblay, M., Teng, Y., Paquette, M., Waters, R., and Conconi, A. (2008). Complementary roles of yeast Rad4p and Rad34p in nucleotide excision repair of active and inactive rRNA gene chromatin. Mol. Cell. Biol *28*, 7504–7513.

Tremblay, M., Toussaint, M., D'Amours, A., and Conconi, A. (2009). Nucleotide excision repair and photolyase repair of UV photoproducts in nucleosomes: assessing the existence of nucleosome and non-nucleosome rDNA chromatin in vivo. Biochem Cell Biol *87*, 337–346.

Troelstra, C., van Gool, A., de Wit, J., Vermeulen, W., Bootsma, D., and Hoeijmakers, J. H. (1992). ERCC6, a member of a subfamily of putative helicases, is involved in Cockayne's syndrome and preferential repair of active genes. Cell *71*, 939–953.

Trumtel, S., Léger-Silvestre, I., Gleizes, P. E., Teulières, F., and Gas, N. (2000). Assembly and functional organization of the nucleolus: ultrastructural analysis of Saccharomyces cerevisiae mutants. Mol Biol Cell *11*, 2175–2189.

Tschochner, H., and Hurt, E. (2003). Pre-ribosomes on the road from the nucleolus to the cytoplasm. Trends Cell Biol. *13*, 255–263.

Tyler, J. K. (2002). Chromatin assembly. Cooperation between histone chaperones and ATP-dependent nucleosome remodeling machines. Eur. J. Biochem. *269*, 2268–2274.

Tyler, J. K., Adams, C. R., Chen, S. R., Kobayashi, R., Kamakaka, R. T., and Kadonaga, J. T. (1999). The RCAF complex mediates chromatin assembly during DNA replication and repair. Nature *402*, 555–560.

Ura, K., and Hayes, J. J. (2002). Nucleotide excision repair and chromatin remodeling. Eur. J. Biochem. *269*, 2288–2293.

Ura, K., Araki, M., Saeki, H., Masutani, C., Ito, T., Iwai, S., Mizukoshi, T., Kaneda, Y., and Hanaoka, F. (2001). ATP-dependent chromatin remodeling facilitates nucleotide excision repair of UV-induced DNA lesions in synthetic dinucleosomes. EMBO J. *20*, 2004–2014.

Ushinsky, S. C., Bussey, H., Ahmed, A. A., Wang, Y., Friesen, J., Williams, B. A., and Storms, R. K. (1997). Histone H1 in Saccharomyces cerevisiae. Yeast *13*, 151–161.

Venema, J., and Tollervey, D. (1999). Ribosome synthesis in Saccharomyces cerevisiae. Annu. Rev. Genet. *33*, 261–311.

Verhage, R. A., Van de Putte, P., and Brouwer, J. (1996). Repair of rDNA in Saccharomyces cerevisiae: RAD4-independent strand-specific nucleotide excision repair of RNA polymerase I transcribed genes. Nucleic Acids Res. *24*, 1020–1025.

Verhage, R., Zeeman, A. M., de Groot, N., Gleig, F., Bang, D. D., van de Putte, P., and Brouwer, J. (1994). The RAD7 and RAD16 genes, which are essential for pyrimidine dimer removal from the silent mating type loci, are also required for repair of the nontranscribed strand of an active gene in Saccharomyces cerevisiae. Mol. Cell. Biol. *14*, 6135–6142.

Verreault, A. (2000). De novo nucleosome assembly: new pieces in an old puzzle. Genes Dev. *14*, 1430–1438.

Vogelauer, M., Cioci, F., and Camilloni, G. (1998). DNA protein-interactions at the Saccharomyces cerevisiae 35 S rRNA promoter and in its surrounding region. J. Mol. Biol. *275*, 197–209.

Wai, H., Johzuka, K., Vu, L., Eliason, K., Kobayashi, T., Horiuchi, T., and Nomura, M. (2001). Yeast RNA polymerase I enhancer is dispensable for transcription of the chromosomal rRNA gene and cell growth, and its apparent transcription enhancement from ectopic promoters requires Fob1 protein. Mol. Cell. Biol. *21*, 5541–5553.

Warner, J. R. (1999). The economics of ribosome biosynthesis in yeast. Trends Biochem Sci *24*, 437–440.

Weintraub, H., and Groudine, M. (1976). Chromosomal subunits in active genes have an altered conformation. Science *193*, 848–856.

Wellinger, R. E., and Thoma, F. (1997). Nucleosome structure and positioning modulate nucleotide excision repair in the non-transcribed strand of an active gene. EMBO J. *16*, 5046–5056.

White, C. L., Suto, R. K., and Luger, K. (2001). Structure of the yeast nucleosome core particle reveals fundamental changes in internucleosome interactions. EMBO J. *20*, 5207–5218.

Willis, N., and Rhind, N. (2009). Regulation of DNA replication by the S-phase DNA damage checkpoint. Cell Div *4*, 13.

Wittner, M., Hamperl, S., Stöckl, U., Seufert, W., Tschochner, H., Milkereit, P., and Griesenbeck, J. (2011). Establishment and maintenance of alternative chromatin states at a multicopy gene locus. Cell *145*, 543–554.

Wolffe, A. P., and Kurumizaka, H. (1998). The nucleosome: a powerful regulator of transcription. Prog. Nucleic Acid Res. Mol. Biol. *61*, 379–422.

Woodcock, C. L., and Ghosh, R. P. (2010). Chromatin higher-order structure and dynamics. Cold Spring Harb Perspect Biol *2*, a000596.

Workman, J. L. (2006). Nucleosome displacement in transcription. Genes Dev. *20*, 2009–2017.

Yamamoto, R. T., Nogi, Y., Dodd, J. A., and Nomura, M. (1996). RRN3 gene of Saccharomyces cerevisiae encodes an essential RNA polymerase I transcription factor which interacts with the polymerase independently of DNA template. EMBO J *15*, 3964–3973.

Yu, Y., and Waters, R. (2005). Histone acetylation, chromatin remodelling and nucleotide excision repair: hint from the study on MFA2 in Saccharomyces cerevisiae. Cell Cycle *4*, 1043–1045.

Yu, Y., Teng, Y., Liu, H., Reed, S. H., and Waters, R. (2005). UV irradiation stimulates histone acetylation and chromatin remodeling at a repressed yeast locus. Proc. Natl. Acad. Sci. U.S.A. *102*, 8650–8655.

Yuan, G.-C., Liu, Y.-J., Dion, M. F., Slack, M. D., Wu, L. F., Altschuler, S. J., and Rando, O. J. (2005). Genome-scale identification of nucleosome positions in S. cerevisiae. Science *309*, 626–630.

Zaragoza, D., Ghavidel, A., Heitman, J., and Schultz, M. C. (1998). Rapamycin induces the G0 program of transcriptional repression in yeast by interfering with the TOR signaling pathway. Mol. Cell. Biol. *18*, 4463–4470.

Zhang, L., Jones, K., and Gong, F. (2009). The molecular basis of chromatin dynamics during nucleotide excision repair. Biochem. Cell Biol. *87*, 265–272.

Zlatanova, J., Seebart, C., and Tomschik, M. (2007). Nap1: taking a closer look at a juggler protein of extraordinary skills. FASEB J. *21*, 1294–1310.

7 Abbreviations

Amp	ampicilline
APS	ammonium persulfate
ATP	adenosine triphosphate
ARS	autonomous replication sequence
bp	base pair(s)
CEN	centromere
CDS	coding sequence
CF	core factor
ChEC	chromatin endogenous cleavage
ChIP	chromain immunoprecipitation
CP	core promoter
CPD	cyclobutane pyrimidine dimer
C-terminal	carboxy-terminal
Da	Dalton
DNA	desoxyribonucleic acid
dNTP	2-desoxyribonucleotide 5' triphosphate
E. coli	*Escherichia coli*
EDTA	ethylene diamine tetra acetate
EGTA	ethylene glycol tetraacetic acid
ENH	enhancer
E-pro	bidirectional Pol II promoter in the rDNA
g	gram(s)
GGR	global genome repair
h	hour(s)
k	kilo
kb	kilo base pair(s)
l	liter(s)
LB	lysogeny broth
mg	milligram(s)
min	minute(s)
ml	milliliter(s)
MNase	micrococcal nuclease
MW	molecular weight
M	molar (mol/l)
NER	nucleotide excision repair
NTS	non-transcribed strand

nm	nanometer(s)
OD	optical density
ORF	open reading frame
P	promoter
PAGE	poly acryl amide electrophoresis
PBS	phophate buffered saline
PCR	polymerase chain reaction
pH	negative decadic logarithm of [H+]
Pol	RNA polymerase
qPCR	quantitative real-time PCR
rDNA	ribosomal DNA
RFB	replication fork barrier
RNA	ribonucleic acid
RP	ribosomal protein
rpm	rotations per minute
rRNA	ribosomal RNA
RT	room temperature
S	sedimentation coefficient
S. cerevisiae	*Saccharomyces cerevisiae*
SDS	sodium dodecyl sulfate
snoRNA	small nucleolar RNA
Taq	Thermus aquaticus
TBP	TATA-box binding protein
TCA	tri chloro acetic acid
TCR	transcription coupled repair
T/E	terminator / enhancer
tel	telomere
TEMED	tetramethylethylenediamine
Tris	tris(hydroxy methyl) amino methane
TS	transcribed strand
U	unit(s)
UAF	upstream activating factor
UE	upstream element
UV	ultra violet
WT	wild-type

8 Publications

Part of this work has been published.

Griesenbeck, J., Wittner, M., Charton, R., and Conconi, A. (2012). Chromatin Endogenous Cleavage and Psoralen Crosslinking Assays to Analyze rRNA Gene Chromatin In Vivo. Methods Mol. Biol. *809*, 291–301.

Wittner, M., Hamperl, S., Stöckl, U., Seufert, W., Tschochner, H., Milkereit, P., and Griesenbeck, J. (2011). Establishment and maintenance of alternative chromatin states at a multicopy gene locus. Cell *145*, 543–554.

Goetze, H., Wittner, M., Hamperl, S., Hondele, M., Merz, K., Stoeckl, U., and Griesenbeck, J. (2010). Alternative Chromatin Structures of the 35S rRNA Genes in Saccharomyces cerevisiae Provide a Molecular Basis for the Selective Recruitment of RNA Polymerases I and II. Mol. Cell. Biol *30*, 2028–2045.

Acknowledgements

Abschließend danke ich allen, die zum Gelingen dieser Arbeit beigetragen haben.

Mein besonderer Dank gilt meinem Mentor PD Dr. Joachim Griesenbeck für die interessante Themenstellung und die großartige Betreuung dieser Doktorarbeit. Vielen Dank für Deine stetige Unterstützung, Förderung, Motivationsspende, ständige Diskussionsbereitschaft und für die spitzenmäßige Zusammenarbeit.

Herzlichen Dank auch an Prof. Dr. Herbert Tschochner für die Möglichkeit diese Promotion an seinem Lehrstuhl durchzuführen. Vielen Dank für die vielen Diskussionen, die stete Unterstützung in allen Belangen und das Erdulden der (doch manchmal etwas lauten) Musik in Deinen Räumen.

Vielen Dank auch an Dr. Philipp Milkereit für die vielen Anregungen und Diskussionen die einen großen Beitrag zum Gelingen dieser Arbeit geleistet haben.

Prof. Dr. Wolfgang Seufert danke ich für die vielen anregenden Diskussionen. Außerdem danke ich ihm und seiner Mitarbeiterin Dr. Heidi Richter für die Hilfe bei den durchflusszytometrischen Analysen.

Herzlichen Dank an Prof. Dr. Antonio Conconi für die Möglichkeit in seinem Labor zu arbeiten und die schöne und konstruktive Zeit in Sherbrooke. Vielen Dank auch an seine Mitarbeiter Romain Charton, Julie Pelloux und Maxime Tremblay für die tolle Zusammenarbeit und die große Hilfsbereitschaft. Besonderer Dank gilt hierbei Romain Charton für die Unterstützung bei der UV-Bestrahlung von Hefezellen.

Bei den Mitgliedern der Chromatin-Subgruppe Hannah Götze, Stephan Hamperl, Virginia Babl, Ulrike Stöckl, Jorge Pérez-Fernández, Herbert Tschochner, Philipp Milkereit und Joachim Griesenbeck möchte ich mich für die gute und effektive Zusammenarbeit in den letzten Jahren bedanken. Besonderer Dank an Stephan Hamperl für die starke Unterstützung bei ChIP Experimenten.

Ich bedanke mich ganz herzlich bei allen Mitgliedern des „House of the Ribosome“ für ihre Hilfsbereitschaft und für die sehr angenehme Arbeitsatmosphäre. Besonders bedanke ich mich bei Gisela Pöll für die vielen aufmunternden Gespräche und für die zahllosen schmackhaften Köstlichkeiten.

Bedanken möchte ich mich auch bei Dr. Helfried Mallow, der leider viel zu früh aus dem Leben geschieden ist.

Für die finanzielle aber vor allem ideelle Unterstützung während meiner Promotion danke ich dem Elitenetzwerk Bayern. Der Bayerischen Forschungsallianz danke ich für die Förderung von Reisen nach Sherbrooke.

Bei meiner Freundin Rebecca bedanke ich mich für die moralische Unterstützung während dieser Promotion und die vielen schönen Tage außerhalb des Labors.

Meinen Eltern Walburga und Robert danke ich für ihre bedingungslose Unterstützung und dafür, dass sie mir diese Ausbildung ermöglicht haben. Vielen Dank!
Merci beaucoup auch an mein Bruderherz Benjamin.